UNIVERSIDAD NACIONAL AUTÓNOMA DE MÉXICO

POSGRADO EN CIENCIAS BIOLÓGICAS

FACULTAD DE ESTUDIOS SUPERIORES IZTACALA

"*Asterohyptis stellulata*: FITOQUÍMICA Y PROPIEDADES BIOLÓGICAS RELACIONADAS CON EL PROCESO DE CICATRIZACIÓN"

TESIS

QUE PARA OPTAR POR EL GRADO DE:

DOCTORA EN CIENCIAS

PRESENTA:

M. en C. Nallely Álvarez Santos

TUTORA PRINCIPAL: Dra. Ana María García Bores
Facultad de Estudios Superiores Iztacala, UNAM.
COMITÉ TUTOR: Dra. Diana Barrera Oviedo
Facultad de Medicina, UNAM.
COMITÉ TUTOR: Dr. Ricardo Reyes Chilpa
Instituto de Química, UNAM.

Los Reyes Iztacala, Tlalnepantla, Estado de México, enero 2024

UNIVERSIDAD NACIONAL AUTÓNOMA DE MÉXICO

POSGRADO EN CIENCIAS BIOLÓGICAS

FACULTAD DE ESTUDIOS SUPERIORES IZTACALA

"*Asterohyptis stellulata*: FITOQUÍMICA Y PROPIEDADES BIOLÓGICAS RELACIONADAS CON EL PROCESO DE CICATRIZACIÓN"

TESIS

QUE PARA OPTAR POR EL GRADO DE:

DOCTORA EN CIENCIAS

PRESENTA:

M. en C. Nallely Álvarez Santos

TUTORA PRINCIPAL: Dra. Ana María García Bores
Facultad de Estudios Superiores Iztacala, UNAM.
COMITÉ TUTOR: Dra. Diana Barrera Oviedo
Facultad de Medicina, UNAM.
COMITÉ TUTOR: Dr. Ricardo Reyes Chilpa
Instituto de Química, UNAM.

Los Reyes Iztacala, Tlalnepantla, Estado de México, enero 2024.

COORDINACIÓN GENERAL DE ESTUDIOS DE POSGRADO
COORDINACIÓN DEL POSGRADO EN CIENCIAS BIOLÓGICAS
FACULTAD DE ESTUDIOS SUPERIORES IZTACALA
OFICIO: CGEP/CPCB/FESI/0935/2023
ASUNTO: Oficio de Jurado

M. en C. Ivonne Ramírez Wence
Directora General de Administración Escolar, UNAM
P r e s e n t e

Me permito informar a usted que en la reunión ordinaria del Subcomité de Biología Experimental del Posgrado en Ciencias Biológicas, celebrada el día **23 de octubre de 2023** se aprobó el siguiente jurado para el examen de grado de **DOCTORA EN CIENCIAS** de la estudiante **ÁLVAREZ SANTOS NALLELY** con número de cuenta **99012643** con la tesis titulada **"Asterohyptis stellulata: fitoquímica y propiedades biológicas relacionadas con el proceso de cicatrización",** realizada bajo la dirección de la **DRA. ANA MARÍA GARCÍA BORES,** quedando integrado de la siguiente manera:

Presidente:	DR. LUIS FELIPE JIMÉNEZ GARCÍA
Vocal:	DR. JOSÉ GUILLERMO ÁVILA ACEVEDO
Vocal:	DR. RUBEN LÓPEZ SANTIAGO
Vocal:	DR. ANDRÉS ELIÚ CASTELL RODRÍGUEZ
Secretario:	DRA. DIANA BARRERA OVIEDO

Sin otro particular, me es grato enviarle un cordial saludo.

A T E N T A M E N T E
"POR MI RAZA HABLARÁ EL ESPÍRITU"
Ciudad Universitaria, Cd. Mx., a 29 de noviembre de 2023

COORDINADOR DEL PROGRAMA

DR. ADOLFO GERARDO NAVARRO SIGÜENZA

POSGRADO EN CIENCIAS BIOLOGICAS
COORDINACIÓN

c. c. p. Expediente del alumno

AGNS/GGM/EARR/ggm

AGRADECIMIENTOS INSTITUCIONALES

Al Posgrado en Ciencias Biológicas de la Universidad Nacional Autónoma de México.

Al Consejo Nacional de Ciencia y Tecnología que otorgó el apoyo económico requerido para la realización de este proyecto otorgando una beca CONAHCyT de posgrado con número CVU 775307.

A la UNAM por el apoyo con los proyectos de investigación PAPIIT con número de registro: PAPIT-DGAPA IN220920; IN212623y por el acceso a la súper computadora Miztli con el número de registro LANCAD-UNAM-DGTIC-413.

A los miembros del Comité Tutor: Dra. Ana María García Bores por su guía como tutor principal, a la Dra. Diana Barrera Oviedo de la Facultad de Medicina, UNAM al Dr. Ricardo Reyes Chilpa del Instituto de química, gracias por guía y sus valiosas aportaciones para la realización de este proyecto.

ÍNDICE GENERAL

RESUMEN

La piel es nuestra principal defensa frente al medio, cuando esta se ve interrumpida comienza un proceso conocido como cicatrización, el cual está dividido en cuatro fases interpuestas: a) hemostasia, b) inflamación, c) proliferación y d) remodelación. Este proceso generalmente es sumamente eficiente, no obstante, puede ser afectado por factores como la infección de heridas y patologías previas como la diabetes, ambas relacionadas con inflamación sostenida e inhibición de cierre de la herida. Por lo cual, es fundamental la búsqueda de tratamientos que permitan un proceso más eficiente. Los productos naturales siempre han sido fuente importante para el descubrimiento de fármacos. *A. stellulata* es una planta utilizada en Tonatico Edo, de México para el tratamiento de heridas, por lo tanto, podría tener actividad cicatrizante. Para evaluar si cuenta con dicha actividad se obtuvo el extracto crudo metanólico (EMAS) de las partes áreas de la planta y los aceites esenciales de hojas y tallo (AEHT) e inflorescencia (AEI), de estos últimos solo se evaluó su actividad antibacteriana debido a su bajo rendimiento. Posteriormente, el EMAS fue particionado y se obtuvieron cuatro particiones nombradas por el solvente en el que son miscibles: PHex, PMeOH, PH_2O y PDMSO. Debido a que los extractos son mezclas de compuestos que en muchas ocasiones actúan de manera sinérgica, se determinó el perfil fitoquímico de *A. stellulata* con el fin de identificar cuáles eran sus componentes principales. Se realizaron un screening de los principales grupos de metabolitos secundarios, cuantificación de fenoles, análisis por HPLC-MS/MS y CG/MS. El EMAS y sus particiones se utilizaron para evaluar las actividades biológicas *in vitro* relacionadas con la cicatrización de heridas: antibacteriana, antioxidante y antiinflamatoria. El EMAS a diferentes concentraciones se integró a la base Beeler para preparar la emulsión que será usada en la evaluación de la actividad cicatrizante, se le realizaron pruebas de estabilidad e irritabilidad en ratones CD1 et/et. La emulsión con EMAS al 5% fue usado para la evaluación de la actividad cicatrizante

in vivo en ratones CD1 et /et con heridas incisionales el tratamiento duro 13 días. El perfil fitoquímico de *A. stellulata* nos indica que cuenta con compuestos fenólicos y terpenicos, probablemente glicosilados, pero no tiene alcaloides. El análisis del EMAS por HPLC-MS-MS permitió identificar dos derivados de quercetina y un glucopiranósido de ácido rosmarínico. El análisis de CG/EM de los aceites esenciales el de AEHT mostró que tiene como compuestos mayoritarios óxido de cariofileno y α-bisabolol; el AEI fue más diverso y sus compuestos principales son germacreno D, cariofileno, α- bisabolol, α-cadinol y óxido de cariofileno. Los resultados de la actividades biológicas, indican que tanto el EMAS y sus particiones tienen actividad bactericida y/o bacteriostática en cepas de *S. aureus* y *S. epidermidis.* El AEHT tiene actividad bactericida y/o bacteriostática en cepas de *S. aureus.* El EMAS, PMeOH, PH_2O y PDMSO tienen actividad antioxidante frente al radical DPPH, la PHex no tiene actividad. El EMAS y sus particiones inhiben *in vitro* la enzima inflamatoria COX-2. En cuanto a la evaluación in vivo se determinó que el uso de la formulación no es irritante en ninguna concentración y todas las formulaciones son estables. La aplicación tópica de EMAS en base Beeler mejoro el depósito y maduración del colágeno, formación de nueva epidermis similar a la normal, mayor contracción de la herida, dermis con folículos pilosos y glándulas sebáceas, hipodermis y una capa de musculo de neoformación. Por lo tanto, podemos concluir que *A. stellulata* cuenta con metabolitos secundarios, que le dan diferentes actividades biológicas que en conjunto permiten la regeneración de tejidos en heridas incisiones de ratones CD1 et/et.

ABSTRACT

The skin is the principal defense against the environment, and when this is interrupted, the wound healing process begins, which is constituted by four interposed phases: a) hemostasia, b) inflammation, c) proliferation, and d) remodeling. Although this process is very efficient; nevertheless, it can be affected by factors such as infection and pre-existing pathologies such as diabetes, both of which are related to sustained inflammation and inhibition of wound closure. Whereby, is fundamental the search for treatments that promote the process to be more efficient. Natural products have always been an important source of inspiration for the discovery of new drugs. *A. stellulata* is a plant used in Tonatico Edo, de México, for the treatment of wounds; therefore, it is probably an agent of wound healing. Methanolic crude extract (EMAS) of aerial parts and essential oils of the stem/leaf (AEHT) and inflorescence (AEI) were used to evaluate this activity. Because of essential oils low yield, only antibacterial activity was evaluated. EMAS was partitioned, and four partitions were obtained named by the solvent in which they are miscible: PHex, PMeOH, PH_2O, and PDMSO. Subsequently, the phytochemical profile of A. stellulata was determined to identify the main groups of secondary metabolites. Screening phytochemicals, quantification of phenols, HPLC-MS/MS, and CG/MS were performed. EMAS and partitions were used for the evaluation of biological activities in vitro: antibacterial, antioxidant, and anti-inflammatory. EMAS at different concentrations was integrated into Beeler base, and the stability of the formulations was evaluated. Subsequently, emulsions were used to evaluate dermal irritability. After, the dermal irritability of the emulsions was evaluated in CD1 et/et mice to select the concentration that would be used in the evaluation of wound healing activity. An EMAS emulsion of 5% was used for the evaluation in vivo of incisional wounds in CD1 et/et mice, and treatment lasted 13 days. The phytochemical profile of *A. stellulata* showed that it has phenolic and terpene compounds, probably glycosylates, but not

alkaloids. HPLC-MS/MS analysis of EMAS allowed the identification of two derivatives of quercetin and a glucopyranoside of rosmarinic acid. CG/MS of AEHT identified the major compounds germacrene D, caryophyllene, α-bisabolol, α-canadiol, and caryophyllene oxide. Results of biological activities showed that EMAS and partitions are bactericides and bacteriostatic against *S. aureus* and *S. epidermidis*. EMAS, PMeOH, PH_2O, and PDMSO had antioxidant activity against DPPH radicals, whereas PHex had no activity. EMAS and partitions inhibit COX-2. *In vivo* evaluation showed that Beeler base and formulations at different concentrations were nonirritant, and all were stable. Topical application of EMAS in Beeler base enhanced many processes such as deposition and maturation of collagen, formation of neo-epidermis similar to normal, better contraction of wound, neo-dermis with hair follicles and sebaceous glands, neo-hypodermis, and muscle of neoformation. In conclusion, *A. stellulata* has secondary metabolites with different biological activities and, in combination, promotes the regeneration of tissues in the incisional wounds of mice CD1 et/et.

1. INTRODUCCIÓN

La piel está compuesta de dos capas principales: la epidermis y la dermis (Emming et al., 2014); que están separadas por una membrana basal; en este órgano se albergan estructuras especializadas como los folículos pilosos, las glándulas sudoríparas y sebáceas; la epidermis es un epitelio plano estratificado que se renueva constantemente, mantiene un equilibrio entre la proliferación de las células basales, la diferenciación y estratificación de las células suprabasales. (Rognoni et al., 2018). La dermis se compone de diferentes subcapas: a) papilar está ubicada cerca de la membrana basal y muestra una alta densidad de fibroblastos y fibras de colágeno delgadas y desorganizadas, b) reticular es la capa central con menor densidad celular, que cuenta con fibras de colágeno gruesas y organizadas, c) hipodermis que es un tejido formado por adipocitos (Lynch et al., 2018).

La piel es el órgano más grande del cuerpo humano, mantiene la homeostasis y protege a los órganos internos (Kim et al., 2019). Por lo cual, es propensa a sufrir daños y que se formen lesiones conocidas como heridas. Para restablecer la homeostasis se da el proceso de cicatrización, el cual busca recuperar la integridad y función del tejido (Rodrigues et al., 2019). La cicatrización es un fenómeno complejo y dinámico que está dividido en cuatro etapas superpuestas: a) hemostasia, b) inflamación, c) proliferación y d) maduración o remodelación (Mi et al., 2022).

En condiciones fisiológicas normales, el proceso de cicatrización es rápido y eficaz. Sin embargo, el envejecimiento, las enfermedades crónicas como la diabetes, las enfermedades vasculares y el cáncer pueden disminuir la capacidad de curación de los tejidos (Bao et al., 2022). En consecuencia, esto promueve la cronicidad de las heridas, caracterizada por la inflamación excesiva y en ocasiones la infección (Sathyanarayanan et al., 2017).

La inflamación crónica se caracteriza por una respuesta continua a lo largo del tiempo (Ptaschinski et al., 2017) y la hiperproducción de radicales libres, los cuales conducen a la inhibición de los mecanismos responsables de las etapas posteriores del proceso de la cicatrización de la herida (Sathyanarayanan et al., 2017). El exceso de radicales libres, provoca estrés oxidativo que puede causar daño a las macromoléculas y por lo tanto daño celular (Krudyavtseva et al., 2016; Sathyanarayanan et al., 2017). En parte esta sobreproducción está relacionada con neutrófilos que presentan cambios fenotípicos, una menor infiltración y una permanencia más prologada en la herida (Las Heras et al., 2020), lo que induce una sobreproducción de ROS y daño a la MEC (Zhao et al., 2016). También, existe un desequilibrio entre los macrófagos M1/M2 lo que mantiene el estado inflamatorio (Baltzis et al., 2014). Durante este proceso hay una sobreproducción de mediadores, uno de estos es COX-2 que a través de la producción de prostaglandinas (PG) contribuye a la inflamación (Romana-Souza et al., 2016). Por lo cual, COX-2 es uno de los principales blancos farmacológicos para tratar la inflamación. Actualmente, se aplican medicamentos antiinflamatorios no esteroideos para su inhibición, pero se ha reportado que pueden retrasar la cicatrización de heridas (Zhao-Fleming et al., 2018).

La infección microbiana es otro fenómeno que inhibe la curación de heridas, prolongando la fase de inflamación y dando origen a heridas crónicas (Zhao et al., 2016; Elzayat et al., 2018). Es muy común en lugares con malas condiciones de higiene (Kramer et al., 2018), o en pacientes con patologías preexistentes como el cáncer (Zhou et al., 2019) o la diabetes (Qiao et al., 2020). La invasión de tejido viable por bacterias patógenas como *Staphylococcus aureus*, *Staphylococcus epidermidis*, *Pseudomonas aeruginosa*, *Escherichia coli* y algunas cepas resistente como *S. aureus* resistente a la meticilina (MRSA), pueden provocar una serie de respuestas locales y sistémicas del huésped, sumado a un control inadecuado de las heridas infectadas, puede retrasar el proceso de

curación o en última instancia, conducir a bacteriemia y septicemia, las cuales pueden ser fatales (Catanzano et al., 2017; Rajoo et al., 2021). Además, las lesiones cutáneas afectan a muchos pacientes en todo el mundo y cuestan miles de millones de dólares a los sectores público y privado (Nussbaum et al., 2018; Chen et al., 2023).

Estos fenómenos conducen a la inhibición de los mecanismos responsables de la sucesión de etapas en el proceso de cicatrización (Sathyanarayanan et al., 2017). Lo cual da como resultado la formación de úlceras o heridas crónicas que afectan la calidad de vida de los pacientes e impacta económicamente tanto al sistema de salud (Han y Ceilley, 2017; Meng et al., 2018). Por lo tanto, es importante la búsqueda de nuevos fármacos con actividad curativa y menos efectos secundarios

Existen varias formulaciones herbales tradicionales que se aplican en la herida, en las que la planta en forma de pasta, decocción, extracto o polvo, mejora y acelera la curación (Nour et al., 2019). Incluso, se ha reportado que se disminuye la formación de cicatrices en los pacientes (Kumar et al., 2007; Chitra et al., 2009). Otras ventajas de plantas medicinales y sus formulaciones son el bajo costo, la disponibilidad y menos efectos secundarios (Bahramsoltani et al., 2014). Los productos naturales siempre han jugado un papel importante en el descubrimiento de fármacos, ya sea por sí mismos o como inspiración para compuestos sintéticos (Almeida et al., 2021).

La aplicación de plantas medicinales como tratamiento, mejora el proceso de cicatrización de heridas debido a la presencia de compuestos activos que pueden ser fenoles, alcaloides y terpenoides. Por ejemplo, la quercetina inhibe la producción de TNFα, IL-1β, IL-6, regulan los niveles de IL-10 y/o aumentan los niveles de expresión de VEGF y TGF-α/β; promueve la diferenciación del fenotipo de macrófagos M1 a M2, lo cual modula la fase inflamatoria (Fu et al., 2020; Ud-Din et al., 2019). Los compuestos terpenoides pueden modular la

inflamación. El kiredol inhibe la expresión de COX-2 (Ren et al., 2020). La periplocina aumenta la proliferación y migración de fibroblastos (Chen et al., 2019). Por lo tanto, la investigación de compuestos y los extractos de plantas medicinales es fundamental para conocer los eventos y fases en los que actúa para mejorar el proceso de cicatrización, lo cual permitirá determinar si las plantas medicinales cuentan con el potencial farmacológico necesario, además de establecer criterios de calidad y la estandarización para su formulación.

Dentro de las plantas medicinales destaca la familia Lamiaceae por su uso etnofarmacológico. En una revisión sobre sus usos y aplicaciones indican que los aceites esenciales tienen fuerte actividad antibacteriana y antioxidante; mientras que los constituyentes polares son conocidos por tener actividades: antiviral, anticancerígena y antiinflamatoria (Frezza et al., 2019). Dicha familia es una de las más diversas de la República Mexicana y presenta un endemismo del 65.82%. Algunos de los géneros presentes en el país son *Salvia*, *Scutellaria*, *Stachys*, *Hyptis* y *Asterohyptis* (Martínez-Gordillo et al., 2013).

Asterohyptis Epling es un género pequeño que fue separado del género *Hyptis* Jacq., éstos permanecieron juntos hasta la propuesta de Epling en 1933. *Asterohyptis* está tipificado por la especie *A. stellulata* (Benth.) Epling y se distingue de *Hyptis* por sus numerosas flores pequeñas que están dispuestas en racimos axilares, lóbulos de la corola no engrosados y anteras no explosivas (Turner, 2011). El género *Asterohyptis* está constituido por cuatro especies distribuidas de México a Centro América (Turner, 2011), de estas, dos son endémicas (Martínez-Gordillo et al., 2013). *A. stellulata*, en el municipio de Tonatico, Edo. de México se utiliza para el tratamiento de heridas (León, en proceso). Debido a este uso tradicional de *A. stellulata* y los antecedentes etnofarmacológicos de la familia, es importante realizar un estudio de sus actividades biológicas como: antimicrobiana,

antioxidante y antiinflamatoria de manera independiente. Así, como determinar si en conjunto afectan el proceso de cicatrización al aplicar el extracto y/o aceites esenciales de la planta de manera tópica en ratones que tengan heridas incisionales. Además, determinar la composición química de la planta nos llevará a discernir los posibles compuestos activos, su mecanismo de acción. Asimismo, nos permitirá tener un probable acercamiento a una formulación farmacológica.

2. HIPÓTESIS

A. stellulata es utilizada para tratar heridas, esto probablemente se deba a la presencia de metabolitos secundarios que le dan cualidades: antimicrobiana, antioxidante, antiinflamatoria y/o cicatrizante. Entonces, al ser aplicada de manera tópica en heridas incisionales en modelo de ratón CD-1 et/et, se observará que las heridas cierran en menor tiempo y presentarán mayor resistencia a la fuerza de tensión. Esto debido a que a nivel histológico habrá re-epitelización, contracción de la herida, así como síntesis y maduración colágeno.

3. OBJETIVO GENERAL:

- Evaluar la actividad cicatrizante de *Asterohyptis stellulata* y conocer su fitoquímica.

3.1. Objetivos particulares

- Investigo el perfil fitoquímico de *A. stellulata* con un screening de los principales grupos de metabolitos secundarios, cuantificación del contenido de fenoles totales, análisis de HPLC-DAD-ESI/MS/MS del extracto metanólico de *A. stellulata* (EMAS) y un análisis de CG/EM de los aceites esenciales de *A. stellulata*.
- Evaluar la actividad antibacteriana de *A. stellulata* en cepas relacionadas a la infección de heridas.
- Determinar la capacidad antioxidante *in vitro* de *A. stellulata* frente al radical DPPH.

- Analizar la capacidad antiinflamatoria de *A. stellulata* a través de la inhibición *in vitro* de COX-2.
- Determinar la estabilidad de la emulsión con *A. stellulata*.
- Evaluar la irritabilidad cutánea de *A. stellulata* en ratones CD-1 et/et.
- Evaluar la capacidad cicatrizante en ratón CD-1 et/et del extracto crudo de *A. stellulata*.

4. ANTECEDENTES

El género Asterohyptis está formado por cuatro especies y sus actividades biológicas han sido poco estudiadas incluyendo la actividad cicatrizante. Sin embargo, para tener un panorama más amplio se revisaron publicaciones que incluyen a *Hyptis* el cual es un género hermano de *Asterohyptis*, el cual tiene varias especies que se usan para tratar heridas (Tabla 1).

Tabla 1. Antecedentes de las actividades biológicas del género *Asterohyptis* e *Hyptis*.

ASTEROHYPTIS	
Autores	**Antecedente**
Jacobo-Herrera et al., 2016	El extracto acuoso de *A. stellulata* es usado de manera tradicional para el tratamiento del vómito.
León, en proceso (Tesis)	En la comunidad de Tonatico Edo. De México *A. stellulata* se utiliza en forma de cataplasma e infusión para el tratamiento de heridas y problemas cutáneos.
Espinosa-González et al., 2021	El extracto MeOH de las partes aéreas de *A. mocininana* (sinonimia *H. mociniana*) presentó actividad antioxidante y efecto fotoquímio preventivo. Se identificaron compuestos derivados de quercetina, pectinólidas y dos derivados del ácido cafeico
HYPTIS	
Autores	**Antecedente**
Shirwaikar et al., 2003	El extracto etanólico de hojas de *H. suaveolens* mejoró el proceso de cicatrización en heridas de incisión, escisión y espacio muerto.
Picking et al., 2013	*Hyptis verticillata* Jacq se utiliza de manera tradicional para tratar heridas.
Bridi et al., 2021	Un estudio de la Subtribu Hyptidinae indica que varias especies del género *Hyptis* son utilizadas de manera tradicional para tratar heridas como: *H. spicigera*, *H. mutabilis*, *H. albida* y *H. obtusiflora*

5. METODOLOGÍA

5.1. Material vegetal

El material vegetal se colectó el 21 de septiembre y el 31 de octubre del 2019, en la comunidad de “San José de los Amates”, Tonatico, Edo. de México. Fue identificado en el herbario IZTA de la FES-Iztacala de la UNAM y tiene el número de registro 3303-IZTA.

5.1.1. Extracto crudo y particiones

El extracto crudo metanólico de *A. stellulata* (EMAS) se obtuvo a partir de 1176.5 g de las partes aéreas previamente secas y molidas, dicho material vegetal se sometió a maceración con metanol por tres días. Posteriormente, se concentró a presión reducida y se eliminó el solvente restante. El rendimiento se calculó de la siguiente manera:

% del CRU = [Peso del extracto seco (g)/Peso del material seco (g)] x 100

Se conservo una parte del EMAS (50.42 g) y el resto (71 g) fue particionado con hexano-metanol, de este procedimiento se obtuvieron cuatro particiones PMeOH, PHex, PDMSO y PH_2O. Las cuales están nombradas por el solvente en el que son miscibles.

5.1.2. Aceites esenciales AEHT y AEI

El aceite esencial de hojas y tallos (AEHT) se obtuvo de 2100 g de material fresco de *A. stellulata*. También, se extrajo el aceite esencial de inflorescencia (AEI) donde se utilizaron 1500 g de material fresco. El material se sometió a hidrodestilación durante 2 horas, utilizando un aparato de tipo clevenger. El aceite esencial se almacenó a 4°C hasta el momento de su uso en los experimentos. El rendimiento del aceite esencial se calculó de la siguiente manera:

% del CRU = [Peso del aceite esencial (g)/Peso del material fresco (g)] x 100

La densidad de los aceites esenciales se determinó pesando por triplicado un volumen conocido (10µL). Debido al rendimiento de los aceites esenciales solo se realizaron las pruebas de actividad antibacteriana y el análisis por CG/EM.

5.2. Perfil fitoquímico de *A. stellulata*

Se realizo la caracterización química de *A. stellulata*, comenzando por una detección preliminar con pruebas coloridas de los principales grupos de metabolitos secundarios y una cuantificación de fenoles totales por el método de Folin-Ciocalteu. Posteriormente, se realizó un análisis del EMAS por HPLC-DAD-ESI/MS/MS. Para los AEHT y AEI se realizó un análisis por CG/MS.

5.2.1. Detección preliminar de los principales grupos de metabolitos por pruebas coloridas de *A. stellulata*.

La detección de los principales grupos de metabolitos secundarios presentes en el EMAS y precipitados de *A. stellulata*, se llevó a cabo con técnicas estándar (Tabla 2). Tubos con 1 mg/mL de EMAS, PMeOH, PHex, PDMSO o PH_2O, se les agrego de 3-5 gotas de reactivo. Los precipitados con los reactivos de Dragendorff y Mayer indican presencia de alcaloides; la coloración azul o verde oscuro con cloruro férrico determina la presencia de compuestos fenólicos; un halo violeta indica glucósidos al realizar el test de Molisch; color verde azulado identifica esteroides; una coloración naranja con el test de Liberman-Burchard es dada por la presencia de lactonas como lactonas sesquiterpénicas y/o cumarinas; finalmente al agitar los tubos por un minuto y observando una espuma persistente indica la presencia de saponinas (Guillén-Meléndez et al., 2022; Sujamol et al., 2021; Yunitasari et al., 2022).

La detección de terpenos se realizó por cromatografía en capa fina con una fase móvil de hexano y etil acetato (8:2), el revelado de las placas se realizó con vainillina-ácido sulfúrico y una incubación de 5 min a 100°C (Ali et al., 2021).

Tabla 2. Reacciones coloridas que se utilizaron para la detección de los principales grupos de metabolitos secundarios presentes en *A. stellulata*.

GRUPO DE METABOLITOS	REVELADOR/AGENTE CROMÓGENO	REACCIÓN POSITIVA
Alcaloides	Reactivo de Dragendorff	Precipitado o color naranja
	Reactivo de Mayer	Precipitado color blanco
Glucósidos	Molish	Halo color morado
Fenoles	Cloruro férrico	Coloración de verde-azul
Saponinas	Espuma	Persistencia de espuma
Lactonas sesquiterpénicas	Reactivo de Baljet	Coloración naranja o roja obscura
Esteroides	Liebermann-Burchard	Color verde intenso
Terpenos	Vainillina-ácido sulfúrico	Revelado de cromatografía en capa fina donde las coloraciones van del rosa al morado.

5.2.2. Cuantificación de fenoles totales

Se utilizó el método de Folin-Ciocalteu para determinar el contenido fenólico total (Rajhi et al., 2022) con modificaciones en consideración a Singleton et al. (1999). Brevemente, se mezclaron 75 µL de EMAS, PMeOH, PHex, PDMSO o PH_2O (1 mg/mL de MeOH) con 1150 µL de agua destilada, 250 µL de reactivo de Folin-Ciocalteu y 1500 µL de carbonato de sodio al 2%. La absorbancia se midió a 760 nm en el Espectrofotómetro Lambda 2S UV/Vis PerkinElmer (USA). Los experimentos se realizaron por triplicado.

5.2.3. Análisis por HPLC-DAD-ESI/MS/MS del EMAS de *A. stellulata*

El análisis fitoquímico del EMAS se realizó según el método descrito por Estrella-Parra et al., (2019) y Espinosa-González et al., (2021), utilizando el mismo sistema HPLC-DAD

(Thermo Dionex Ultimate 3000 HPLC, UV-ESI-MS, software Chromeleon) y ESI/MS/MS (sistema Orbitrap Fusion Tri-hybrid, software Xcalibur, Thermo Scientific Xcalibur V.4.1.5.0).

Se utilizó una columna Nucleodex β-OH (200 mm x 4 mm, 5 µm; Macherey-Nagel, 720,124). La muestra se analizó mediante una base móvil en gradiente: A) ácido fórmico al 0.1% en agua (v/v); B) ácido fórmico al 0.1% en acetonitrilo (v/v); y C) ácido fórmico al 0.1% en metanol (v/v); comenzando con 95% A, 2% B y 3% C, cambiando a 54% A, 23% B y 23% C después de 20 min y terminando con 95% A, 2% B y 3% C después 30 minutos. El flujo fue de 0.6 mL/min.

También, se realizó el análisis de masa de los siguientes patrones comerciales: catequina (C1251), quercetina (Q0125), ácido gálico (G7384) y ácido shikímico (S5375), de Sigma-Aldrich. Además, se consultaron las bases de datos espectrales como mzCloud y MassBank para determinar los patrones de fragmentación.

5.2.4. CG-EM del AEHT y AEI de *A. stellulata*

El análisis fitoquímico de los aceites esenciales AEHT y AEI se realizaron en el Instituto de Química de la UNAM. Las muestras fueron diluidas en 1 mL de diclorometano. Posteriormente, se inyectaron al cromatógrafo de gases acoplado a espectrometría de masas. Para el análisis se utilizó un cromatógrafo de gases (CG) Agilent Technologies 7890B y un detector de espectrometría de masas (EM) Agilent Tecnologies 5977D.

Se utilizó una columna capilar HP-5MS 30m x 0.25 mm x 0.25mm, como fase móvil Helio a 1 mL/min, con una temperatura del inyector de 280°C, comenzando con una temperatura de 40°C por minuto, rampa 18°C/min y una temperatura final de 300°C por 5 minutos. El tiempo de análisis fue de 25 minutos. El detector de espectrometría de masas por impacto

electrónico fue de 70eV y con rango de 30-600 (m/z). La identificación de compuestos se hizo a través de la comparación la biblioteca NIST 14.

5.3. ACTIVIDAD ANTIBACTERIANA DE *A. stellulata*

5.3.1. Microorganismos utilizados en los bioensayos

La actividad antibacteriana de *A. stellulata* fue estudiada en las siguientes cepas bacterianas: *Staphylococcus aureus* 23MR, *S. aureus* ATCC 2913, *S. aureus* CC, *S. aureus* CUSI, *S. aureus* FES-C, *Staphylococcus epidermidis* ATCC 12228, *S. epidermidis* FES-C, *Micrococcus luteus* ATCC 10240, *Pseudomonas aeruginosa* ATCC27853, *Escherichia coli* 82MR, *Enterobacter aerogenes* ATCC 13048 y *Salmonella typhi* ATCC 19430. Fueron elegidas ya que son de importancia médica, por causar infecciones y sus subsecuentes complicaciones en el tratamiento de heridas (Abbas et al., 2015, Caldwell, 2020; Elzayat et al., 2018).

La actividad antibacteriana de *A. stellulata* se evaluó de acuerdo con la directriz M100 del Clinical and Laboratory Standard Institute. (CLSI 2020).

5.3.2. Determinación cualitativa de la actividad antibacteriana

La actividad antimicrobiana cualitativa se determinó por el método de difusión en agar de Kirby-Bauer (CLSI, 2020). Los inóculos bacterianos se ajustaron al estándar 0.5 de Mc Farland (1 x 108 UFC/mL). Se prepararon los discos de papel filtro de 5mm de diámetro, se impregnaron con 2 mg de las particiones (EMAS, PMeOH, PHex, PDMSO o PH_2O). Para los aceites esenciales se aplicaron los siguientes volúmenes de acuerdo con su densidad AEHT 7.5 µL y del AEI 6 µL. El antibiótico Cloranfenicol fue utilizado como control positivo (30 µg/5 µL) y DMSO como control negativo (10 µL). Los inóculos se sembraron en placas con agar Müller-Hinton, los sensidiscos se colocaron sobre la superficie del agar y se

incubaron por 24 horas a 37°C. Los halos de inhibición se reportan en mm. Cada bioensayo se realizó por triplicado. Las sustancias que tuvieron actividad se les determinó la concentración mínima inhibitoria (CMI) y concentración bactericida mínima (CBM).

5.3.3. Determinación cuantitativa de la actividad antibacteriana

A las cepas que fueron sensibles en la prueba de Kirby-Bauer, se les determinó la concentración mínima inhibitoria (CMI), que es la concentración mínima que inhibe el crecimiento visible de los microorganismos y la concentración bactericida mínima (CBM) que se define como la concentración mínima que elimina a más del 99.9% de los microorganismos con la técnica de microdilución en caldo (CLSI, 2020).

A partir de inóculos al 1.5 x 10^8 UFC/mL que tenían una absorbancia de 0.242 ± 0.019 a 560 nm, se preparó el inóculo experimental para lo cual se tomaron 100 µL y se agregaron a 100 mL de solución salina (0.9%) para obtener una concentración de 1.5 x 10^5 UFC/mL, de este se agregaron 50 µL a tubos Eppendorf 600 µL. El EMAS, las particiones y el AEHT se utilizaron a las siguientes concentraciones 0.612, 0.125, 0.250, 0.5, 1, 2 y 4 mg/mL. El EMAS y las particiones fueron disueltos en 1% de DMSO y 1% de Tween 80 (para mejorar la solubilidad en el medio) en el caldo Müller-Hinton; el AEHT fue disuelto solamente en caldo y Tween 80 al 1% (volumen final de 50 µL).

Los controles fueron los siguientes: testigo -sin sustancia a evaluar y sin bacteria-, control negativo -con caldo y Tween 80-, control de crecimiento -con Tween 80 y bacteria-, éste se realizó para observar que el material con el que disolvió el aceite esencial no afectará el crecimiento de las bacterias, control con caldo y bacteria; y control positivo -con cloranfenicol 30 µg/mL y bacteria-. En todos los casos el volumen final fue de 200 µL. Posteriormente se incubaron por 24 horas a 37°C.

Después del periodo de incubación se agregaron 50 µL de cloruro de tetrazolio (TTC 0.08%), se incubaron por 30 minutos y finalmente se observó la sobrevivencia bacteriana por el cambio de coloración; rojo hay sobrevivencia mientras que sin color hay muerte celular; también se puede observar la baja de intensidad cuando hay reducción considerable del crecimiento bacteriano, lo cual nos permite determinar la CMI. Una repetición se dejó sin TTC para posteriormente ser sembrada en cajas con agar Müller-Hilton, las cuales se incubaron por 24 horas, esto permite observar el crecimiento bacteriano y corroborar las lecturas con el TTC.

5.4. Actividad antioxidante de *A. stellulata* sobre el radical DPPH

La actividad antioxidante se evaluó mediante la capacidad de reducción del radical 2,2-difenil-1-picrilhidracilo (DPPH) (Guija-Poma et al., 2015). Este método está basado en la reducción del radical DPPH por la sustancia a evaluar. El DPPH es un radical que presenta una coloración púrpura con un máximo de absorción a 515 nm, cuando este es reducido por el compuesto antioxidante la coloración se torna amarilla. Para llevar a cabo dicho método, se realizaron diluciones en DMSO de cada una de las sustancias a evaluar: EMAS, PMeOH, PHex, PH_2O o PDMSO (5-640 µg/mL). En una placa de 96 pozos se agregaron 50 µL de cada dilución de las muestras a evaluar a 150 µL de una solución de DPPH (250 µM) en metanol. La mezcla se incubó a temperatura ambiente por 30 minutos en obscuridad. Finalmente, se midió la absorción a 515 nm. Como control positivo se utilizó quercetina (1-10 µg/mL).

Los datos se expresaron como porcentaje de decoloración, obtenidos mediante la siguiente formula:

$$\% \text{ decoloración} = (\text{Absorbancia}_{\text{muestra}} / \text{ Absorbancia}_{\text{DPPH}}) \text{ X } 100$$

Con el porcentaje de decoloración, a partir de un análisis de regresión, se obtuvo la concentración antioxidante media (CA_{50}), es decir, la cantidad necesaria de una sustancia para reducir en un 50% los radicales libres, por lo tanto, un valor bajo de (CA_{50}) representa una alta capacidad antioxidante. Se realizaron ocho repeticiones de cada medición en tres experimentos independientes.

5.5. Actividad antiinflamatoria: ensayo *in vitro* de COX-2

El EMAE fue estudiado en cuanto a su capacidad de inhibición *in vitro* de COX-2 para determinar los valores de CI_{50}, es decir, la concentración de la fracción o extracto que inhibe el 50% de la actividad de la enzima (Abdelall et al., 2019).

Se utilizó el kit de COX-2 (human) (Cayman Chemical, USA), de acuerdo con las indicaciones del fabricante. El EMAS fue previamente disuelto en DMSO quedando a las concentraciones finales de 12.5, 25, 50 y 100 µg/mL. PMeOH, PHex, PDMSO y PH_2O fueron disueltas en DMSO a una sola concentración de 100 µg/mL. El Celecoxib es un fármaco de referencia antiinflamatorio específico para COX-2, por lo que fue ocupado como control positivo con tres concentraciones 1, 10 y 100 µM. Los tubos con la reacción se prepararon de la siguiente manera: 160 µL de Buffer de reacción, 10 µL de Hemo, 10 µL de COX-2 y 10 µL del inhibidor (EMAE, partición o Celecoxib). También, se prepararon dos tubos más; uno sin inhibidores que representa el 100% de la actividad de COX-2 y otro con la enzima desnaturalizada por temperatura (100°C por 3 minutos).

Todos los tubos de reacción fueron incubados durante 10 minutos a 37°C y se les agrego 10 µL de ácido araquidónico, son incubados nuevamente a 37°C durante tres minutos exactos y se les agrega cloruro de estaño con el objetivo de parar la reacción enzimática. Las PG que se produjeron durante el periodo de reacción se cuantificaron por ELISA. Se realizaron diluciones 1:2000 y 1:4000 de cada tubo de reacción, estas diluciones son las

que se utilizaron para el ELISA. Los pozos contenían 50 µL de cada tubo de reacción, 50 µL de tracer y 50 µL de anticuerpo. Para poder determinar la concentración de PG de los tubos de reacción se realiza una curva patrón con diferentes concentraciones de un estándar de PG (15.6-2,000 pg/mL), los pozos con el estándar contenían lo mismo que los tubos de reacción. La placa se dejó incubar en obscuridad y agitación por 18 horas. Después, de este periodo se lava la placa cinco veces y de manera consecutiva. Posteriormente, se agregan a cada pozo 200 µL del reactivo de Ellmann's y se incuba nuevamente por 30-60 min. Pasado este periodo se leyó a una absorbancia de 420 nm. Los datos se analizaron con un ajuste de curva logística de 4 parámetros. Lo cual nos permite determinar la concentración de PG. El % de inhibición se determinó con la siguiente formula:

% de inhibición = ([Concentración de PG con COX-2 al 100%] – [Concentración de PG con cada inhibidor]/ Concentración de PG con COX-2 al 100%) x 100

Posteriormente con los porcentajes de inhibición y la concentración se determina la CI_{50}, con un análisis de regresión lineal.

5.7. Formulación de la emulsión con *A. stellulata* y medida de estabilidad

Se utilizó una emulsión que contenía base Beeler y el EMAS. Esta base fue seleccionada porque permite la penetración de moléculas polares de alto tamaño molecular en el estrato córneo con una distribución homogénea tanto en la epidermis como en la dermis de ratones sin pelo (Boiy et al., 2007) La base Beeler se preparó de acuerdo con las indicaciones de la Agencia Española de Medicamentos y Productos Sanitarios (AEMPS, 2019), con modificaciones menores (glicerina en sustitución del propilenglicol). El EMAS a diferentes concentraciones 1, 5 y 10% (p/p) se agregaron a la base Beeler, se mezcló homogéneamente para obtener al emulsión de EMAS. A las formulaciones se les ajustó el

pH a 6 con trietanolamina, que es el pH de la piel cercano al de los ratones (pH 6.4) y al de los humanos (pH 5.5).

Las formulaciones (1 mL) fueron evaluadas en apariencia, color y olor a las 24 h de su preparación y durante 6 meses (Xavier-Santos et al., 2022). También, se sometieron a una prueba de centrifugación para determinar su estabilidad a 12000 rpm durante 30 minutos (Centrifuga 5418 Eppendorf, Hamburgo). Terminado el periodo de centrifugación se observan si existen cambios visuales en la formulación. Posteriormente, se determina el índice de formación de crema (IC) y se analizó por el método de emulsificación (Wu et al., 2022), se calculó con la ayuda de la siguiente fórmula:

$$\mathbf{CI\ (\%) = (Hs/Ht)\ x\ 100}$$

Donde CI = índice de formación de crema, Hs = altura de la emulsión superior, Ht = Altura de la emulsión total.

Además, se determinó la estabilidad de EMAS con un escaneo UV (200-200 nm), donde se midieron la emulsión EMAS previamente demulsificación con metanol (32 µg/mL), EMAS a la misma concentración y metanol como blanco (Butnariu, 2014; Wu et al., 2022)

5.8. Prueba de irritabilidad en ratón CD-1 et/et de EMAE

Para evaluar la irritabilidad de los compuestos se utilizó el método descrito por Drize (1944) y OECD guideline (2015) for testing chemicals 404, modificando el modelo animal por la cepa de ratón que se utilizara en el protocolo de cicatrización. Se utilizaron ratones de seis a ocho semanas de la cepa CD1 et/et -ratones sin pelo-, estuvieron en condiciones estándar de ciclo luz y oscuridad, temperatura ambiente 25°C, agua y alimento *ad libitum*. Los ratones fueron acondicionados durante siete días antes del protocolo de investigación (Putri et al., 2019). Se seleccionaron los ratones que presentaban piel intacta, fueron separados en

grupos de tres ratones en cajas individuales, una por cada tratamiento: EMAS, PMeOH, PHex, PH_2O o PDMSO.

El día 0 del experimento se aplicaron tópicamente 0.1 mL con una jeringa de insulina de los tratamientos en la zona dorsal de los ratones. La aplicación fue en forma de cuadrante como se observa en la figura 1, los diferentes tratamientos fueron aplicados directamente en un parche adhesivo para heridas (10 cm x 10 cm Farmacia del Ahorro®) y después se colocó en el dorso del ratón. Los cambios en la aplicación de zona están dados en el sentido de las manecillas del reloj en cada ratón (figura 1).

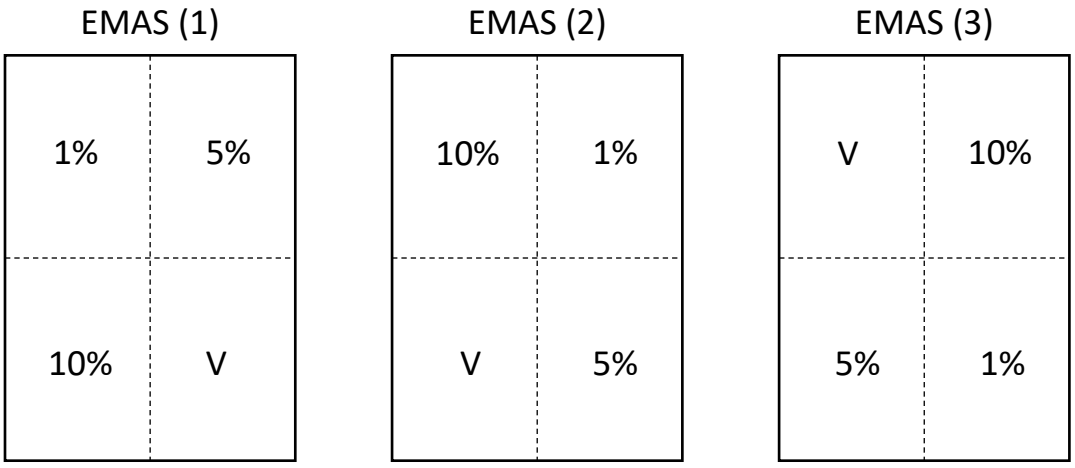

Figura 1. Aplicación en cuadrantes de las cremas a diferentes concentraciones y el vehículo (V) en el dorso de ratones CD-1 et/et. En las tres repeticiones se puede observar como la aplicación va cambiando de zona en sentido de las manecillas del reloj.

Debido a que la prueba se hace sin anestesiar a los animales, los ratones se inmovilizaron con el mismo parche y se colocaron en cajas de acrílico de manera individual por una hora, el cual es el tiempo indicado para la prueba de irritabilidad. La inmovilización permite que la aplicación permanezca en contacto con una sola área del dorso, sin que el ratón se desprenda el parche o ingiera parte de la formulación. Después de transcurrida la hora, se quita el parche, la zona del dorso se limpia con agua estéril para eliminar los restos de los tratamientos y se realiza la primera observación, las siguientes se hacen cada 24 horas

durante tres días (24, 48 y 72 horas) después de la aplicación y se tomaron anotaciones de acuerdo con las tablas establecidas por Drize (1944) y OECD guideline (2015) (Tabla 3) para determinar la formación de eritema o edema en la zona de la aplicación. El eritema es el enrojecimiento difuso o en manchas de la piel, producido por la congestión de los capilares. Mientras, que el edema es la inflamación producida por acumulación excesiva de líquido seroalbuminoso en el tejido celular.

Tabla 3. Escalas de evaluación de eritema y edema (Drize 1944; OECD guideline 2015).

ERITEMA	
No eritema	**0**
Eritema	**1**
Eritema bien definido	**2**
Eritema de moderado a severo	**3**
Eritema severo	**4**
Calificación máxima posible de eritema: 4	
EDEMA	
No edema	**0**
Edema muy ligero apenas perceptible	**1**
Edema ligero con bordes sobresalientes con elevación definida	**2**
Edema moderado, con una elevación máxima de 1 mm aproximadamente	**3**
Edema severo, elevación mayor de 1 mm extendiéndose más allá del sitio de aplicación	**4**
Calificación máxima posible de edema: 4	

Una vez obtenidas las lecturas de eritema, se promediaron las calificaciones de las evaluaciones: 1, 24, 48 y 72 horas, para las tres repeticiones (3 ratones) de cada una de las concentraciones de los tratamientos a evaluar y el vehículo. El mismo procedimiento se utiliza para evaluar el edema. A partir de estos promedios, calcular el índice de irritación primaria con la siguiente fórmula:

Índice de irritación primaria = promedio de eritema + promedio de edema

La interpretación de los resultados con base en el índice de irritación primaria se da con base a las siguientes categorías (Tabla 4).

Tabla 4. Índice de irritación primaria (Drize 1944; OECD guideline 2015)

INDICE DE IRRITACIÓN PRIMARIA	
No irritante	0-1
Ligeramente irritante	1.1-2
Moderadamente irritante	2.1-5
Irritante moderado a severo	5.1-6
Irritante severo	6.1-8

5.9. Evaluación de la actividad cicatrizante

Para estudiar las propiedades cicatrizantes de *A. stellulata* se utilizaron ratones *Mus musculus* de la cepa CD-1 et/et se realizó el protocolo con ligeras modificaciones de acuerdo con lo establecido por García-Bores y colaboradores (2020).

Los ratones fueron previamente anestesiados con isoflurorano para realizar una herida incisional de aproximadamente 17 mm. Los animales fueron divididos en dos partes: A) evaluaciones físicas (fuerza de tensión, velocidad y tiempo de reepitelización total de la herida) y B) análisis histológico (reepitelización; tamaño de la zona cicatrizada -TZC-, disposición y maduración del colágeno; tejido de granulación y determinación de la fase del proceso de cicatrización). Los animales se dividieron en los siguientes grupos (5 individuos/grupo): 1) grupo EMAS (aplicación del EMAS al 5% en base beeler); 2) grupo vehículo (aplicación de base beeler sin extracto); y 3) grupo Recoverón® (aplicación del medicamento estándar para heridas). Los diferentes tratamientos se aplicaron de manera tópica desde el primer día que se realizó la herida (día 0) hasta el cierre total (día 13).

5.9.1. Evaluaciones físicas del proceso de cicatrización de heridas

La longitud de la herida se midió diariamente para determinar la velocidad de cierre (mm/día) y el tiempo total de reepitelización (días). Al final los organismos fueron

sacrificados en cámara de CO_2. Posteriormente, se determinó la fuerza de tensión (g) necesaria para abrir la herida con un tensiómetro calibrado de 1000 g. Todos los procedimientos se realizaron de acuerdo con la NOM-062-ZOO-1999.

5.9.2. Análisis histológico de la piel en la zona cicatrizada

Los ratones para el análisis histológico fueron sacrificados bajo las mismas condiciones que los anteriores. Después, se tomaron muestras de piel en la zona de cicatrización de la herida y piel adyacente. Las muestras se fijaron en solución tampón de paraformaldehído PBS al 2% (p/v) (pH 7.2) durante 24 horas. Posteriormente, se deshidrataron con una secuencia de soluciones etanólicas (70, 80, 95, 96 y 100% v/v), se aclararon con dos cambios de xilol, para después ser incluidos en parafina. Las muestras se cortaron por la mitad para obtener las partes distal y media de la herida para su inclusión. Luego, se realizaron cortes de 3 µm de grosor, se tiñeron con Hematoxilina-Eosina esto permitió reconocer la estructura general del tejido, otras sesiones fueron reñidas con la tinción tricrómica de Masson que nos ayudó a observar la maduración del colágeno (García-Bores et al., 2020).

Los parámetros que se consideraron en el diagnóstico histológico fueron los siguientes: a) reepitelización, b) TZC (las medidas se obtuvieron con el software NIS-Elements BR - versión 3.2- proporcionado por Nikon Instruments), c) grosor, disposición y maduración colágeno, d) Tejido de granulación, e) la fase del proceso de cicatrización de las muestras (considerando las capas de la piel normal, glándulas sebáceas y folículos pilosos). Los resultados de la aplicación de EMAS (5%) se compararon con los ratones del grupo de referencia con aplicación del fármaco Recoveron® (C+) (acexamato de sodio en crema) y el grupo con aplicación del vehículo base Beeler (C-).

6. ANÁLISIS ESTADÍSTICOS

Los datos de la cuantificación de fenoles, la actividad antioxidante sobre DPPH, la inhibición de COX, la actividad cicatrizante por el método del tensiómetro y la velocidad de cierre de las heridas se sometieron a análisis de varianza de un factor (ANOVA $p > 0.05$). Las actividades que tuvieron diferencias significativas se les realizo una prueba de Tuckey's. Los datos de las medidas diarias de la herida a un análisis de regresión lineal para determinar la velocidad de cierre. Todos los análisis fueron realizados con el programa GraphPad Prism 9.

7. RESULTADOS

7.1. MATERIAL VEGETAL

7.1.1. EMAS y particiones

El rendimiento total del EMAS fue de 121.42 g (10.32%) a partir de 1176.5 g de planta seca de *A. stellulata*. Para poder evaluar las actividades biológicas se reservó una parte del EMAS (50.42 g). Al resto (71 g) se le realizó una partición con metanol/hexano de la cual se obtuvieron: la PMeOH, PHex, PH_2O y PDMSO su rendimiento en gramos y porcentaje está dado a partir de los 71 g del CRU que fue procesado, es decir, el 100% del extracto que se particionó. El mayor rendimiento lo tiene la PMeOH, seguida del PDMSO, la PHex y el PH_2O (Tabla 5).

Tabla 5. Rendimientos de la partición del EMAS de *A. stellulata*.

EMAS de *A. stellulata* (71g = 100%)			
PMeOH	**PHex**	**PH_2O**	**PDMSO**
31.46g (44.23%)	10.18g (14.31%)	4.89 g (6.87%)	13.33g (18.74%)

El rendimiento total del extracto crudo metanólico de *A. stellulata* fue de 121.42 g (10.32%) a partir de 1176.5 g de planta seca. CRU=crudo, PMeOH=partición metanólica, PHex=partición hexánica, PH_2O=partición miscible en agua y PDMSO=partición miscible en dimetilsullfóxido.

7.1.2. Aceites esenciales AEHT y AEI

El AETH tuvo un rendimiento de 0.83%, color amarillo y una densidad de 0.83 ± 0.0219 g/mL. Mientras, que el AEI tuvo un rendimiento de 1.0%, coloración amarilla y densidad de 0.67 ± 0.01549 g/mL. Debido al rendimiento los aceites esenciales solo fueron utilizados para evaluar su actividad antibacteriana y realizar el análisis de CG/MS.

7.2. Perfil fitoquímico de *A. stellulata*

7.2.1. *Screening* fitoquímico de los principales grupos de metabolitos de *A. stellulata*.

El EMAS, PMeOH y PH_2O tuvieron reacción positiva con cloruro férrico, la cual revela la presencia de fenoles. En cuanto a la prueba de Molish todos fueron positivos para compuestos glicósilados, teniendo una reacción más intensa en el extracto EMAS, la PMeOH y PDMSO; en menor proporción la PHex y PH_2O. La reacción con vainillina-ácido sulfúrico nos muestra que la PHex y la PDMSO tienen terpenos. En PHex, PH_2O y PDMSO cuenta con lactonas (sesquiterpénicas o cumarinas) de acuerdo con lo observado al agregar el reactivo de Baljet. El EMAS, PHex y PDMSO tienen metabolitos del tipo esteroide por la reacción con Liebermann-Buchard. Para la prueba de saponinas solo se observó la formación de espuma en EMAS. Mientras, ninguno tiene compuestos del tipo alcaloide ya que no se formaron precipitados con los reactivos de Dragendorff y Mayer (Tabla 6).

Tabla 5. Screening fitoquímico de metabolitos secundarios de *A. stellulata*.

METABOLITO	REACTIVO	*A. stellulata*				
		EMAS	PMeOH	PHex	PH_2O	PDMSO
Fenoles	$FeCl_3$	++	+++	-	++	-
Alcaloides	Mayer	-	-	-	-	-
	Dragendorff	-	-	-	-	-
Glicósidos	Molish	+++	+++	+	++	+++
Saponinas	Espuma	+	-	-	-	-
Terpenos	Vainillina	-	-	+++	+	+
Lactonas Sesquiterpénicas	Baljet	-	-	++	+	++
Esteroides	Liebermann-Buchard	+	-	++	-	+

* El signo (+) significa que el resultado es positivo, mayor reacción positiva (+++), media (++), baja (+) y reacción negativa (–). CRU=crudo, PMeOH=partición metanólica, PHex=partición hexánica, pH_2O=precipitado miscible en agua y pDMSO=precipitado miscible en dimetilsullfóxido.

7.2.2. Cuantificación de fenoles totales

La PMeOH tuvo la mayor concentración de fenoles totales (178.218 ± 0.015 mg EAG/ g de extracto), después la PDMSO (151.1 ± 0.031 mg de EAG /g de extracto) seguida del EMAS (133 ± 0.044 mg de EAG /g de extracto), el PH_2O (131.823 ± 0.019 mg de EAG/g de extracto) y finalmente la PHex (32.06 ± 0.001 mg de EAG/g de extracto). Hasta el momento no se ha informado la concentración de fenoles totales de *A. stellulata* u otro miembro del género *Asterohyptis*.

7.2.3. Análisis por HPLC-DAD-ESI/MS/MS del EMAS de *A. stellulata*

En el análisis HPLC-DAD-ESI-MS/MS se identificaron tres compuestos (Figura 2): 2-(3,4-dihidroxifenil)-5,7-dihidroxi-3-[2,3,4-trihidroxi-5 -(hidroximetil) ciclohexoxi] cromen-4-ona (I), quercetina-3-O-glicósido (II) y 2-O-(4-hidroxi-cinamoil), 4'-O-D-glicopiranósido (glicósido del ácido rosmarínico) (III).

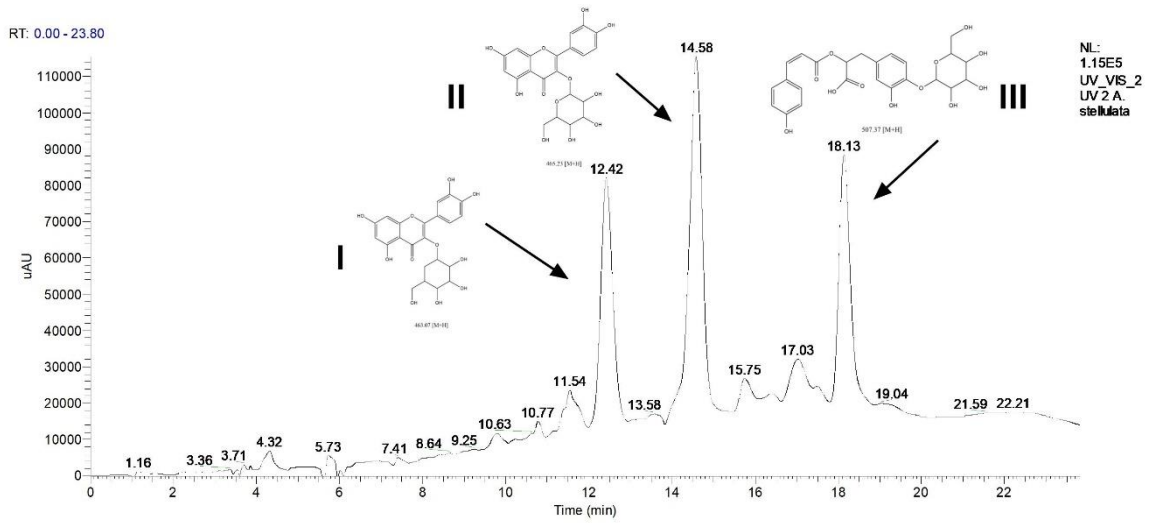

Figura 2. Cromatograma AsM. I. 2-(3,4-dihidroxifenil)-5,7-dihidroxi-3-[2,3,4-trihidroxi-5-(hidroximetil) ciclohexoxi] cromen-4-ona (463,07 m/z [M+H]), II. quercetina-3-O-glicósido (465,23 m/z [M+H]), III. 2-O-(4-hidroxi-cinamoil),4'-O-D-glicopiranósido (507.37 [M+H]). UV: 254 nm.

7.2.3.1. Análisis de masas de derivados de compuestos de quercetina

Se identificaron dos derivados de compuestos de quercetina (I y II) (Fig. 2. I y II). La aglicona quercetina presentó un fragmento de 303 m/z [M+H] (> 15%). Los iones presentes en los compuestos y en el estándar de quercetina son: 80, 156, 212, 280, 303 m/z [M+H].

El compuesto I (TR: 12.42 min) tiene un ión molecular de 463.07 m/z [M+H] (Fig. 3). La fragmentación del ciclitol presentó pérdida de cuatro grupos hidroxilo (68 u) que corresponden al fragmento 395.13 m/z [M+H]. Además, el ion de 303 m/z [M+H] es el de la aglicona, este mismo está presente en el estándar de quercetina, en los informes de espectros de PubChem y el estudio de Espinosa-González (et al., 2021). Posteriormente, hay pérdida de metinos y metilenos, respectivamente.

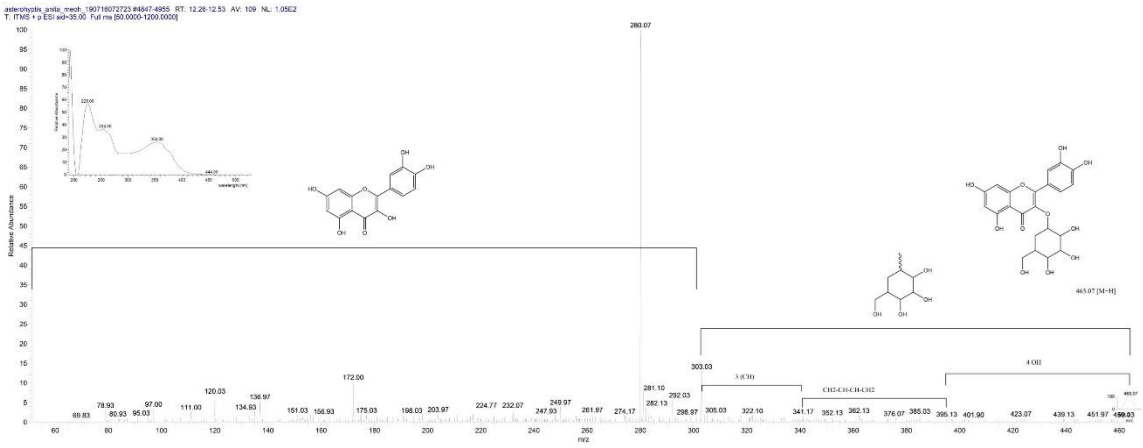

Figura 3. Patrón de fragmentación del compuesto I. 2-(3,4-dihidroxifenil)-5,7-dihidroxi-3-[2,3,4-trihidroxi-5-(hidroximetil) ciclohexoxi] cromen-4-ona (463,07 m/z [M+H]). La detección de masas se realizó en modo positivo [M+H].

El compuesto II (TR: 14.58 min) tiene un ion molecular es de 465.23 m/z [M+H] (Fig. 4). Región de glucósido, presenta pérdida de cuatro hidroxilos (68 u) que corresponden al fragmento de 397.17 m/z [M+H]. De igual manera presenta un heteroátomo de oxígeno en que corresponde al 329 m/z [M+H]. Luego, la fragmentación del enlace éter origina un fragmento de 303 m/z [M+H], correspondiente a la quercetina aglicona, este ion está representado en el patrón de fragmentación del estándar quercetina, al reporte de espectros en MassBank y al estudio de Espinosa-González y colaboradores (2021). Finalmente, se forma un fragmento de 153 m/z [M+H] por la retrorreacción Diels-Alder en el anillo C de la aglicona de quercetina.

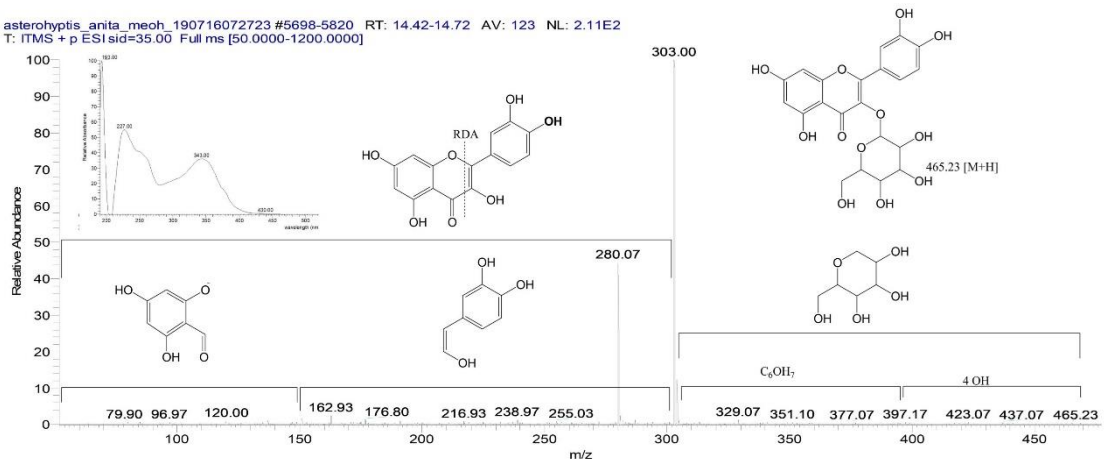

Figura 4. Patrón de fragmentación del compuesto II. Quercetina-3-O-glicósido (465,23 m/z [M+H]). La detección de masas se realizó en modo positivo [M+H].

7.2.3.2. Análisis de masas del glicósido del ácido rosmarínico

El compuesto III (TR: 18.13 min) tiene un ión molecular de 507.37 m/z [M+H] (Fig. 5). La región de glicopiranósido presenta pérdida de grupos hidroxilo (68 u) originando fragmento 439.17 m/z [M+H]. Posteriormente, por doble transposición de hidrógeno a oxígeno del enlace éter, se libera una molécula de agua (18 u), rompiendo el anillo del heterociclo, y liberando una cadena alifática de C_6H_5 (75 u), formando un fragmento de 344 m/z [M+H], que corresponde a aglicona. Esto, por una transposición de hidrógeno rompiendo el enlace éster originando un fragmento de 148.97 m/z [M+H]. Por otra parte, la aglicona pierde el grupo ácido, formando el fragmento más abundante 287 m/z [M+H]. Los siguientes fragmentos son pérdida de oxígeno (16 u) 271 m/z [M+H], formando orto-dihidroxibenceno 148.97 m/z [M+H], esta pérdida dos oxígenos (32 u) y un reordenamiento de McLafferty formando un grupo de propilio.

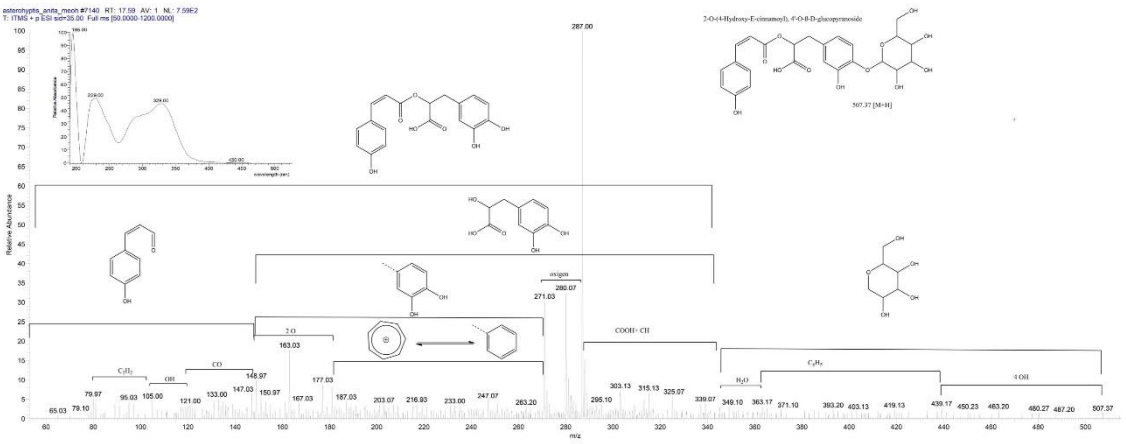

Figura 5. Patrón de fragmentación del compuesto III. 2-O-(4-hidroxi-cinamoil),4'-O-D-glicopiranósido (507.37 [M+H]. La detección de masas se realizó en modo positivo [M+H].

7.2.4. CG-EM del AEHT y AEI de *A. stellulata*.

7.2.4.1. CG-EM del AEHT

La caracterización química del AEHT por CG-EM permitió identificar 11 compuestos de los cuales 9.10% fueron monoterpenos y 90.90% sesquiterpenos. Los principales constituyentes son: óxido de cariofileno (20.48%) y α-bisabolol (13.60%) (Figura 6 y tabla 7).

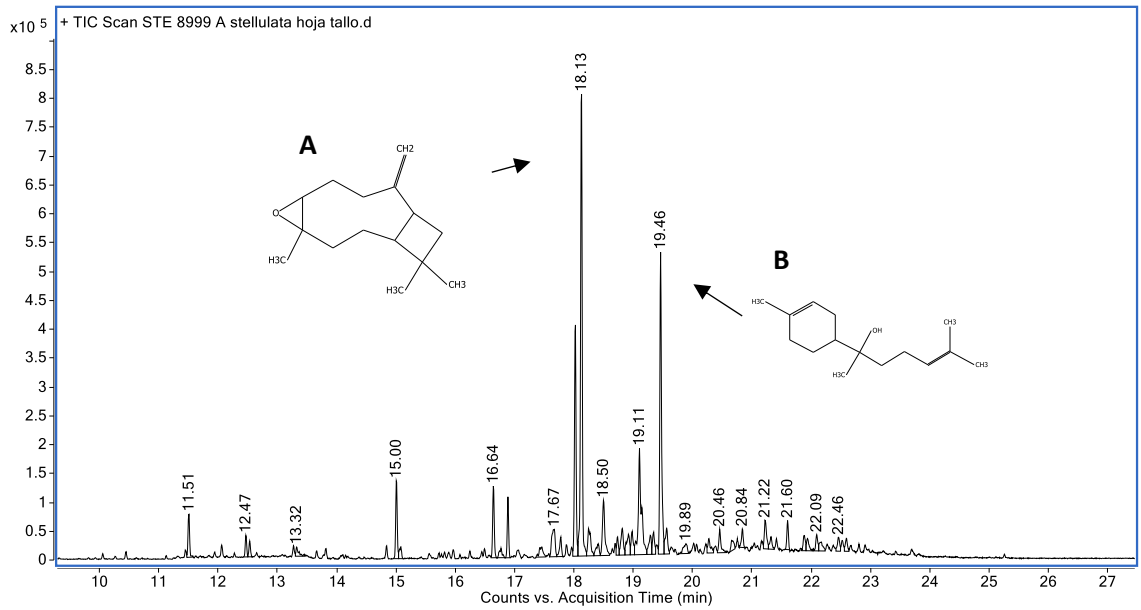

Figura 6. Cromatograma de CG-EM del AEHT de *A. stellulata*. A) óxido de cariofileno y B) α-bisabolol.

Tabla 7. Constituyentes del AEHT de *A. stelullata* identificados CG-EM.

TR	Molécula	%Área
11.51	criptona	1.83
12.47	3-isopropilbenzaldehido	0.83
13.32	cuminol	0.67
15.00	(-)-β-borboneno	3.13
16.64	naftaleno, decahidro-4a-metil-1-metileno-7-(1-metiletenil)-, [4aR-(4a.α.,7.α.,8a.β.)]-	
16.89	β-bisaboleno	2.13
18.03	β-spatulenol	9.72
18.13	óxido de cariofileno	20.48
18.50	(1R,3E,7E,11R)-1,5,5,8-Tetrametil-12-oxabiciclo [9.1.0] dodeca-3,7-dieno (derivado del humuleno)	3.55
19.11	2-furanmetanol, tetrahidro-α,α.,5-trimetil-5-(4-metil-3-ciclohexeno-1-il), [2S-[2-α,5-β(R*)]]- (derivado del bisabolol)	8.39
19.46	α-bisabolol	13.60
TOTAL		62.5%

Los constituyentes no identificados y con porcentajes menores a 0.5% fueron omitidos.TR: tiempo de retención, AEHT: aceite esencial de hoja tallo.

7.2.4.2. CG-EM del AEI

El análisis por CG-EM del AEI mostró una mayor diversidad de compuestos que respecto al de AETH. Se identificaron 22 de los cuales 13.16% fueron monoterpenos y 84.21% sesquiterpenos. Los componentes principales fueron el germacreno D (19%), cariofileno (11.96%), el α- bisabolol (9.62%), el α-cadinol (5.80%) y el óxido de cariofileno (5.42%) (Figura 7 y tabla 8).

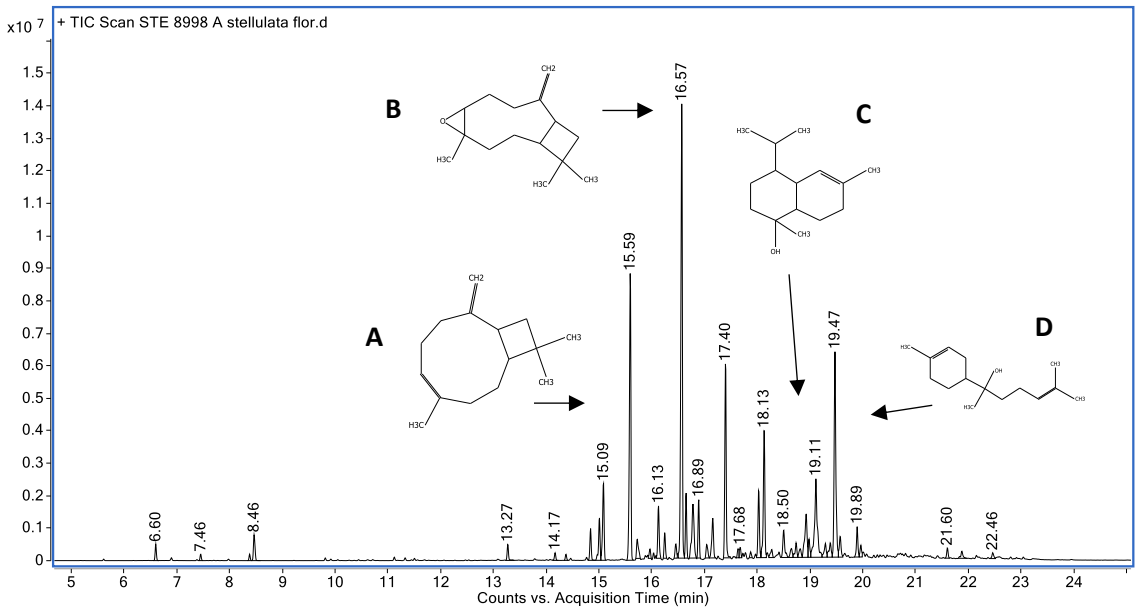

Figura 7. Cromatograma de CG-EM del aceite esencial de inflorescencias de *A. stellulata*. A) cariofileno (TR 15.59); B) Germacreno D (TR 16.47); C) α-cadinol (TR 19.11) y D) α-bisabolol (TR 19.47)

Tabla 8. Constituyentes del AEI de *A. stelullata* identificados por el análisis de CG-EM.

TR	Molécula	%Área
6.60	α-pineno	0.54
7.46	β-pineno	0.22
8.38	o-cimeno	0.21
8.46	D-limoneno	0.21
13.27	acetato de bornilo	1.10
14.17	elemeno isómero	0.29
14.38	α-cubebeno	0.22
14.84	α-copaeno	1.15
15.01	(-)-β-borboneno	1.75
15.59	cariofileno	11.96
16.13	humuleno	2.04
16.25	alloaromadendreno	0.92
16.46	δ-muuroleno	0.59
16.57	germacreno D	19.00
16.89	β-bisaboleno	2.01
17.40	ciclohexeno, 4-[(1E)-1,5-dimetil-1,4-hexadien-1-yl]-1-metil	7.44
18.13	óxido de cariofileno	5.42
18.93	tau-cadinol	2.79
19.11	α-cadinol	5.80
19.47	α-bisabolol	9.62
TOTAL		73.28%

Los constituyentes no identificados fueron omitidos.TR: tiempo de retención, AEI: aceite esencial de inflorescencia.

7.3. ACTIVIDAD ANTIBACTERIANA DE *A. stellulata*

7.3.1. Determinación cualitativa de la actividad antibacteriana

7.3.1.1. EMAS y particiones

La evaluación cualitativa de la actividad antibacteriana de EMAS, PMeOH, PHex, PH_2O y PDMSO de *A. stellulata* mostraron actividad sobre cinco cepas gram positivas (Tabla 9). El EMAS tuvo actividad en *S. aureus* FES-C y *S. epidermidis* FES-C. La PMeOH presento actividad sobre *S. aureus* ATCC29213, *S. aureus* CC y *P. aureginosa* ATCC27853. La PHex fue activa frente a *S. aureus* ATCC 29213, *S. aureus* CC, *S. aureus* FES-C y *S. epidermidis* ATCC 12228. La PDMSO tiene actividad en *S. aureus* ATCC29213, *S. aureus* CC, *S. aureus* FES-C y *S. epidermidis* FES-C. La PH_2O mostró actividad en *S. aureus* ATCC29213, *S. aureus* CC, *S. epidermidis* ATCC 12228 y *S. epidermidis* FES-C.

Todos los tratamientos fueron activos al menos en una cepa de *S. aureus* y *S. epidermidis* (Tabla x). Los mayores halos de inhibición los presentaron la PHex (7.68 ± 0.68), el PH_2O (7.46 ± 0.05) sobre *S. epidermidis* ATCC 12228 y la PMeOH (7.05 ± 0.20) sobre *S. aureus* ATCC 29213. El EMAS fue el que inhibió el menor número de microorganismos *S. aureus* FES-C y *S. epidermidis* FES-C. Estos resultados mostraron diferencias estadísticamente significativas ($p < 0.05$) en comparación con el cloranfenicol (control positivo).

Tabla 9. Actividad cualitativa antibacteriana del EMAS y particiones de *A. stellulata.*

Cepa	Tratamientos (mm)					Cloranfenicol (30 µg)
	EMAS	PMeOH	PHex	PDMSO	PH_2O	
S. aureus (+) 23 MR	NA	NA	NA	NA	NA	24.30 ± 0.44
S. aureus (+) ATCC 29213	NA	7.05 ± 0.20	6.13 ± 0.20	6.40 ± 0.57	5.98 ± 0.65	22.37 ± 0.98
S. aureus (+) CC	NA	6.16 ± 0.37	NA	5.16 ± 0.20	6.28 ± 0.45	20.42 ± 1.20
S. aureus (+) CUSI	NA	NA	NA	NA	NA	23.02 ± 0.92
S. aureus (+) FES-C	5.96 ± 0.06	NA	5.73 ± 0.25	5.83 ± 0.14	NA	23.13 ± 1.35
S. epidermidis (+) ATCC 12228	NA	NA	7.68 ± 0.68	NA	7.46 ± 0.05	23.95 ± 2.53
S. epidermidis (+) FES-C	6.66 ± 0.26	NA	NA	6.01 ± 0.55	6.04 ± 0.18	21.12 ± 1.69
M. luteos (+) ATCC 1024Oa	NA	NA	NA	NA	NA	13.75 ± 2.37
P. aureginosa (-) ATCC27853	NA	NA	NA	NA	NA	21.12 ± 1.69
E. coli (-) 82MR	NA	NA	NA	NA	NA	27.22 ± 1.91
E. aerogenes (-) ATCC 13048	NA	NA	NA	NA	NA	25.73 ± 1.62
S. typhi (-) ATCC 19430	NA	NA	NA	NA	NA	26.63 ± 1.89

Todos los tratamientos estuvieron a una concentración de 2mg por sensidisco. Los resultados se presentan como el promedio de los halos de inhibición (mm) de tres repeticiones ± Desviación estándar. Bacterias gram positivas (+), Bacterias gram negativas (-), No activo (NA), Cloranfenicol (C+), EMAS: extracto crudo metanólico de *A. stellulata*, PMeOH: partición metanólica, PHex: partición hexánica, PDMSO: partición miscible en dimetilsulfóxido, PH_2O: precipitado acuoso.

7.3.1.2. AEHT y AEI

El AETH tuvo actividad sobre las diferentes cepas de *S. aureus*. Mientras, el AEI tuvo actividad sobre la mayoría de las cepas de *S. aureus*, con excepción de *S. aureus* CC (Tabla 10).

Tabla 10. Actividad antibacteriana de los aceites esenciales de *A. stellulata*.

Cepa	Halos de inhibición (mm)		
	AEHT	AEI	Cloranfenicol (C+)
S. aureus 23 MR	6.00 ± 0.00	6.00 ± 0.00	22.00 ± 0.28
S. aureus CUSI	7.60 ± 0.06	7.60 ± 0.06	20.00 ± 0.00
S. aureus FES-C	6.00 ± 0.00	5.50 ± 0.00	22.50 ± 0.70
S. aureus ATCC29213	6.00 ± 0.00	6.30 ± 0.06	25.00 ± 0.00
S. aureus CC	6.10 ± 0.28	NA	20.00 ± 0.00

N.A. No activo. *Halos en mm. (Promedio ± desviación estándar). AEHT: aceite esencial de hojas y tallos, AEI: aceite esencial de inflorescencia.

7.3.2. Determinación cuantitativa de la actividad antibacteriana

Las cepas que tuvieron actividad en el protocolo de difusión en agar se les determinó su CMI y CBM (Tabla 11). La PH_2O tiene una CMI de 1 mg/mL y CBM de 2 mg/mL sobre *S. epidermidis* FES-C.

Las cepas *S. aureus* ATCC 29213 y *S. aureus* CC fueron ligeramente susceptibles a los diferentes extractos: PMeOH, PHex, PDMSO y PH_2O en la prueba cualitativa. Sin embargo, su CMI está por encima de la concentración más alta evaluada de 4 mg/mL. Por lo tanto, la CBM no se pudo determinar.

Tabla 11. Valores de CMI y CBM de *A. stellulata*.

Cepa	Tratamientos (mg/mL)									
	EMAS		PMeOH		PHex		PDMSO		PH_2O	
	CMI	CBM	CMI	CBM	CMI	CBM	CMI	CBM	CMI	CBM
S. aureus ATCC 29213	-	-	> 4	-	> 4	-	> 4	-	> 4	> 4
S. aureus CC	-	-	> 4	-	> 4	-	> 4	-	> 4	> 4
S. aureus FES-C	> 4	-	-	-	> 4	-	> 4	-	-	-
S. epidermidis ATCC 12228	-	-	-	-	> 4	-	-	-	**1**	**2**
S. epidermidis FES-C	> 4	-	-	-	-	-	> 4	-	> 4	> 4

Los resultados se presentan en mg/mL del promedio de las tres repeticiones. No fueron evaluadas por falta de actividad (-), EMAS: extracto crudo metanólico de *A. stellulata*, PMeOH: partición metanólica, PHex: partición hexánica, PDMSO: partición miscible en dimetilsulfóxido, PH_2O: precipitado acuoso.

7.4. Actividad antioxidante de *A. stellulata* sobre el radical DPPH

La actividad antioxidante de *A. stellulata* fue determinada por el método de reducción del DPPH se evaluaron EMAS, PMeOH, PHex, PH_2O y PDMSO.

La PMeOH presentó la mayor actividad antioxidante (CA_{50} = 102.79 ± 3.15 µg/mL), seguido por el EMAS (CA_{50} = 112.84 ± 3.71 µg/mL), después la PDMSO (CA_{50} = 122.65 ± 10.98 µg/mL), la PH_2O (CA_{50} = 137.79 ± 6.05 µg/mL) y por último la PHex (CA_{50} = 1496.53 ± 30.79 µg/mL). El estándar quercetina tuvo la mayor actividad antioxidante (CA_{50} de 5.01 ± 0.1

µg/mL). El análisis de ANOVA indica que existen diferencias significativas ($p < 0.05$ o p=1.79e-16). La prueba de Tuckey´s muestra que estas diferencias son entre el estándar y EMAS, PMeOH, PHex, PH_2O y PDMSO. La PHex también mostro diferencia con el resto de las sustancias evaluados como se puede observar en la Tabla 12.

Tabla 12. Actividad antioxidante de *A. stellulata* sobre el radical DPPH.

DPPH (CA_{50} µg/mL)					
Quercetina	**EMAS**	**PMeOH**	**PHex**	**PH_2O**	**PDMSO**
5.01 ± 0.1*****	112.84 ± 3.71	102.79 ± 3.15	1496.53 ± 30.79†	137.79 ± 6.05	122.65 ± 10.98

Cada valor corresponde al promedio de tres experimentos diferentes ± valores de desviación estándar. CA_{50} = concentración antioxidante media. Diferencia significativa de quercetina (*) ($p < 0.05$ o p=1.79e-16) con respecto al resto de las sustancias. Diferencia significativa de PHex (†) ($p < 0.05$ o p=1.79e-16) con respecto al resto de las sustancias.

El estándar quercetina tuvo el valor de CA_{50} menor. Pero, se debe considerar que esto es debido a que se trata de un compuesto puro con alta actividad antioxidante, en comparación con EMAS, PMeOH, PHex, PH_2O y PDMSO que aún son una mezcla compleja de compuestos que pueden tener o no dicha actividad. Mientras, que las diferencias entre éstos y la PHex es por su baja capacidad antioxidante CA_{50} de 1496.53 ± 30.79 µg/mL; lo anterior podría ser porque dicha actividad se le atribuye principalmente a lo compuestos fenólicos que se encuentran presentes en EMAS, PMeOH y PH_2O.

7.5. Actividad antiinflamatoria de EMAS: ensayo *in vitro* de COX-2

El EMAS tiene una CI_{50}= 28 µg/mL, el Celecoxib CI_{50}= 22.35 µM y las particiones tuvieron diferentes porcentajes de inhibición a la concentración de 100 µg/mL (Tabla 13). Hasta el momento de la búsqueda, no se han encontrado investigaciones sobre la inhibición de COX-2 con *Asterohyptis* o *Hyptis*.

Tabla 13. Inhibición *in vitro* de COX-2 por *A. stellulata*.

TRATAMIENTO	% DE INHIBICIÓN (100 µg/mL)	CI_{50}
EMAS	94.69	28 **µg/mL**
PMeOH	82.40	−
PHex	96.92	−
PDMSO	88.330	−
PH_2O	92.1390	−
Celecoxib	−	44.35 **µM**

COX-2: ciclooxigenasa 2, CI_{50}: Concentración inhibitoria media, EMAS: extracto metanólico de *A. stellulata*, PMeOH: partición metanólica, PHex: partición hexánica, PDMS: Partición dimetilsulfóxido, PH_2O: partición acuosa, - = dato sin evaluar.

7.7. Formulación de la emulsión y medida de estabilidad

Las formulaciones desarrolladas no mostraron cambios visibles durante los 6 meses de observación. Después, de la centrifugación se mantuvo la estabilidad de la formulación con un IC = 100 y no hubo cambios en el aspecto visual de la formulación. El escaneo UV (200-400 nm) de la base demulsificada y EMAS a la misma concentración no mostró cambios e el patrón de absorción.

7.8. Prueba de irritabilidad en ratón CD-1 et/et de EMAE

Las observaciones de la piel de ratón expuestas a la aplicación de las diferentes concentraciones (1, 5 y 10%) del EMAS y las particiones de *A. stellulata* no mostraron características de edema o eritema en las observaciones a 1, 24, 48 y 72 horas postratamiento (Tabla 14). Los resultados nos permiten inferir que la aplicación tópica de la crema con diferentes concentraciones no induce irritación en la piel de ratón CD-1 et/et.

Tabla 14. Evaluaciones obtenidas en la prueba de irritabilidad dérmica primaria de *A. stellulata*.

Tx´s		Tiempo (h)			
		1	24	48	72
EMAS	1%	0	0	0	0
	5%	0	0	0	0
	10%	0	0	0	0
PMeOH	1%	0	0	0	0
	5%	0	0	0	0
	10%	0	0	0	0
PHex	1%	0	0	0	0
	5%	0	0	0	0
	10%	0	0	0	0
PDMSO	1%	0	0	0	0
	5%	0	0	0	0
	10%	0	0	0	0
PH_2O	1%	0	0	0	0
	5%	0	0	0	0
	10%	0	0	0	0
Vehículo	0%	0	0	0	0

TX's: tratamientos, EMAS: extracto crudo metanólico de *A. stellulata*, PMeOH: partición metanólica, PHex: partición hexánica, PDMSO: partición dimetilsulfóxido, PH_2O: partición acuosa.

Es importante resaltar que el cambio de la tonalidad de la piel que se observaron después de 1 hora de aplicación es debido al contacto con las formulaciones, ya que a pesar de que se limpió el área con agua estéril y gasas, la piel conservó parte de los compuestos de la planta (Tabla 15).

Tabla 15. Imágenes del dorso de los ratones a los que se les realizó la prueba de irritabilidad dérmica primaria de la aplicación tópica de *A. stellulata.*

H	TX´s EMAS	PMeOH	PHex	PDMSO	PH_2O
1	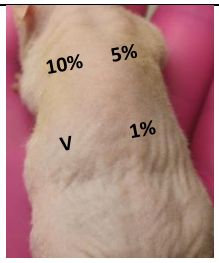		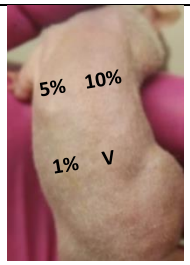	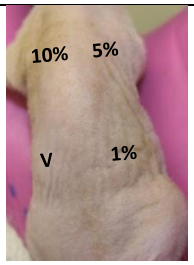	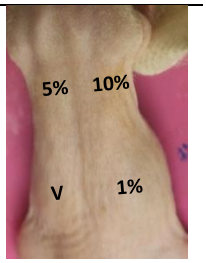
24					
48					
72					

En las imágenes de la primera observación (1 hora) del ratón elegido para las fotos, se muestra el cuadrante de la aplicación de los tratamientos 1%, 5%, 10% y el vehículo (V). Las imágenes de las revisiones posteriores son del mismo individuo, por lo cual, ya no se dibujó el cuadrante nuevamente. H: horas, TX's: tratamientos, EMAS: extracto crudo metanólico de *A. stellulata*, PMeOH: partición metanólica, PHex: partición hexánica, PDMSO: partición miscible en dimetilsulfóxido, PH_2O: precipitado acuoso.

Estos resultados no permitirán continuar con los protocolos de actividad cicatrizante y discernir la concentración idónea para evaluar dicha actividad. Dados los resultados podríamos ocupar incluso la dosis máxima. Sin embargo, se ha reportado que las dosis altas no necesariamente son mejores, incluso pueden llegar a ser citotóxicas y disminuir el proceso de cicatrización (Chiocchio et al., 2019). Por lo cual, se decidió utilizar la concentración intermedia, es decir, 5% del EMAS para evaluar la actividad cicatrizante.

7.9. Evaluación de la actividad cicatrizante

7.9.1. Evaluaciones físicas del proceso de cicatrización de heridas

La cicatrización de heridas se evaluó con el EMAS a una concentración de 5% (Tabla 16). El grupo con la aplicación de *A. stellulata* tuvo resistencia a la fuerza de tensión y velocidad de cierre de la herida, similar al grupo Recoverón® y mayor que el grupo con aplicación del vehículo. Todos los grupos tuvieron el cierre total de la herida al día 13. La velocidad del cierre de la herida fue similar entre los grupos tratados con *A. stellulata* (1.479 ± 0.043) y el Recoverón® (1.509 ± 0.040), las heridas tratadas con el vehículo-base Beeler- tuvieron la menor velocidad de cierre (1.330 ± 0.039).

Tabla 16. Resumen de los resultados de las evaluaciones físicas con los diferentes tratamientos: *A. stellulata*, Recoverón® y Vehículo. Aplicación tópica en ratón CD-1 et/et.

Grupos	Fuerza de tensión (g)	Cierre total de la herida (días)	Velocidad del cierre de la herida (mm/día)
A. stellulata	960 ± 89.44	13	1.479 ± 0.043
Recoverón®	940 ± 89.44	13	1.509 ± 0.040
Vehículo	774 ± 217.67	13	1.330 ± 0.039

7.9.2. Análisis histológico de la piel en la zona cicatrizada

Las secciones de piel donde se encuentra la zona cicatrizada se tiñeron con Hematoxilina-Eosina para reconocer la estructura general del tejido, observar la formación de neodermis -reepitelización-, definir el tamaño de la zona cicatrizada -TZC- (la zona en la que se hizo la herida y se recuperó con la aplicación de los distintos tratamientos), la revisión del tejido de granulación nos permite reconocer grupos celulares presentes en la zona, infiltrado inflamatorio, angiogénesis e incluso procesos de regeneración por la presencia de glándulas y folículos. Mientras, la tinción tricrómica de Masson se utilizó para observar el grosor, disposición y maduración del colágeno en la zona cicatrizada.

7.9.2.1. Reepitelización y tamaño de la zona cicatrizada

Las secciones de la zona cicatrizada con la aplicación de los diferentes tratamientos mostraron diferencias en la reepitelización (Figura 8). Los ratones tratados con *A. stellulata* y Recoverón® muestran una epidermis similar a la piel normal (Fig. 8. A, B, C y D), mientras que el grupo vehículo (Fig. 8. E y F) muestra una epidermis visiblemente más delgada.

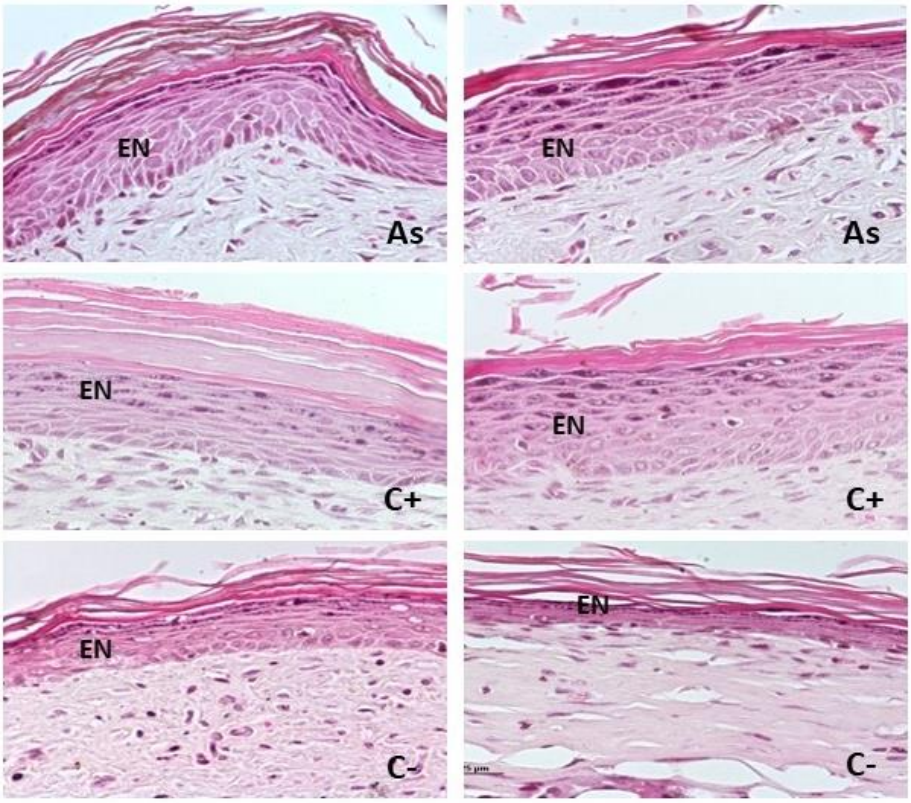

Fig. 8. Imágenes representativas del análisis histológico de secciones de la epidermis de neoformación teñidas con H&E en la herida cicatrizada (centro) con los diferentes tratamientos (400x). A) y B) Tratamiento con *A. stellulata* (As); C) y D) Tratamiento con Recoverón® (C+); E) y F) Tratamiento con vehículo (C-). EN: epidermis de neoformación.

Asimismo, el TZC fue menor en el grupo *A. stellulata* 473.82 ± 166.72 µm (Fig. 9 A y B), seguido por el grupo Recoverón® 1406.85 ± 1059.92 µm (Fig. 9 C y D), y finalmente el grupo vehículo 1736.08 ± 854.64 µm (Fig. 9 E y F). La reepitelización y la contracción de la herida (reducción del tejido de granulación -zona cicatrizada- para resolver la separación producida en los bordes de la herida) son características de la fase proliferativa (Low et al.,

2021). Por lo tanto, *A. stellulata* promueve el progreso de la fase proliferativa a la remodelación.

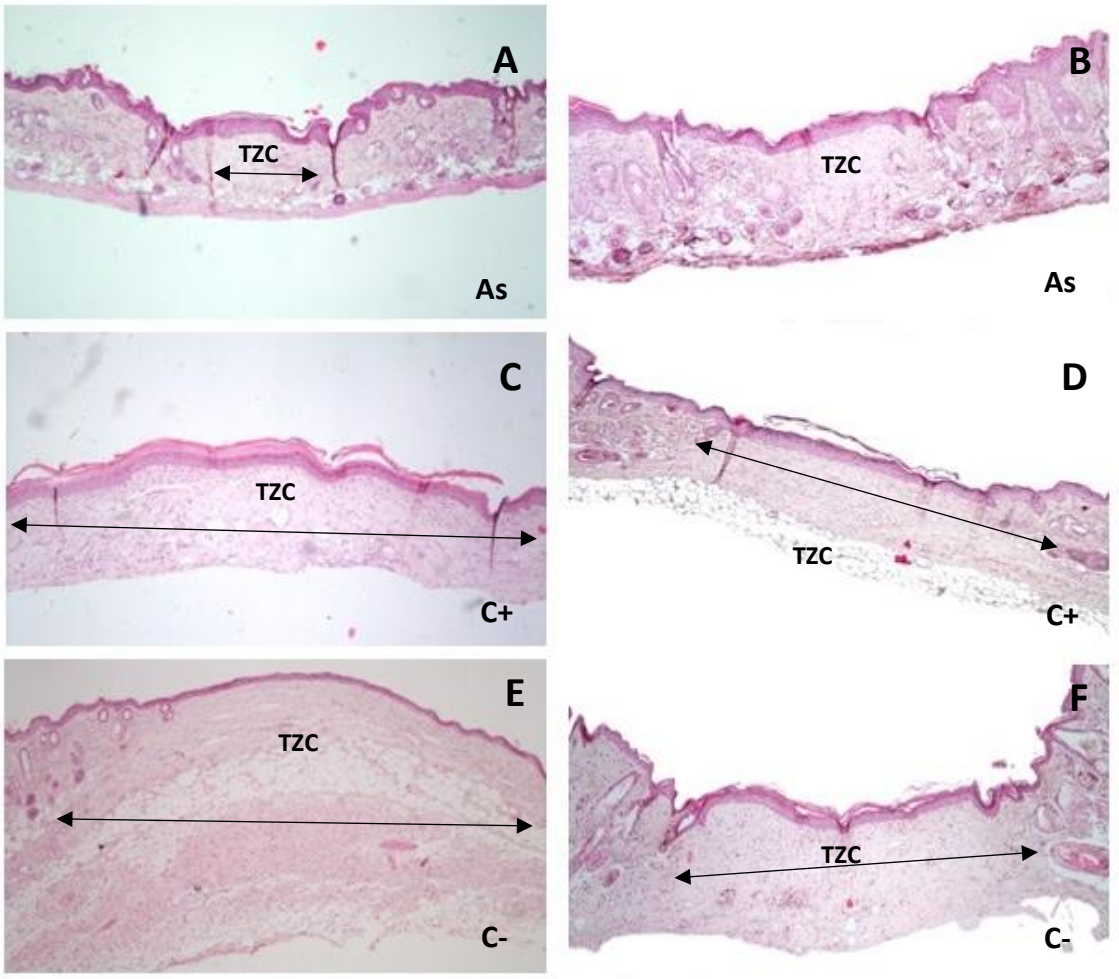

Fig. 9. Imágenes representativas del análisis histológico de secciones zona cicatrizada teñidas con H&E en la herida cicatrizada (centro) con los diferentes tratamientos (400x). A) y B) Tratamiento con *A. stellulata* (As); C) y D) Tratamiento con Recoverón® (C+); E) y F) Tratamiento con vehículo (C-). TZC: tamaño de la zona cicatrizada.

7.9.2.2. Grosor, disposición y maduración del colágeno

Al grupo de ratones que se les aplicó de manera tópica *A. stellulata* mostró mejor desempeño en la distribución y maduración del colágeno (Fig. 10 A y B), formando fibras densas y organizadas, similar al grupo Recoverón® (Fig. 10 C y D); de forma contraria, la piel tratada con el vehículo tuvo menor maduración y organización del colágeno (Fig. 10 E y F). La matriz extracelular como componente principal tiene al colágeno, es la proteína más abundante en el tejido de la piel, y la proporción adecuada es esencial durante la

formación del tejido conectivo y el proceso de cicatrización de heridas (Pérez-Contreras et al., 2022). Además, como se mencionó anteriormente, en la fase de remodelación es fundamental el cambio de colágeno tipo III a colágeno tipo I (Wang et al., 2018). Estos resultados están relacionados con la resistencia a la tracción reportada para los diferentes tratamientos, lo que confirma que la aplicación tópica de *A. stellulata* aceleró el progreso a la fase de remodelación.

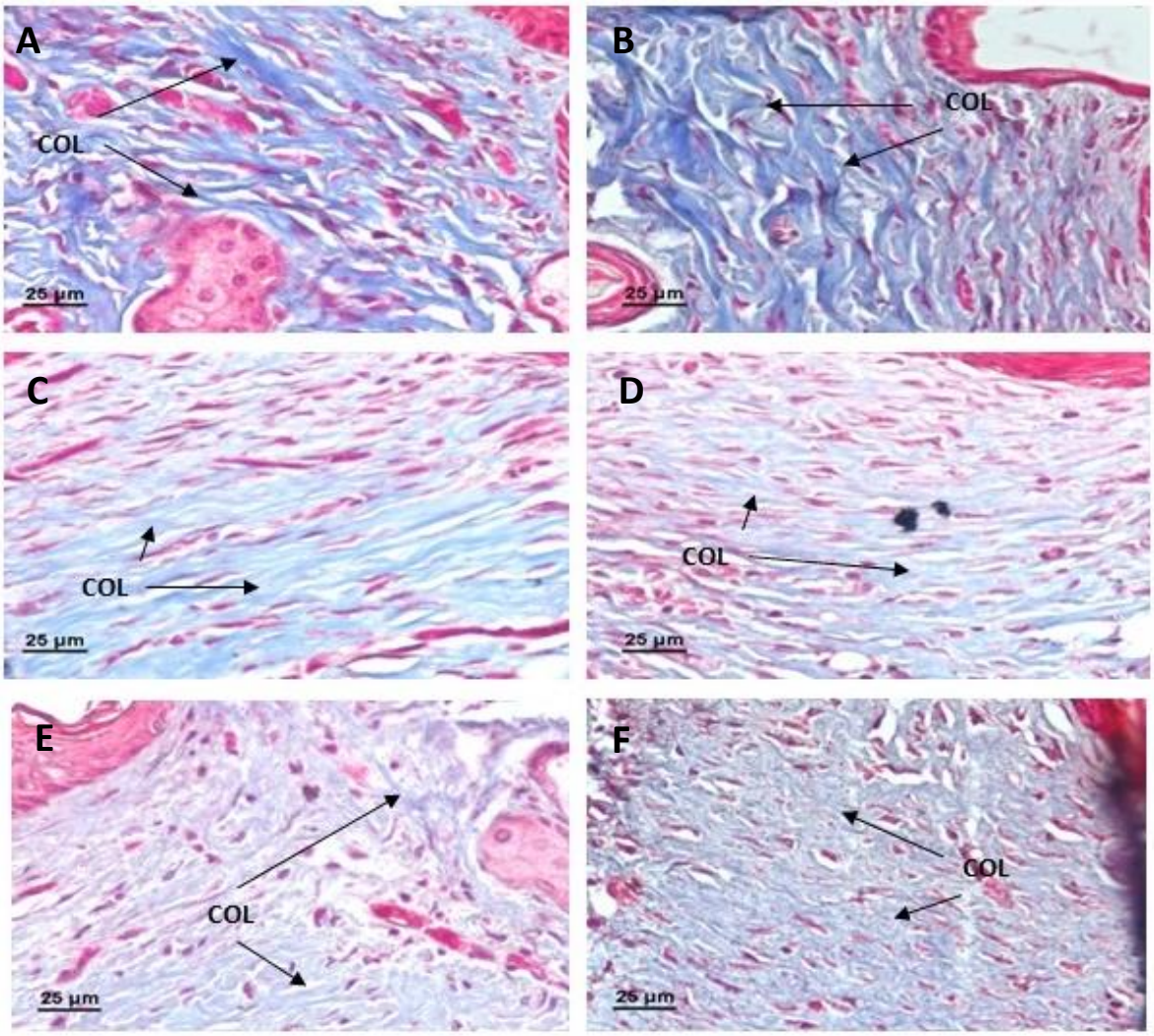

Fig. 10. Imágenes representativas del análisis histológico del colágeno teñido con Masson's en los costados de la zona cicatrizada con los diferentes tratamientos (400x). A) y B) Tratamiento con *A. stellulata* (As); C) y D) Tratamiento con Recoverón® (C+); E) y F) Tratamiento con vehículo (C-). COL: colágeno.

7.9.2.3. Tejido de granulación

El estudio histológico del tejido de granulación -zona cicatrizada- (Figura 11) es consistente con los resultados anteriores. Las secciones del grupo *A. stellulata* presentan menor número de fibroblastos/miofibroblastos, abundantes vasos sanguíneos y no se observó infiltrado inflamatorio (Fig. 11 A y B). Por su parte, el grupo Recoverón® presenta profusión de fibroblastos reactivos, pocos vasos sanguíneos y nula presencia de infiltrado inflamatorio (Fig. 11 C y D). Finalmente, en el grupo vehículo tiene un número intermedio de fibroblastos, pocos vasos sanguíneos y neutrófilos (Fig. 11 E y F).

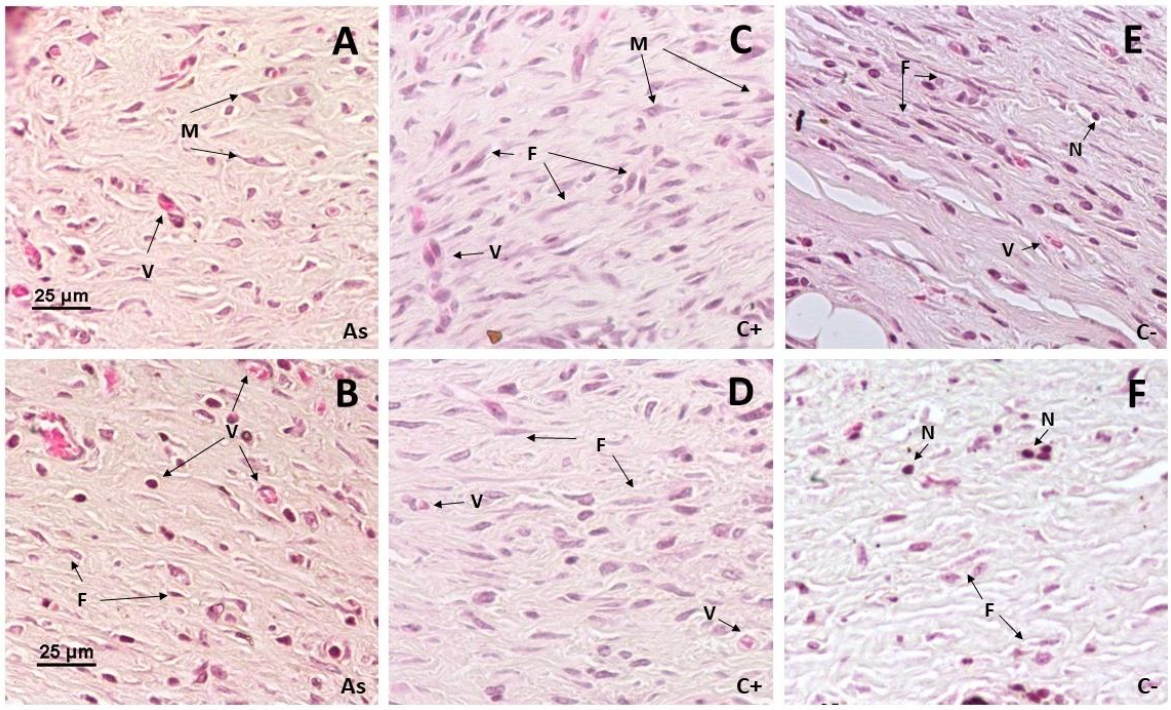

Fig. 11. Imágenes representativas del análisis histológico de secciones de tejido de granulación teñidas con H&E en la herida cicatrizada (centro) con los diferentes tratamientos (400x). A) y B) Tratamiento con *A. stellulata* (As); C) y D) Tratamiento con Recoverón® (C+); E) y F) Tratamiento con vehículo (C-). F: fibroblasto, M: miofibroblasto, V: vaso sanguíneo, N: neutrófilo.

El conjunto de resultados de las evaluaciones físicas (Tabla 15) y los resultados del análisis histológico, nos permiten determinar la fase de cicatrización y/o la regeneración de las secciones de piel a las que se les aplicaron los diferentes tratamientos (Tabla 17).

Tabla 17. Resumen de los resultados del análisis histológico de los tejidos con tratamientos: *A. stellulata*, Recoverón® y Vehículo. Aplicación tópica en ratón CD-1 et/et.

Grupos	TZC (µm)	COL	E	D	TG				Fases (transición)
					F	M	N	V	
A. stellulata	437.82 ± 166.72	**+++**	R	R	**+**	**++**	**-**	**+++**	Remodelación/Regeneración
Recoverón® (C+)	1406.85 ± 1059.92	**+++**	R	NR	**+++**	**+**	**-**	**++**	Proliferación/Remodelación
Vehículo (C-)	1736.08 ± 854.64	**++**	R	NR	**++**	**-**	**+**	**+**	Inflamación/Proliferación

TZC: tamaño de la zona cicatrizada, COL: colágeno, E: epidermis, D: dermis, TG: tejido de granulación, R: regeneración, NR: sin regeneración, F: fibroblastos, M: miofibroblastos, N: neutrófilos, V: vasos sanguíneos, -: ausentes, +: pocos, ++: regulares, +++: muchos.

El grupo vehículo (C-)se encuentra en la transición de la inflamación a la proliferación (Tabla 17), por la presencia de neutrófilos, pocos fibroblastos, colágeno inmaduro, menor resistencia a la tensión, tamaño mayor en la zona cicatrizada, permanencia del tejido de granulación y sin formación de las capas características de la piel normal (Fig. 12 A y B).

El grupo Recoverón® se encuentra entre la proliferación y la remodelación (Tabla 17), tienen abundantes fibroblastos, pocos miofibroblastos, nuevos vasos sanguíneos, ausencia de neutrófilos, colágeno maduro y mejor resistencia a la tensión, tamaño mayor en la zona cicatrizada, permanencia del tejido de granulación y sin formación de las capas características de la piel normal (Fig. 12 A y C).

Los ratones tratados con *A. stellulata* (Tabla 17) presentan miofibroblastos, abundantes vasos sanguíneos, ausencia de neutrófilos, epidermis nueva similar a la normal, colágeno maduro, menor tamaño de la zona cicatrizada (contracción de la herida) y disminución del tejido de granulación (Fig. 12 A y D). Esto implica que están en fase de remodelación, incluso es posible un proceso de regeneración, ya que la zona cicatrizada es pequeña y presenta capas características de la piel normal -músculo, hipodermis, dermis-, así como folículos pilosos y glándulas sebáceas (Figura 12 D, E y F).

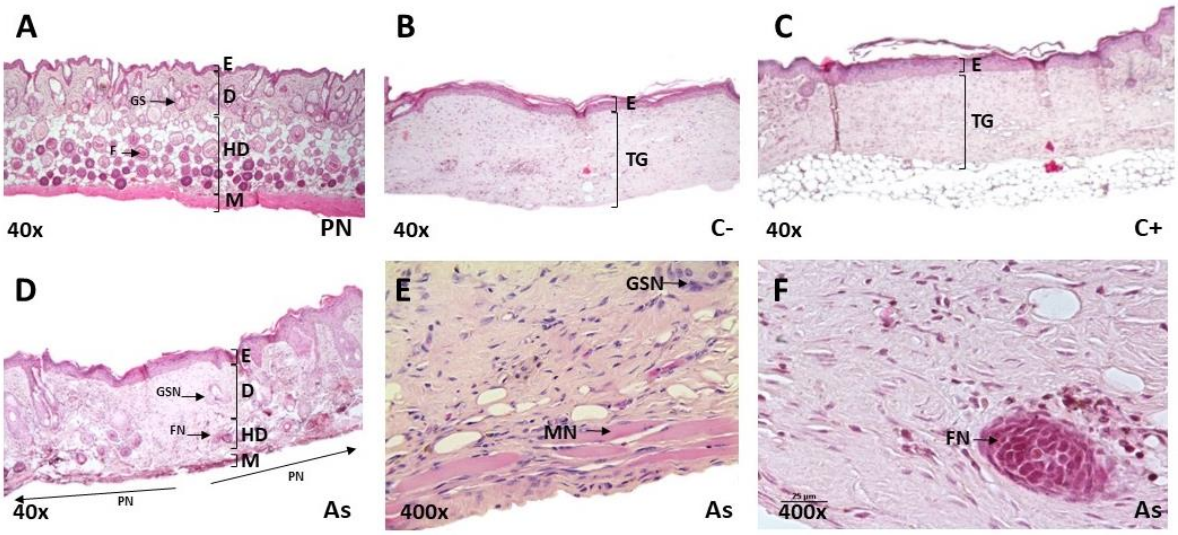

Fig. 12. Comparación de piel normal y los tejidos de ratones CD-1 et/et con la aplicación de los diferentes tratamientos. A) Piel normal de CD-1 et/et (40x); B) Zona cicatrizada del grupo vehículo; C) Zona cicatrizada del grupo Recoveron®; D) Zona cicatrizada/regenerada del grupo *A. stellulata* (40X); E) Regeneración de músculo y glándula sebácea de neoformación del grupo *A. stellulata* (400x); D) Folículo de neoformación del grupo *A. stellulata* (400x). As: *A. stellulata,* C-: grupo vehículo, C+: grupo Recoverón®, PN: piel normal, E: epidermis, D: dermis, HD: hipodermis, M: músculo, GS: glándula sebácea, F: folículo, GSN; glándula sebácea de neoformación, NF: folículo de neoformación, NM: músculo de neoformación.

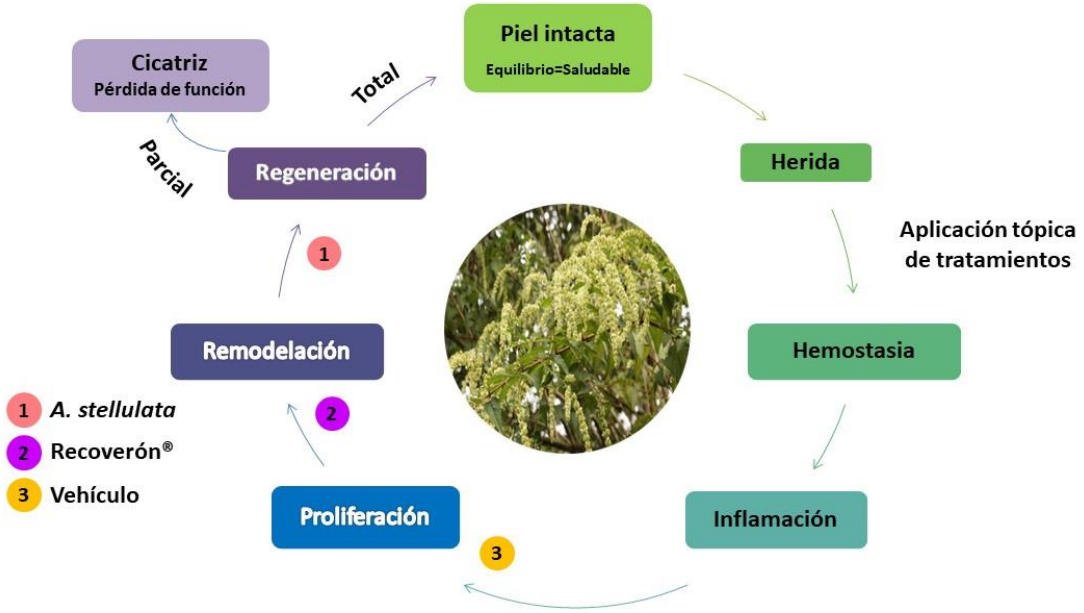

Fig. 13. Resumen de la actividad cicatrizante de los diferentes tratamientos, haciendo énfasis en la fase en la que se encontraban los tejidos analizados con la aplicación de los distintos tratamientos.

8. DISCUSIÓN

8.1. Perfil fitoquímico

8.1.1. Aceites esenciales

El AEHT tiene como principales constituyentes el óxido de cariofileno (20.48%) y α-bisabolol (13.60%). el óxido de cariofileno se encuentra como constituyente principal en especies del género *Hyptis* como: *H. mutabilis* (Bridi et al., 2020), *H. atrorubens* (Kerdudo et al., 2016) e *H. pectinata* (Nascimento et al., 2008). Además, el óxido de cariofileno cuenta con actividad analgésica y antiinflamatoria, mostrando actividad similar a la aspirina (Chavan et al., 2010). El β- cariofileno aplicado en forma de hidrogel mejoró el cierre de la herida en modelo murino gracias a su efecto antinflamatorio (Parisotto-Peterle et al., 2020). Además, cuanta con actividad antibacterial sobre *P. aeruginosa*, *S. aureus* y *E. coli*, también mejora la acción del antibiótico norfloxacina, gentamicina y eritromicina cuando se utilizan en combinación (Santos et al., 2021).

El α-bisabolol es un sesquiterpeno que no ha sido reportado para *Asterohyptis* o *Hyptis*, hasta el momento. Sin embargo, su presencia en el aceite esencial es de suma importancia ya que tiene diversas actividades farmacológicas como antiinflamatorio, antibacteriano, calmante e hidratante de la piel (Kim et al., 2021). Siento, la mayoría de ellas importantes en el proceso de cicatrización. El α-bisabolol tiene actividad antiinflamatoria ya que se sabe que puede actuar regulando de manera negativa la expresión de los genes de iNOS y COX-2 mediante la inhibición de la señalización de NF-kB (Kim et al., 2011). También, se ha relacionado que su presencia en el aceite esencial de Manzanilla (*Chamomille* sp.) promueve la cicatrización de heridas, reduciendo la inflamación a través de la disminución de los niveles de IL-1β (Gad et al., 2019), lo cual podría relacionarse a la regulación negativa sobre la expresión genética de COX-2.

El AEI tiene como componentes principales el germacreno D (19%), cariofileno (11.96%), el α- bisabolol (9.62%) y el α-cadinol (5.80%). El óxido de cariofileno. el germacreno D se ha identificado en los aceites esenciales de *H. mutabilis* (Silva et al., 2013), *H. lanceolata* (Tchoumbougnang et al., 2005), *H. monticola* (Perera et al., 2017) y *H. suaveolens* (Tesch et al., 2015). El α-cadinol ha sido identificado en especies como *H. villosa* (Franco et al., 2011) y en *H. fructicosa* (Silva et al., 2013). El α-cadinol cuenta con actividad antiinflamatoria sobre macrófagos RAW 264.7 activados por lipopolisacáridos (Tung et al., 2010). Además, se ha comprobado que tiene alta afinidad con COX-2, similar al ligando estándar rofecoxib, por lo cual su actividad antiinflamatoria tal vez sea a través de la inhibición de esta enzima (Omolara et al., 2020).

Debido al bajo rendimiento de los aceites esenciales solo se evaluó la actividad antibacteriana. Sin embargo, la mezcla de compuestos presentes en los aceites pareciera tener potencial en la curación de heridas.

8.1.2. EMAS y particiones

El *screanning* farmacológico nos indica que *A. stellulata* cuenta con compuestos del tipo fenol y terpeno principalmente, así como ausencia de alcaloides, lo cual coincide con los perfiles fitoquímicos del género *Hyptis* ya que hasta el momento de la búsqueda no se han descrito compuestos de este tipo. Mientras, en sus PHex, PH_2O y PDMSO dio reacción positiva al reactivo de Baljet que permite identificar compuestos con lactonas insaturadas. El análisis fitoquímico de *A. mociniana* (Sinonimia *Hyptis mociniana*) indica que cuenta con derivados del tipo pectinolido -α-pironas- (Espinosa-González et al., 2021). Las α-pironas han sido identificadas en especies del género *Hyptis* (Almtorp et al., 1991; Pereda–Miranda et al., 2001; Boalino et al 2003; Costa et al., 2014). Por lo cual es probable que estas sustancias estén presentes en *A. stellulata*.

A. stellulata tuvo una cuantificación de fenoles totales entre 32.06 a 178.218 mg de EAG/g de extracto, en comparación con especies del género *Hyptis* (≥ 300 mg de EAG/g extracto), tiene una menor concentración de fenoles totales. Por ejemplo, *Hyptis crenata* Pohl ex Benth en su extracto metanólico tenía 373.0 ± mg de EAG/g de extracto (Rebelo et al., 2009), *Hyptis fructicosa* en su extracto crudo hidroetanólico tuvo 360.51 ± mg de EAG/g de extracto (de Lima et al., 2013) and *Hyptis suaveolens* en su extracto etanólico presento 336.496 ± 0.005 mg de EAG/g de extracto y el acuoso con 253.68 ± 0.03 mg de EAG/g de extracto (Sanchez-Aguirre et al., 2020).

Los compuestos fenólicos (ácidos fenólicos, flavonoides, taninos, lignanos, estilbenos, etc.) son ampliamente conocidos por sus actividades antioxidantes, antiinflamatorias (Khan et al., 2019) y antimicrobianas (Ivanov et al., 2022). Además, el extracto rico en fenoles de *Ipomoea pes-capre* mejoró el proceso de cicatrización de heridas (Xavier-Santos et al., 2022). Por lo tanto, la presencia de estos compuestos en el extracto podría estar relacionado con las actividades biológicas de *A. stellulata*. Además, se ha considerado que las preparaciones herbales que mejoran la cicatrización, es porque cuentan con propiedades antioxidantes, antiinflamatorias y antimicrobianas (Kumar et al., 2019).

El análisis por HPLC de EMAS permitió la dilucidación de compuestos del tipo fenólico: derivados de quercetina y ácido rosmarínico. Isoquercitrosido, boehmerina y ácido rosmarínico glicosilados fueron identificados en *A. mociniana* (Espinosa-González et al., 2021). El ácido rosmarínico se encuentra ampliamente distribuido en especies de *Hyptis* como: *H. capitata* (Almtorp et al., 1991), *H. verticillata* (Kuhn et al., 1993), *H. pectinata* (Falcao et al., 2016), *H. campestris*, *H. radicans*, *H. meridionalis*, *H. comaroides*, *H. lacutris*, *H. lappulacea* y *H. multibracteata* (do Santos et al., 2018); *H. suaveolens*, *H. pectinata*, *H. marrubioides* (Vilasboas-Campos et al., 2021). Así como los glicósidos de quercetina que han sido identificados en *H. fasciculata* -isoquercetina- (Silva et al., 2009), *H. atrorubens* -

hiperosido e isoquercetina- (Abedi et al., 2013), *H. suaveolens* -rutina, quercetina e isoquercetina (Bezerra et al., 2017; Vilasboas-Campos et al., 2021), *H. pectinata* y H. *marrubioides* -isoquercetina (Vilasboas-Campos et al., 2021).

Los compuestos identificados en *A. stellulata* cuentan con diferentes actividades relacionadas con la curación de heridas como se comentará más adelante.

8.2. Actividad antibacteriana

La incidencia de enfermedades infecciosas nuevas y recurrentes; la resistencia a los antibióticos ha aumentado en gran medida la susceptibilidad de la curación tardía de las heridas (Kumar et al., 2019) y el hecho de que la planta cuente con actividad antimicrobiana es de suma importancia, pues al evitar el desarrollo de infecciones favorece un proceso de cicatrización normal.

El género ha sido poco estudiado y no cuenta con reportes sobre su actividad antimicrobiana, por lo cual nuevamente se discutirá con los reportes existentes de algunas especies del género *Hyptis*.

El AEHT de *A. stellulata* fue evaluado contra diferentes cepas tuvo actividad sobre cepas aisladas de casos clínicos *S*. *aureus* CUSI y *S. aureus* FES-C con un CMI de 2 mg/mL, aunque inhibió el crecimiento en el resto de las cepas *S. aureus*. Especies del género *Hyptis* tiene reportes de la actividad antibacteriana sobre *S. aureus* con aceites esenciales de diferentes especies. *H. suaveolens* (HI: 14 mm con 5 mg/mL) (Asekun et al., 1999), *H. mutabilis* (HI: 7 mm con 50µL) (Oliva et al., 2006), *H. martiussii* (CMI: 32-1024 µL/mL) (Andrade et al., 2017) y *H. pectinata* (CMI: 12.50 µL/mL) (Santos et al., 2008). El AEHT tiene como componentes principales óxido de cariofileno, (20.48%) y α-bisabolol (13.60%). El β-cariofileno tiene actividad antibacteriana sobre *P. aeruginosa*, *S. aureus* y *E. coli*, mejora la acción del antibiótico norfloxacina, gentamicina y eritromicina cuando se utilizan

en combinación (Santos et al., 2021). La aplicación de α-bisabolol en combinación con aminoglucósidos y beta lactámicos, mejora su actividad antimicrobiana, se cree que esto es debido a que dicho compuesto podría interactuar con la membrana citoplasmática o proteínas presentes en ella, aumentando la permeabilidad e incrementando la entrada del antibiótico (Galvão et al., 2018). Además, el aceite esencial con α-bisabolol (93.7%) de *Nectandra megapotamica* tiene actividad antibiofilm sobre *S. aureus* resistente a meticilina y *P. aeruginosa* (Souza et al., 2019). Por lo tanto, la actividad antibacteriana del AETH podría ser debido a sus componentes principales.

La actividad antibacteriana del EMAS, PMeOH, PHex y PDMSO de *A. stellulata* fue moderada con una CMI > 4 mg/mL sobre cepas gram positivas: *S. aureus* y *S. epidermidis*. La PH_2O tiene una CMI de 1 mg/mL y CBM de 2 mg/mL sobre *S. epidermidis* FES-C. Especies de *Hyptis* han mostrado actividad antimicrobiana y en algunos casos se determinó el compuesto que les podría estar brindando dicha actividad. *H. crenata* en su extracto etanólico (CMI 250 µg/mL), fracción de diclorometano (CMI 62.5 µg/mL), fracción hexánica (CMI 125 µg/mL), fracción acetato de etilo (CIM 125 µg/mL) y su fracción hidrometanólica (CMI >10000 µg/mL) tuvieron actividad sobre *S. aureus* ATCC 25923, pero no tuvieron actividad sobre *E. coli* ATCC 25922 y *P. aeruginosa* ATCC 27853 (Violante et al., 2012). *H. sidifolia* su extracto etanólico mostró actividad sobre *S. aureus* con una MIC 1 mg/mL (Bussmann et al., 2010). El compuesto cirsimaritina (flavonoide metilado) de *H. albida* tuvo actividad antibacteriana sobre *S. aureus* (MIC 31.25 µg/mL), los compuestos α-pirona de *H. oblongifolia* tuvieron actividad sobre *B. subtilis* (MIC 100 µg/mL) pero no sobre *S. aureus* (Rojas et al., 1992). No obstante, *H. pectina* su compuesto α-pirona pectinokido H tiene una CMI de 20 µg/mL frente a una cepa multirresistente *S. aureus* ATCC 6538 (Fragoso-Serrano et al., 2005). Los componentes principales del EMAS son compuestos derivados de la quercetina y el ácido rosmarínico, ambos con actividad antimicrobiana. La quercetina tiene efectos bacteriostáticos sobre diferentes cepas incluyendo *S. aureus*, dañando las paredes

celulares y membranas (Wang et al., 2018). El ácido rosmarínico al ser integrado a un biopolímero provocaron morfología mórbida y lisis en las bacterias de la cepa *S. aureus* (Ge et al., 2018). Por lo tanto, probablemente la actividad antibacteriana de *A. stellulata* esté relacionada a sus constituyentes principales.

Los agentes con CMI mayores a 4 mg/mL son considerados bacteriostáticos (como es el caso de *A. stellulata* en algunas cepas) y se ha reportado que en muchos casos esta actividad es mejor para el tratamiento de infecciones (Wald-Dickler et al., 2018). Además, plantas como *Elaeis guineensis* tiene actividad bacteriostática (6.25 mg/mL) sobre *S. aureus* y promueve la regeneración de tejidos (Rajoo et al., 2021). Una posible razón es qué la actividad antibacteriana moderada mantiene una tasa lenta de crecimiento bacteriano, permitiendo al sistema inmunitario eliminar cualquier patógeno restante de manera más eficiente (Álvarez-Santos et al., 2022).

Además, *S. aureus* es la causa más importante de infecciones de piel y tejidos blandos en el hospital y en la comunidad en todo el mundo, puede diseminarse a áreas más profundas de la piel y eventualmente llegar al torrente sanguíneo provocando enfermedad sistémica y/o afectando órganos distales (Gonzalez et al., 2019). También, *S. epidermidis* se asocia frecuentemente con bacteriemia y es una de las principales preocupaciones con respecto al tratamiento de las infecciones estafilocócicas es la resistencia a los antibióticos (Eftekhar y Raei 2011). Además, *S. epidermidis* es una de las bacterias que habitualmente infecta las heridas retrasando el proceso de curación (Asada et al., 2012; Catanzano et al., 2017). Por lo cual, es fundamental la búsqueda de alternativas para su tratamiento como son los productos naturales presentes en plantas, los cuales pueden tener una actividad antibacteriana moderada, que permita que el sistema inmune genere una respuesta coordinada de los agentes de la inmunidad innata, como los queratinocitos, las células

endoteliales, las células inmunitarias residentes en la piel y los neutrófilos reclutados y eliminar el patógeno de la piel (González et al., 2019; Caldwell, 2020).

8.3. Antioxidante y antiinflamatoria

El EMAS, las particiones PMeOH y PH_2O presentaron las actividades antioxidantes más altas, estos resultados coinciden con los resultados de la cuantificación de fenoles totales. Los compuestos fenólicos son conocidos por su capacidad de sufrir series de reacciones de reducción y oxidación; debido a los efectos de resonancia localizados en el anillo aromático y a la presencia de grupos hidroxilos; por lo que son capaces de reducir a los radicales libres o especies reactivas de oxígeno (Dzah 2014; Zuo et al., 2018). La estructura química será la que determine su eficiencia como antioxidante (De Lira Mota et al., 2009; Dzah 2014). Ya que también, pueden tener grupos metoxilo y/o azucares en sus estructuras. Las propiedades químicas, físicas y biológicas de los compuestos se ven significativamente afectadas por la glicosilación (Choi et al., 2012). Esto podría afectar la actividad antioxidante de los compuestos de *A. stellulata* ya que de acuerdo con la reacción de Molish el EMAS y las particiones tienen compuestos glicosilados, por lo cual esta podría ser la razón de que presente una CA_{50} mayor en comparación con *A. mocininana* CA_{50} de 29.06 ± 2.69 ppm (Espinoza-González et al., 2021). Especies del género *Hyptis* tienen actividad antioxidante sobre DPPH variable por ejemplo *H. heterodon* con una CA_{50} de 233.4 ± 1.3 µg/mL (Silva et al., 2005) es menos antioxidante que *A. stellulata*, pero *H. suaveolens* colectada en Veracruz, Méx., el extracto etanólico de hojas presento una CA_{50} de 3.56 ± 0.04 µg/mL (Sánchez-Aguirre et al., 2020) tiene mejor actividad antioxidante. Esta modificación en la actividad antioxidante está relacionada directamente con la composición química de las plantas sometidas a diferentes condiciones bióticas y abióticas. La PDMSO tuvo actividad antioxidante similar con una cuantificación de fenoles totales similar a las particiones polares. No obstante, le reacción colorida fue la menos intensa, porque

probablemente tenga compuestos con actividad antioxidante del tipo terpénico. En el género *Hyptis* como se indicó anteriormente cuenta con terpenos del tipo abietano; en: *H. carvalhoi* se han identificado el galdosol (1), rosmanol (2) y derivados (Barros de Lima et al., 2012) y en *H. dilatata* rosmanol (2) y sus derivados (Urones et al., 1998). Algunos de estos cuentan con actividad antioxidante (Nakatani 1994) ya que tienen un anillo C aromático y presenta de uno a dos grupos hidroxilo (Barros de Lima et al., 2012). Los polifenoles pueden dividirse en otros subgrupos: ácidos fenólicos, flavonoides, taninos, lignanos y estilbenos, muchos de estos cuentan con actividades biológicas importantes, destacando la actividad antioxidante mediante la inducción de la expresión de enzimas antioxidantes, quelar los iones metálicos e inhibir la reacción de Fenton (Aruoma 2003; Halliwell 2008; Yan et al., 2020). Además, se les han atribuido cualidades antiinflamatorias (Ghuman et al., 2019).

La actividad antiinflamatoria de los polifenoles se da mediante la regulación de vías de señalización en células del sistema inmune mediante la regulación de los procesos inflamatorios asociados a neutrófilos, monocitos/macrófagos, mastocitos y linfocitos T. Dentro de los procesos que se conocen esta la disminución de citocinas proinflamatorias: TNFα, IL-1, IL-2, IL-6 e IL-8 (vía NF-κB); la regulación de la cascada de señales para genes asociados a la inflamación (vía MAPK); además se ha observado que los polifenoles tiene una capacidad para modular mecanismos epigenéticos, la inhibición de las enzimas COX-2 y LOX (vía ácido araquidónico) (Khan et al., 2019).

El EMAS y sus particiones inhiben la enzima COX-2. Hasta el momento de la búsqueda, no se han encontrado investigaciones sobre la inhibición de COX-2 con *Asterohyptis* o *Hyptis*. *A. stelullata* tuvo una CI_{50}= 28 µg/mL en otras especies se han determinado CI_{50} menores, por ejemplo: la fracción metanólica de *Betula utilis* tuvo un IC_{50}= 4.26 µg/mL (Vishwakarma et al., 2022a), *Lantana camara* un CI_{50}= 4.06 µg/mL (Vishwakarma et al., 2022b) y *Hedera*

helix con una CI_{50}= 3.36 µg/mL (Shokry et al., 2022). Sin embargo, *A. stellulata* tuvo actividades similares en su porcentaje de inhibición con plantas con actividad antiinflamatoria como *Ajuga bracteosa* que mostró 42.38% de inhibición de COX-2 a una concentración de 25 µg/mL (Gautam et al., 2011). El efecto de la inhibición total de COX-2 en heridas podría incluso disminuir el proceso de cicatrización ya que afecta la respuesta inflamatoria necesaria para la curación, reduciendo la contracción de la herida, la reepitelización, angiogénesis y componentes de la MEC (Dong et al., 1993; Romana-Souza et al., 2016). Por lo cual, la actividad modera del extracto podría beneficiar al cierre de la herida sin inhibir totalmente a COX-2 y permitir que el proceso inflamatorio cumpla sus funciones.

La actividad desinflamatoria de *A. stellulata* podría estar relacionada con los compuestos identificados por HPLC/MS-MS. Es importante considerar que los compuestos identificados en el extracto están glicosilados en comparación con sus agliconas que han sido investigadas en los procesos de inflamación y cicatrización. Por lo tanto, esto podría afectar su actividad.

La quercetina es un compuesto que promueve el proceso de curación en ratones con heridas por escisión disminuyendo la inflamación a través del cambio de fenotipo de miofibroblasto M1 proinflamatorio a M2 antiinflamatorio (Choudhary et al., 2020; Fu et al., 2020). Se ha reportado que actúa sobre la vía del ácido araquidónico actuando sobre lipooxigenasa y no sobre COX-2, también, se considera que su actividad antiinflamatoria está relacionada con su capacidad antioxidante, la inhibición de vías como NF-κB y MAPK (Khan et al., 2019).

El ácido rosmarínico (AR) cuenta con diversos reportes sobre su capacidad de inhibición de COX-2 (Dahchour, 2022; Swarup et al., 2007) y de su expresión (Ghasemzadeh et al.,

2016). Además, modula la inflamación a través de las vías NF-κB, MAPK y Nrf2 (Vasileva et al., 2021). Además, la aplicación de AR disminuyo la formación de cicatrices y promovió la regeneración de tejidos (Chhabra et al., 2020; Küba et al., 2021; Wani et al., 2019).

Por lo tanto, la inhibición de COX- 2 por el EMAS podría estar relacionado con su actividad cicatrizante al modular la inflamación. Probablemente, a través de los glicósidos AR y quercetina. Sin embargo, es importante considerar su papel en otras vías de señalización relacionadas con la inflamación como NF-κB, MAPK y Nrf2. Por lo cual, sería necesario analizar este punto en estudios posteriores.

8.4. Prueba de irritabilidad

La aplicación tópica de la crema con diferentes concentraciones no induce irritación en la piel de ratón CD-1 et/et. Hasta el momento de la búsqueda solo se encontró una investigación sobre la toxicidad tópica de una especie de *Hyptis*: *H. verticillata* Jacq., se probó su toxicidad dérmica con la aplicación de 4g/kg del extracto crudo acuoso en conejos albino Nueva Zelanda y no presentó irritación local (Picking et al., 2013). La mayoría de las investigaciones sobre su toxicidad se han hecho con estudios de toxicidad agua con administración oral y no se consideran tóxicos, por ejemplo, *H. suaveolens* no se consideró toxica ya que no hubo muerte animal con dosis de hasta 5 g/kg del extracto acuoso (Santos et al., 2007); el extracto crudo acuoso de *H. verticillata* en pruebas con ratones, la ingesta de 1 g/kg por 5 días consecutivos no provocó mortalidad y no aparecieron signos de intoxicación; además, cuando se le da la decocción de 1 mL por animal por día (4mg) no hubo mortalidad, ni signos de toxicidad y la necropsia muestra que no existió daño interno (Picking et al., 2013).

Estos resultados permitieron continuar con los protocolos de actividad cicatrizante y elegir la concentración para evaluar dicha actividad. Dados los resultados podríamos ocupar la

dosis máxima, sin embargo, se consideraron los resultados de las pruebas biológicas como la actividad antioxidante, ya que, en algunas ocasiones los antioxidantes a dosis altas pueden actuar como prooxidantes (Pérez 2003).

8.5. Actividad cicatrizante/regeneración

El tratamiento tópico con el vehículo (C-) se encuentra en la transición de la inflamación a la proliferación, por la presencia de neutrófilos, pocos fibroblastos, colágeno inmaduro, menor resistencia a la tensión, tamaño mayor en la zona cicatrizada, permanencia del tejido de granulación y sin formación de las capas características de la piel normal. En la inflamación, las células fagocíticas, incluidos los neutrófilos y los macrófagos, previenen la infección y eliminan los desechos celulares (Yazarlu et al., 2021), liberan citocinas, quimiocinas y factores de crecimiento, participan en el reclutamiento y la activación de fibroblastos y células epiteliales para la etapa proliferativa (Low et al., 2021). No obstante, de acuerdo con los resultados obtenidos con *A. stellulata* nos indica que puede ser un vehículo adecuado para la liberación de compuestos presentes en el EMAS. Debido a que la eficacia curativa de quercetina y sus derivados está limitada por su baja solubilidad y permeación cutánea (Zhou et al., 2021).

La aplicación tópica de Recoverón® (C+) en los ratones provocó un proceso de cicatrización más rápido, necesitó una fuerza de tensión ligeramente menor que el tratamiento con *A. stellulata* para abrir la zona de cicatrización de la herida, coincidiendo con los datos histológicos en los cuales se observa una TZC grande, pero con fibras densas y organizadas de colágeno. El grupo tratado con Recoverón® se encuentra entre la proliferación y la remodelación, porque tienen abundantes fibroblastos, pocos miofibroblastos, nuevos vasos sanguíneos, ausencia de neutrófilos, colágeno maduro y mejor resistencia a la tensión, tamaño mayor en la zona cicatrizada, permanencia del tejido de granulación y ausencia de las capas características de la piel. La proliferación se

caracteriza por la angiogénesis, proliferación de fibroblastos (nueva MEC/colágeno tipo III), queratinocitos (reepitelización) y células endoteliales (vasos sanguíneos) (Low et al., 2021; Yazarlu et al., 2021). En última instancia, los fibroblastos y los queratinocitos producen TGF-β que conduce a la diferenciación de los miofibroblastos, regulando el cierre de la herida (Yazarlu et al., 2021) y el comienzo de la fase de remodelación.

La aplicación tópica de *A. stellulata* promueve la cicatrización y regeneración de la piel. El análisis histológico permitió identificar epidermis similar a la normal, zonas de cicatrización pequeñas, la formación de capas características de la piel -músculo, hipodermis, dermis-, así como folículos pilosos y glándulas sebáceas. Se observo que los individuos tratados con *A. stellulata* presentaban una mejor distribución y maduración del colágeno, lo cual coincide con la fuerza de tensión para abrir la herida en comparación con los controles. Como se mencionó anteriormente, en la fase de remodelación es fundamental el cambio de colágeno tipo III a colágeno tipo I el cual es más resistente (Wang et al., 2018). En cuanto a los grupos celulares los ratones tratados con *A. stellulata* presentan miofibroblastos, abundantes vasos sanguíneos, ausencia de neutrófilos, características de la fase de remodelación. Incluso, es evidente un proceso de regeneración ya que la piel de la zona donde se realizó la herida es muy similar a la piel normal de los ratones CD1 et/et.

Existen datos en los que el proceso de cicatrización se identifica por la formación de cicatriz y perdida de función del tejido, en otros caso se estipula que puede llegar a la restauración del tejido. Akita y colaboradores (2019) consideran que la cicatrización de heridas puede estar implicada en la regeneración de tejidos y el retorno a su estado original. Para que se de este último fenómeno existen diversas condiciones que permiten el restablecimiento del tejido a su normalidad, en ratones *Acomys* spp. con heridas excisionales puede regenerar completamente el tejido por la presencia de blastema, pero los ratones CD-1 solo cicatrizan (Gawriluk et al., 2016). Por lo general, las heridas de la piel producen MEC desorganizada

conocida comúnmente como cicatriz (Castaño et al., 2018). En esta se puede observar fibrosis dérmica variable, epidermis borrada, glándulas sebáceas y folículos limitados o ausentes, lo que provoca una pérdida de estructura y función (Sun et al., 2016), lo cual se observa en los controles. También, se considera que los tratamientos que acortan el proceso de cicatrización disminuyen la formación de cicatrices (Süntar et al., 2010). Lo cual concuerda parcialmente con nuestros resultados, ya que la aplicación de *A. stellulata* acelera el proceso de cicatrización, Recoverón® también, pero en este caso se observa tejido cicatricial. Por lo tanto, considerando que la cicatrización solo conlleva a la formación de cicatriz -perdida de función- y la regeneración el restablecimiento de las condiciones normales, se puede concluir que la aplicación tópica de *A. stellulata* en ratones CD-1 et/et disminuye la formación de cicatrices y promueve la regeneración de la piel. Dichos sucesos están asociados a los metabolitos secundarios presentes en el EMAS, ya que es sabido que pueden actuar por diferentes vías y promover la curación de heridas (Álvarez-Santos et al., 2023).

A. stellulata tiene glicósido de quercetina, este compuesto se ha reportado en plantas que mejoran la cicatrización/regeneración de heridas. El extracto metanólico de *Euphorbia characias* subsp. *wulfenii* (Hoppe ex W.D.J. Koch) Radcl.-Sm., promovió el avance a la fase de remodelación y disminuyo la formación de cicatrices, en los cortes histológicos del artículo se observa la formación de folículos pilosos con la aplicación del extracto, pero no lo reportan en el escrito, en cuanto a sus fracciones tienen quercitrina, hiperósido y guaijaverina, pero al aplicarlas de manera individual no mejoraron la actividad (Özbilgin, et al., 2018). Esto podría ser indicativo de que el extracto crudo al contener todos los metabolitos juntos estos podrían estar actuando de manera sinérgica. *Sambucus ebulus* L. tiene quercetina 3-O-glucósido, aislado de una de sus fracciones, pero la actividad cicatrizante fue menor que el extracto metanólico inicial (Süntar et al., 2010). Además, en

el extracto de acetato de etilo de *Eugenia pruniformis* Cambess se identificaron quercetina, kaempferol e hiperósido (43 % p/p), este extracto aceleró la cicatrización de heridas y la remodelación dérmica (Galhardo de Albuquerque et al., 2016). Por lo tanto, podemos considerar que la aplicación de extractos crudos -mezcla de metabolitos- aceleran y mejoran la curación de heridas. Aunque se ha visto que la aplicación de las agliconas de los compuestos identificados en el EMAS promueve la curación de heridas por si solos o en la aplicación conjunta con biomateriales. La quercetina acelera el proceso de contracción de la herida, incrementa el número de fibroblastos, mejora el depósito de colágeno y promueve la diferenciación de macrófagos del tipo M1 -proinflamatorio- al M2 -antiinflamatorio- (Fu, et al., 2020). Este cambio de fenotipo está asociado a la regulación de vías de señalización incrementado Nrf2 y regulado NFκB (Wang y He 2022). El incremento de la expresión de M2 juega un papel importante en la resolución de la inflamación, actividad antifibrótica (inhibición de formación de cicatriz) y regeneración de tejidos (Monovarian et al., 2019). Además, cuando la quercetina es integrada a nanopartículas se ha observado que funciona como bacteriostático y promueve la regeneración de la piel al ser aplicada en ratones con heridas excisionales (Li et al., 2022). También, al ser integrada en liposomas y posteriormente a un hidrogel disminuyo la fibrosis y la formación de cicatriz (Jangde et al., 2018). Por lo tanto, la presencia de los derivados de quercetina en *A. stellulata* podría promover la cicatrización y regeneración de heridas.

El otro metabolito presente en el EMAS de *A. stellulata* fue el glucopiranósido del ácido rosmarínico. Hasta el momento no se han encontrado reportes de las actividades de dicho metabolito, pero si la aglicona es decir el ácido rosmarínico. La aplicación tópica de crema con ácido rosmarínico (10 %) redujo el tamaño de la herida y produjo menos cicatrización, pero el tiempo de cicatrización se prolongó y la epitelización fue menor (Küba et al., 2021). Además, la aplicación de ácido rosmarínico en nanopartículas y gel tiene actividades

antibacterianas, antioxidantes y cicatrizantes, incluso disminuye la formación de cicatrices y promueve la regeneración de tejidos (Wani et al., 2019; Chhabra, 2020).

El extracto crudo de *A. stellulata* es una mezcla con diferentes metabolitos secundarios, entre ellos derivados de quercetina y ácido rosmarínico. Estos compuestos podrían mejorar la actividad de cicatrización de heridas. Sin embargo, es posible que otros metabolitos no identificados tengan también cualidades curativas y actúen de manera sinérgica, ya que los reportes indican que al hacer fracciones y subfracciones disminuye la actividad (Süntar et al., 2010; Özbilgin, et al., 2018).

Es fundamental continuar con la investigación de los posibles mecanismos de acción de *A. stellulata* en la regeneración de heridas cutáneas, ya que es sabido que tanto la quercetina como el ácido rosmarínico actúan en diferentes vías de señalización relacionadas con la curación de heridas (Khan et al., 2019; Vasileva et al., 2021; Alvarez-Santos et al., 2023). Por lo cual un estudio a mayor profundidad permitiría en un futuro la formulación de un fitofármaco para el tratamiento de heridas.

9. CONCLUSIONES

- *A. stellulata* tiene compuestos fenólicos y terpenos en su composición química, pero no contiene alcaloides.
- El rango de fenoles totales de *A. stellulata* va de 178.218 ± 0.015 a 131.823 ± 0.019 mg de EAG/g de extracto en la parte polar y de 32.06 ± 0.001 mg EAG/ g de extracto en la fracción hexánica.
- El extracto crudo de *A. stellulata* cuenta derivados de quercetina y un glucopiranósido de ácido rosmarínico.
- El aceite esencial de hojas y tallos tiene como compuestos mayoritarios óxido de cariofileno y α-bisabolol.

- El aceite esencial de inflorescencia tiene como compuestos mayoritarios germacreno D, cariofileno, α- bisabolol, α-cadinol y óxido de cariofileno.
- *A. stellulata* y sus particiones tienen actividad bactericida y/o bacteriostática frente a *S. aureus* y *S. epidermidis.*
- El aceite esencial de *A. stellulata* tiene actividad bactericida y bacteriostática en diferentes cepas de *S. aureus*.
- El EMAS, PMeOH, PH_2O y PDMSO cuentan con actividad antioxidante frente al radical DPPH
- La PHex de *A. stellulata* no tiene actividad antioxidante frente al radical DPPH.
- *A. stellulata* tiene actividad inhibitoria sobre COX-2 *in vitro*.
- *A. stellulata* no es un irritante dérmico al aplicarse de manera tópica en el dorso de ratones CD-1 et/et.
- La aplicación del EMAS de *A. stellulata* integrado a la base Beeler mejoró el proceso de cicatrización/regeneración en heridas incisionales de ratón CD-1 et/et.
- *A. stellulata* cuenta con metabolitos secundarios, que le dan diferentes actividades biológicas que en conjunto permiten la regeneración de tejidos en heridas incisiones en ratones CD1 et/et.

10. REFERENCIAS BIBLIOGRÁFICAS

Abbas, M., Uçkay, I., Lipsky, B.A. 2015. In diabetic foot infections antibiotics are to treat infection, no to heal wounds. Expert Opin Pharmacother. 16:821-832.

Abdelall, E.K.A., Kamel, G.M. 2016. Synthesis of new thiazolo-celecoxib analogues as dual cyclooxygenase-2/15-lipoxygenase inhibitors: Determination of regio-specific different pyrazole cyclization by 2D NMR. Eur J Med Chem. 118:250-258.

Abedini, A., Roumy, V., Mahieux, S., Biabiany, M., Standaert-Vitse, A., Rivière, C., Sahpaz, S., Bailleul, F., Neut, C., Hennebelle, T. 2013. Rosmarinic acid and its methyl ester as antimicrobial components of the hydromethanolic extract of *Hyptis atrorubens* Poit. (Lamiaceaee). Evid Based Complement Alternat Med. 2013:604536.

AEMPS. 2019. Monografías, excipientes. In R. B. Tarno, F. L. Escribano,T., Vara, & P. I. Alcaraz (Eds.), Formulario nacional. Madrid: Ministerio de Sanidad, Consumo y Bienestar Social (p. 277).

Akdemir, Z., Kahraman, C., Tath, I.I., Akkol, E. K., Süntar, I., Keles, H. 2011. Bioassay-guided isolation of anti-inflammatory, antinociceptive and wound healer glycosides from the flowers of *Verbascum mucronatum* Lam. J Ethnopharmacol. 136:436-443.

Akita, S. 2019. Wound repair and regeneration: mechanisms, signaling. Int J Mol Sci. 20:6328.

Ali, A. M. A., El-Nour, M. E., Yagi, S. M., Qahtan, Alatar, A. A., Abdel-Salam, E. M., Sengin, G. 2021. Cytotoxicity, phytochemical screening and genetics analysis of ginger (*Zingiber officinale* Rosc.) callus and rhizome. S Afr J Bot. 151:54-59.

Almeida, M. C., Resende, D. I. S. P., da Costa, P. M., Pinto, M. M. M., Sousa, E. 2021. Tryptophan derived natural marine alkaloids and synthetic derivatives as promising antimicrobial agents. Eur J Med Chem. 209:112945.

Almtorp, G. T., Hazell, A. C., Torssell, B. G. 1991. A lignan and pyrone and other constituents from *Hyptis capitata*. Phytochemistry. 30:2753-2756.

Álvarez-Santos, N., Estrella-Parra, E.A., Benítez-Flores, J.C., Serrano-Parrales, R., Villamar-Duque, T.E., Santiago-Santiago, M.A., González-Valle, M.R., Avila-Acevedo, J.G., García-Bores, A. 2022. *Asterohyptis stellulata*: Phytochemistry and wound healing activity. Food Bioscience. 50(Part B):102150.

Álvarez-Santos, N., García-Bores, A.M., Barrera-Oviedo, D., Hernández-Delgado, C.T., Estrella-Parra, E.A., Avila-Acevedo, J.G., Secondary metabolites in wound healing: a review of their mechanisms of action. Chapter 10. Studies in Natural Product Chemistry.

Andrade, T. A., Freitas, T. S., Araújo, F. O., Menezes, P. P., Dória, G. A. A., Rabelo, A. S., Quintans-Júnior, L.J., Santos, M. R. V., Bezerra, D. P., Serafini, M. R., Menezes, I. R. A., Nunes, P. S., Araújo, A. A. S., Costa, M. S., Campina, F. F., Santos, A.T.L., Silva, A.R.P., Coutinho, H. D. M. 2017. Physico-chemical characterization and antibacterial activity of inclusion complexes of *Hyptis martiusii* Benth essential oil in β-cyclodextrin. Biomed Pharmacother. 89:201-207.

Aruoma, O.I. 2003. Methodological considerations for characterizing potential antioxidant actions of bioactive components in plant foods. Mutat Res. 523-524:9-20.

Asada, M., Nakagami, G., Minematsu, T., Nagase, T., Akase, T., Huang, L., Yoshimura, K., Sanada, H. 2012 Novel models for bacterial colonization and infection of full-thickness wounds in rats. Wound Repair Regen. 20(4):601-10.

Asekun, O. T., Ekundayo, O., Adeniyi, B. A. 1999. Antimicrobial activity of the essential oil of *Hyptis suaveolens* leaves. Fitoterapia. 70:440-442.

Bahramsoltani, R., Hosein, F. M., Rahimi, R. 2014. Medicinal plants and their natural components as future drugs for the treatment of burn wounds: an integrative review. Arch Dermatol Res. 306:601-617.

Baltzis, et al. 2014. Pathogenesis and treatment of impaired wound healing in diabetes mellitus: new insights. Adv Ther. 31:817-836

Bao, L., Cai, X., Zhang, M., Xiao, Y., Jin, J., Quin, T., Li, Y. 2022. Bovine collagen oligopeptides accelerate wound healing by promoting fibroblast migration via PI3K/Akt/mTOR signaling pathway. J Funct Foods. 90:104981.

Barros de Lima, K.S., Ávila, P.A.T., Silva, G.M.L., Sousa, L.M.A., Rocha, S.E. 2012. Abietane diterpenes from *Hyptis carvalhoi* Harley. Biochem Syst Ecol. 44:240-242.

Bezerra, J. W. A., Costa, A. R., da Silva, M. A. P., Rocha, M. I., Boligon, A. A. da Rocha, J. B. T., Barros, L. M., Kamdem, J. P. 2017. Chemical composition and toxicological evaluation of *Hyptis suaveolens* (L.) Poiteau (LAMIACEAEE) in Drosophila melanogaster and Artemia salina. S Afr J Bot. 113:437-442.

Bhatia, N., Kaur, G., Soni, V. Kataria, J., Dhawan, R.K. 2016. Evaluation of the wound healing potential of isoquercetin-based cream on scald burn injury in rats. Burns Trauma. 4:1-8.

Boalino, D. M., Connolly, J. D., McLean, S., Reynolds, W. F., Tinto, W. F. 2003. α-pirones and a 2(5H)-furanone from *Hyptis pectinate*. Phytochemistry. 64:1303-1307.

Boiy, A., Roelandts, R., Roskams, T., de Witte, P.A.M. 2007. Effects of vehicles and esterification on the penetration and distribution of hypericin in the skin of hairless mice. Photodiagnosis Photodyn Ther. 4:130–139.

Bridi, H., Carvalho, M.G., Lino, V.P.G. 2021. Subtribe Hyptidinae (Lamiaceae): A promisin source of bioactive metabolites. J Ethnopharmacol. 264:113225.

Bussmann, R.W, Malca-García, G., Glenn, A., Sharon, D, Chait, G., Díaz, D., Pourmand, K., Jonat, B., Somogy, S., Guardado, G., Aguirre, C., Chan, R., Meyer, K., Kuhlman, A., Townesmith, A., Effio-Carbajal, J., Frías-Fernandez, F., Benito, M. 2010. Minimum inhibitory concentrations of medicinal plants used in Northern Peru as antibacterial remedies. J Ethnopharmacol. 132:101-8.

Butnariu, M. 2014. Detection of the polyphenolic components in *Ribes nigrum* L. Ann Agric Environ Med. 21:11–14.

Caldwell, M. D. 2020. Bacteria and antibiotics in wound healing. Surg Clin North Am. 100:757-776.

Carvalho, M.T.B., Araújo-Filho, H.G., Barreto, A.S., Quintana-Júnior, L.J., Quintans, J.S.S., Barreto, R.S.S. 2021. Wound healing properties of flavonoids: A systematic review highlighting the mechanisms of action. Phytomedicine. 90:153636.

Castaño, O., Pérez-Amodio, S., Navarro-Requena, C., Mateos-Timoneda, M.A., Engel, E. 2018. Instructive microenvironments in skin wound healing: Biomaterials as signal releasing platforms. Adv Drug Deliv Rev. 129 (2018) 95-117.

Catanzano, O., D'Esposito, V., Pulcrano, G., Maiolino, S., Ambrosio, M. R., Esposito, M., Miro, A., Ungaro, F., Formisano, P., Catania, M. R. 2017. Ultrasmall silver nanoparticles

loaded in alginate–hyaluronic acid hybrid hydrogels for treating infected wounds. Int J Polym Mater. 66 (12):626-634

Chavan, M. J., Wakte, P. S., Shinde, D. B. 2010. Analgesic and anti-inflammatory activity of Caryophyllene oxide from *Annona squamosa* L. bark. Phytomedicine.17:149-151.

Chen, L., Jiang, P., Li, J., Xie, Z., Xu, Y., Qu, W., Feng, F., Liu, W. 2019. Periplocin promotes wound healing through the activation of Src/ERK and PI3K/Akt pathways mediated by Na/K-ATPase. Phytomedicine. 57:72-83.

Chen, L., Jiang, P., Li, J., Xie, Z., Xu, Y., Qu, W., Feng, F., Liu, W. 2019. Periplocin promotes wound healing through the activation of Src/ERK and PI3K/Akt pathways mediated by Na/K-ATPase. Phytomedicine. 57:72-83

Chhabra, P., Chauhan, G., Kumar, A. 2020. Augmented healing of full thickness chronic excision wound by rosmarinic acid loaded chitosan encapsulated graphene nanopockets. Drug Dev Ind Pharm. 46:878-888.

Chiocchio, I., Poli, F., Governa, P., Biagi, M., Lianza, M. 2018. Wound healing and in vitro antiradical activity of five *Sedum* species grown within two sites of community importance in Emilia-Romagna (Italy). Plant Biosystems -An International Journal Dealing with all Aspects of Plant Biology, 15:610–615.

Chitra, S., Patil, M. B., Ravi, K. 2009. Wound healing activity of *Hyptis suaveolens* (L.) poit (Lamiaceae). Int J PharmTech Res. 1(3):737-744.

Choi, D.Y., Lee, Y.J., Hong, J.T., Lee, H.J. 2012. Antioxidant properties of natural polyphenols and their therapeutic potentials for Alzheimer's disease. Brain Res Bull. 87(2-3):144-53.

Choudhary, A., Kant, V., Jangir, B.L., Joshi, V.G. 2020. Quercetin loaded chitosan tripolyphosphate nanoparticles accelerated cutaneous wound healing in Wistar rats. Eur J Pharmacol. 880:173172.

CLSI. 2020. Performance standards for antimicrobial susceptibility testing. CLSI supplement M100, Wayne, Pennsylvania.

Costa, V. C., Tavares, J. F., Silva, A. B., Duarte, M. C., Agra, M. F., Barbosa-Filho, J. M., Souza, I. L. L., da Silva, B. A., Silva, M. S. 2014. Hyptenolide, a new a-pyrone with spasmolytic activity from *Hyptis macrostachys*. Phytochem Lett. 8:32-37.

Dahchour, A. 2022. Anxiolytic and antidepressive potentials of rosmarinic acid: A review with a focus on antioxidant and anti-inflammatory effects. Pharmacological Research. 184:106421.

de Lima, A.C.B., Paixao, M.S., Melo, M., de Santana, M.T., Damascena, N.P., Dias, A.S., Porto, Y.C.B.S., Fernandes, X.A., Santos, C.C.S., Lima, C.A., Quintans Júnior, L.J., Estevan, C.S., Araújo, B.S. 2013. Orofacial antinociceptive effect and antioxidant properties of the hydroethanol extract of *Hyptis fruticosa* salmz ex Benth. J Ethnopharmacol. 146:192-197.

de Lima, S.L., de Freitas, S.C., Vey, P.T., Leitao, G.A., da Silva, P.P., Erbice, B.A., Baldisserotto, B. 2021. Ethanolic extract of *Hyptis mutabilis* (Rich.) Briq.: An effective sedative and antioxidant agent in fish. J Ethnopharmacol. 531:735940.

de Lira Mota, K.S., Días, G.E., Pinto, M.E., Luiz-Ferreira, A., Souza-Brito, A.R., Hiruma-Lima, C.A., Barbosa-Filho, J.M., Batista, L.M. 2009. Flavonoids with gastroprotective activity. Molecules. 14(3):979-1012.

do Santos, P. K., Sedano-Partida, M. D., Sala-Carvalho, W. R., Ortega, S. J. L. B., da Silva-Luz, C. L., Furlan, C. M. 2018. Biological activity of *Hyptis* Jacq. (Lamiaceaee) is determined by the environment. Ind Crops Prod. 112:705-715.

Dong, Y.L., Fleming, R.Y., Yan, T.Z., Herndon, D.N., Waymack, J.P. 1993. Effect of ibuprofen on the inflammatory response to surgical wounds. J Trauma. 35(3):340-343.

Draize, J.H, Woodard, G. 1944. Methods for the study of irritation and toxicity of substances applied topically to the skin and mucous membranes. J Pharmacol Exp Ther. 82(3):377-90.

Dzah, C.S., Duan, Y., Zhang, H., Wen, C., Zhang, J., Chen, G., Ma, H. 2020. The effects of ultrasound assisted extraction on yield, antioxidant, anticancer and antimicrobial activity of polyphenol extracts: A review. Food Bioscience. 35:100547.

Eftekhar, F., Raei, F. 2011.Correlation of minimum inhibitory concentration breakpoints and methicillin resistance gene carriage in clinical isolates of *Staphylococcus epidermidis*. Iran J Med Sci. 36(3):213-216.

Elzayat, E. M. Auda, S. H., Alanazi, F. K. Al-Agmay, M. H. 2018. Evaluation of wound healing activity of henna, pomegranate and myrrh herbal ointment blend. SPJ. 26:733-738.

Elzayat, E.M. Auda, S.H., Alanazi, F.K. Al-Agmay, M.H. 2018. Evaluation of wound healing activity of henna, pomegranate and myrrh herbal ointment blend. Saudi Pharm J. 26:733-738.

Eming, S.A., Martin, P., Tomic-Canic, M. 2014. Wound repair and regeneration: mechanisms, signaling, and translation. SciTransl Med. 6:1-36

Epling, C. 1933. *Asterohyptis*: A Newly Proposed Genus of Mexico and Central America. Bull Torrey Bot Club. 60:17-21.

Espinosa-González, A. M., Estrella-Parra, E.A., Nolasco-Ontiveros, E., García-Bores, A. M., García-Hernández, R., López-Urrutia, E., Campos-Contreras, J.E., González-Valle, M. del R., Benítez-flores, J. del C., Céspedes-Acuña, C. L., Alarcón-Enos, J., Rivera-Cabrera, J. C., Avila-Acevedo, G. 2021. *Hyptis mociniana*: phytochemical fingerprint and photochemoprotective effect against UV-B radiation-induced erythema and skin carcinogenesis. Food Chem Toxicol. 151:112095.

Estrella-Parra, E. A., Espinosa-González, A. M., García-Bores, A. M., Zamora-Salas, S. X., Benítez-Flores, J. C., González-Valle, M. R., Hernández-Delgado, C. T., Peñalosa-Castro, I., Avila-Acevedo, J. G. 2019. Flavonol glycosides in *Dyssodia tagetiflora* and its temporal variation, chemoprotective and ameliorating activities. Food Chem Toxicol. 124:411-422.

Fairweather, M., Heit, Y.I., Buie, J., Rosenber, L.M., Briggs, A., Orgill, D.P., Bertagnolli, M.M. 2015. Celecoxib inhibits early cutaneous wound healing. J Surg Res. 194(2): 717-724.

Falcao, E. E. A., de Souza, S. A., Camara, C. A., Quintans, J. S.S., Santos, P. L., Correira, M. T. S., Silva, T. M. S., Lima, A. A. N., Quintans-Húnior, L. J., Guimaraes, A. G. 2016. In vitro and in vivo determination of antioxidant activity and mode of action of isoquercitrin and *Hyptis fasciculata.* Rev Bras Pharmacogn. 26:203-208.

Fragoso-Serrano, M., Gibbons, S., Pereda-Miranda, R. 2004. Anti-Staphylococcal and cytotoxic compounds from *Hyptis pectinata*. Plant Med. 71:278-280.

Frezza, C., Venditti, A., Serafini, M., Bianco. 2019. Phytochemistry, chemotaxonomy, ethnopharmacology, and nutraceutics of Lamiaceaee. Stud Nat Prod Chem. 62, 125–178.

Fu, J., Huang, J., Lin, M., Xie, T., You, T. 2020. Quercetin promotes diabetic wound healing via switching macrophages from M1 to M2. J Surg Res. 246:213-223.

Gad, H. A., Abd, E. R. F., Hamdy, G. M. 2019. Chamomile oil loaded solid lipid nanoparticles: A naturally formulated remedy to enhance the wound healing. J Drug Deliv Sci Technol. 50:329-338.

Galhardo de Albuquerque, R.D.D., Perini, J.A., Machado, D.E., Angell-Gamba, Esteves, T., R.S., Santos, M.G., Passos Oliveira, A., Rocha, L. Wound Healing Activity and Chemical Standardization of *Eugenia pruniformis* Cambess. Pharmacogn Mag. 12:288-294.

Galvão, R., F. F., Colares A. V., de Fatima, A., N. C., Galvão-Rodrigues, F. F., Lima, M. M., Bezerra, M. B. M. F., da Costa, J. G M. 2018. *In vitro* antimicrobial activity of the essential oil from *Vanillosmopsis arborea* Barker (Asteraceae) and its major constituent, α-bisabolol. Microbial Pathogenesis. 125:144-149.

García-Bores, A. M., Álvarez-Santos, N., López-Villafranco, M. E., Jácquez-Ríos, M. P., Aguilar-Rodríguez, S., Grego-Valencia, D., Espinosa-González, A. M., Estrella-Parra, E. A., Hernández-Delgado, C. T., Serrano-Parrales, R., González-Valle, M. R., Benítez-Flores, J. C. 2020. *Verbesina crocata*: A pharmacognostic study for the treatment of wound healing. Saudi J Biol Sci. 27:3113-3124.

Gautam, R., Jachak, S.M., Saklani, A. 2011. Anti-inflammatory effect of *Ajuga bracteosa* Wall Ex Benth. mediated through cyclooxygenase (COX) inhibition. J Ethnopharmacol. 133 (2):928-930.

Gawriluk, T.R., Simkin, J., Thompson, K.L., Biswas, S.K., Clare-Salzler, Z., Kimani, J.M., Kiama, S.G., Smith, J.J., Ezenwa, V.O., Seifert, A.W. 2016. Comparative analysis of ear-hole closure identifies epimorphic regeneration as a discrete trait in mammals. Nat Commun. 7:11164.

Ge, L., Zhu, M. Li, X., Xu, Y., Ma, X., Shi, R., Li, D., Mu, C. 2018. Development of active rosmarinic acid-gelatin biodegradable films with antioxidant and long-term antibacterial activities. Food Hydrocolloids. 83:308-316.

Ghasemzadeh, R.M., Amin, B., Mehri, S., Mirnajafi-Zadeh, S.J., Hosseinzadeh, H. 2017. Anti-inflammatory effects of ethanolic extract of *Rosmarinus officinalis* L. and rosmarinic acid in a rat model of neuropathic pain. Biomed Pharmacother. 86:441-449.

Ghuman, S., Ncube, B., Finnie, J.F., McGaw, L.J., Mfotie Njoya, E., Coopoosamy, R.M., Van Staden, J. 2019. Antioxidant, anti-inflammatory and wound healing properties of medicinal plant extracts used to treat wounds and dermatological disorders. S Afr J Bot. 126:232-240.

Gonzalez, C.D., Ledo, C., Cela, E., Stella, I., Xu, C., Ojeda, D.S., Frenette, P.S., Gómez, M.L. 2019. The good side of inflammation: Staphylococcus aureus proteins SpA and Sbi contribute to proper abscess formation and wound healing during skin and soft tissue infections. Biochim Biophys Acta Mol Basis Dis. 1865:2657-2670.

Guija-Poma, E., Inocente-Camones, M.A., Ponce-Pardo, J. y Zarzosa-Norabuena. 2015. Evaluación de la técnica 2,2-Difenil-I-Picrilhidrazilo (DPPH) para determinar capacidad antioxidante. Horizonte Medico. 15:57-60.

Guillén-Meléndez, G.A., Soto-Domínguez, A., Loera-Arias, M.J., Castillo-Velázquez, U., Villa-Cedillo, S., Piña-Mendoza, E.I., Estrada-Castillón, E., Chávez-Montes, A., González-Alcocer, A., Becerra-Verdín, E.M., Castañeda-Martínez, A., Pérez-Hernández, R.A., Salas-Treviño, D. 2022. Effect of methanolic extract of *Mimosa malacophylla* A. Gray in vero and HEK-293 cell lines, and in the morphology of kidney and bladder of rats with induced urolithiasis. J Ethnopharmacol. 297:115552.

Gurtner, G.C., Werner, S., Barradon, Y., Longaker, M.T. 2008. Wound repair and regeneration. Nature. 453:314-321

Halliwell, B. 2008. Are polyphenols antioxidants or pro-oxidants? What do we learn from cell culture and in vivo studies? Arch Biochem Biophys. 476:107-112.

Han, G., Ceilley, R. 2017. Chronic wound healing: a review of current management and treatments. Adv Ther. 34:599-510.

Ivanov, M., Kostic, M., Stojkovic, D., Sokovic, M. 2022. Rosmarinic acid-Modes of antimicrobial and antibiofilm activities of common plant polyphenol. S Afr J Bot. 146:521-527.

Jangde, R., Srivastava, S., Singh, M.R., Singh, D. 2018. *In vitro* and *in vivo* characterization of quercetin loaded multiphase hydrogel for wound healing application. Int J Biol Macromol 115:1211-1217.

Kerdudo, A., Njoh Ellong, E., Gonnot, V., Boyer, L., Michel, T., Adenet, S., Rochefort, K., Fernandez, X., 2016. Essential oil composition and antimicrobial activity of *Hyptis atrorubens* Poit. from Martinique (F.W.I.). J. Essent. Oil Res. 28:436–444

Khan, H. Sureda, A., Belwal, T., Cetinkaya, S., Süntar, I., Tejada, S., Devkota, H.P., Ullah, H., Aschener, M. 2019. Polyphenols in the treatment of autoimmune diseases. Autoimmun Rev. 18:647-657.

Kim, H. S., Sun, X., Lee, J.H., Kim, H.W., Fu, X., Leong, K.W. 2019. Advanced drug delivery systems and artificial skin grafts for skin wound healing. Adv Drug Deliv Rev. 146:209-239.

Kim, H.S., Lee, J.H., Kim, H.W., Fu, X., Leong, K.W. 2019. Advanced drug delivery systems and artificial skin grafts for skin wound healing. Adv Drug Deliv Rev. 146:209-239

Kim, S., Jung, E., Kim, J. H., Park, Y. H., Lee, J., Park, D., 2011. Inhibitory effects of (−)-α-bisabolol on LPS-induced inflammatory response in RAW264.7 macrophages. Food Chem Toxicol. 49:2580-2585.

Kim, T. Y., Park, H., Kim, S. K., Kim, S. J., Parck, Y. C. 2021. Production of (−)-α-bisabolol in metabolically engineered Saccharomyces cerevisiae. J Biotechnol. 340:13-21.

Kramer, A., Dissemond, J., Kim, S., Willy, C., Mayer, D., Papke, R., Tuchmann, F., Assadian, O. 2018. Consensus on Wound Antisepsis: Update 2018. Skin Pharmacol Physiol. 31:28-58.

Küba, M.C., Türkoglu, A., Oguz, A., Tuncer, M.C., Kaya, S., Basol, Ö., Bilge, H., Tatli, F. 2021. Comparison of local rosmarinic acid and topical dexpanthenol applications on wound healing in a rat experimental wound model. Folia Morphol. 80:618-624.

Kudryavtseva, A.V. Krasnov, G.S., Dmitriev, A.A., Alekseev, B.Y., Kardymon, O.L., Sadritdinova, A.F., Fedorova, M.S., Pokrovsky, A.V., Melnikova, N.V., Kaprin, A.D., Moskalev, A.A. y Snezhkina, A.V. 2016. Mitochondrial dysfunction and oxidative stress in aging and cancer. *Oncotarget*. 7(29):44879-44905.

Kudryavtseva, A.V. Krasnov, G.S., Dmitriev, A.A., Alekseev, B.Y., Kardymon, O.L., Sadritdinova, A.F., Fedorova, M.S., Pokrovsky, A.V., Melnikova, N.V., Kaprin, A.D., Moskalev, A.A. y Snezhkina, A.V. 2016. Mitochondrial dysfunction and oxidative stress in aging and cancer. Oncotarget. 7(29):44879-44905.

Kuhnt, M., Rimpler, H., Heinrich, M. 1993. Lignans and others compounds from the mixe indian medicinal plant *Hyptis verticillata*. Phytochemistry. 36(2):485-489.

Kumar, D. S., Choudhuri, P.K., Srivastava, R., Sharma, M. 2019. Antimicrobial, anti-inflammatory and wound healing activity of polyherbal formulation. Biomed Pharmacother. 111:555-567.

Las Heras, K., Igartua, M., Santos-Vizcaino, E., Hernández, R.M. 2020. Chronic wounds: current status, available strategies and emerging therapeutic solutions. J Control Release. 328:532-550

León, E.D.A. 2023. Flora Medicinal de Tonatico, Estado de México. Tesis de licenciatura para obtener el título de Bióloga. FES Iztacala. UNAM. México. (En proceso).

Li, J., Chou, H., Lei, L., Li, H., Cui, Z. 2020. Wound healing activity of neferine in experimental diabetic rats through the inhibition of inflammatory cytokines and nrf-2 pathway. Artif Cells Nanomed Biotechnol. 48:96-106.

Li X, Yang X, Wang Z, Liu, Y., Guo, J., Zhu, Y., Shao, J., Li, J., Wang, L., Wang, L. 2022. Antibacterial, antioxidant and biocompatible nanosized quercetin-PVA xerogel films for wound dressing. Colloids Surf B: Biointerfaces 209-112175.

Low, J.S. Mak, K.K., Zhang, S., Pichika, M.R., Marappan, P., Mohandas, K., Balijepalli, M.K. 2021. In vitro methods used for discovering plant derived products as wound healing agents – An update on the cell types and rationale. Fitoterapia. 154:105026.

Lynch, M.D., Watt, F.M. 2018. Fibroblast heterogeneity: implications for human disease. The Journal of Clinical Investigation. 128:26-35

Martínez-Gordillo, M., Fragoso-Martínez, I., García-Peña, M. R., Montiel, O. 2013. Géneros de Lamiaceaee de México, diversidad y endemismo. Rev Mex Biodiv. 84:30-86.

Meng, Z., Zhou, D., Gao, Y., Zeng, M., Wang, W. 2018. miRNA delivery for skin wound healing. Adv Drug Deliv Rev. 129: 308-318.

Mi, Y., Zhong, L., Lu, S., Hu, P., Pan, Y., Ma, X., Yan, B., Wei, Z., Yang, G. 2022. Quercetin promotes cutaneous wound healing in mice through Wnt/β-catenin signaling pathway. J Ethnopharmacol. 290:115066.

Monavarian, M., Kader, S., Moeinzadeh, S., Jabbari, E. 2019. Regenerative Scar-Free Skin Wound Healing. Tissue Eng Part B Rev. 25(4):294-311.

Nakatani, N. 1994. Chemistry of antioxidants from Labiatae Herbs. Food Phytochemicals for Cancer Prevention II. Chapter 16. 144-153

Nascimento, P.F.C., Alviano, W.S., Nascimento, A.L.C., Santos, P.O., Arrigoni-Blank, M. F., De Jesus, R.A., Azevedo, V.G., Alviano, D.S., Bolognese, A.M., Trindade, R.C., 2008. *Hyptis pectinata* essential oil: chemical composition and anti-*Streptococcus mutans* activity. Oral Dis. 14, 485–489

NOM-062-ZOO-1999. Especificaciones técnicas para la producción, cuidado y uso de los animales de laboratorio. Diario Oficial de la Federación. 107-165.

Nour, S., Baheiraei, N., Imani, R., Khodaei, M., Alizadeh, A., Rabiee, N., Moazzeni, S. M. 2019. A review of accelerated wound healing approaches: biomaterialassisted tissue remodeling. J Mater Sci: Mater Med. 30:120.

Nussbaum, S.R., Carter, M.J., Fife, C.E., Da Vanzo, J., Haught, R., Nusgart, M., Cartwright, D. 2018. An economic evaluation of the impact, cost, and medicare policy implications of chronic nonhealing wounds. Value in Health. 21:27-32.

OECD. (2015). In Test No. 404 acute: Dermal irritation/corrosion. OECD (pp. 1–8).

Oliva, M. M., Demo, M. S., Lopez, A. G., Lopez, M. L., Zygadlo, J. A. 2006. Antimicrobial activity and composition of *Hyptis mutabilis* essential oil. J Herbs Spices Med. 11:57-63.

Omolara, T. J., Odoh, K. d., Obiora, N. C., Oduje, A. A., Adegboyega, A. E. 2020. Biochemical evaluation and molecular docking assessment of the anti-inflammatory potential of *Phyllanthus nivosus* leaf against ulcerative colitis. Heliyon. 6:e03893.

Özbilgin, S., Acikara, Ö.B., Akkol, E.K., Süntar, I., Keles, H., Iscan. G.S. 2018. In vivo wound-healing activity of *Euphorbia characias* subsp. *wulfenii*: Isolation and quantification of quercetin glycosides as bioactive compounds. J Ethnopharmacol. 224:400-408.

Parisotto-Peterle, J., Bidone, J., Grolli, L. L., de Moraes, S. G.A., Correa, F. M., da Silva, M. M., Horn, a. P., dos Santos, M. K., da Viega, V. F., Pereira, L. R., Ferreira, H. t., Lima, d. c., Scherer, K. L. 2020. Healing activity of hydrogel containing nanoemulsified β-caryophyllene. Eur J Pharm Sci. 148:105318.

Pereda-Miranda, R., Fragoso-Serrano, M., Cerda-García-Rojas, C. M. 2001. Application of molecular mechanics in the total stereochemical elucidation of spicigerolide, a cytotoxic 6-tetraacetyl-oxyheptenyl-5,6-dihydro-α-pyrone from *Hyptis spicigera*. Tetrahedron. 57:47-53.

Perera, W.H., Bizzo, H.R., Gama, P.E., Alviano, C.S., Salimena,F.R.G., Alviano, D.S., Leitao, S.G. 2016. Essential oil constituents from high altitude Brazilian species with antimicrobial activity: *Baccharis parvidentata* Malag., *Hyptis monticola* Mart. ex Benth. and *Lippia origanoides* Kunth. Journal of Essenntial Oil Research. 29(2):109-116.

Pérez, T.G. 2003. Los flavoides: antioxidantes o prooxidantes. Rev Cubana Invest Biomed. 22:48-57.

Pérez-Contreras, C.V., Alvarado-Flores, J., Orona-Ortiz, a., Balderas-López, J.L., Salgado, R.M., Zacaula-Juárez, N., Krötzsch, E., Navarrete, A. 2022. Wound healing activity of the hydroalcoholic extract and the main metabolites of *Amphipterygium adstringens* (cuachalalate) in a rat excision model. J Ethnoparmacol. 293:115313.

Pérez-Contreras, C.V., Alvarado-Flores, J., Orono-Ortiz, A., Balderas-López, J.K., Salgado, R.M., Zcaula-Juarez, N., Krötzsch, E., Navarrete, A. 2022. Wound healing activity of the hydroalcoholic extract and the main metabolites of *Amphipterygium adstringens* (cuachalalate) in a rat excision model. J Ethnopharmacol. 293:115313.

Picking, D., Delgoda, R., Boulogne, I., Mirchell, S. 2013. *Hyptis verticillata* Jacq: Are view of its traditional uses, phytochemistry, pharmacology and toxicology. J Ethnopharmacol. 147:16-41.

Ptaschinski, C., Hrycaj, S. M., Schaller, M. A., Wellik, D. M., Lukacs, N. 2017. Hox5 paralogous genes modulate Th2 cell function during chronic allergic inflammation via regulation of Gata3. J Immunol. 188:501-509.

Putri, D.L., Hasanah, F., Srirustami, R., Repi, Purnomo, R., Harsodjo, S. 2019. Wound healing properties of *Epiphyllum oxypetalum* (DC.) Haw. leaf extract in streptozotocin-induced diabetic mice by topical application. Wound Medicine. 26:100160.

Qiao, Y., He, J., Chen, W., Yu, Y., Li, W., Du, Z., Xie, T., Ye, Y., Hua, S. Y., Zhong, D., Yao, K., Zhou, M. 2020. Light-activatable synergistic therapy of drug-resistant bacteria-infected cutaneous chronic wounds and nonhealing keratitis by cupriferous hollow nanoshells. ACS nano. 14:3299-3315.

Rajhi, I., Boulaaba, M., Baccouri, B., Rajhi, F., Hammami, J., Barhoumi, F., Flamini, G., Mhadhbi, H. 2020. Assessment of dehulling effect on volatiles, phenolic compound, and antioxidant activities of faba beans seeds and flours. S Afr J Bot. 147:741-753.

Rajoo, A., Ramanathan, S., Mansor, S.M., Sasidharan, S. 2021. Formulation and evaluation of wound healing activity or Elaeis guineensis Jacq leaves in a Staphylococcus aureus infected Sprague Dawley rat model. J Ethnopharmacol. 266:113414.

Rebelo, M.M., Silva, J.K.R.D., Andrade, E.H.A., Maia, J.G.S. 2009. Antioxidant capacity and biological activity of essential oil and methanol extract of *Hyptis crenata* Pohl ex Benth. Rev Bras Farmacog. 19:230-235.

Ren, J., Yang, M., Chen, J., Ma, S., Wang, N. 2020. Anti-inflammatory and wound healing potential of kirenol in diabetic rats through the suppression of inflammatory markers and matrix metalloproteinase expressions. Biomed Pharmacother. 129:110475.

Rodriguez, M., Kosaric, N., Bonham, C.A., Gurtner, G.C. 2019. Wound healing: a celular perspective. Physiol Rev. 99:665-706.

Rognoni, E., Watt, F.M. 2018. Skin cell heterogeneity in development wound healing, and cancer. Trends Cell Biol. 28:709-722

Rojas, A., Hernández, L., Pereda-Miranda, R., Mata, R. 1992. Screening for antimicrobial activity of crude drug extracts and pure natural products from Mexican medicinal plants. J Ethnopharmacol. 35:275-283.

Romana-Souza, B., dos Santos, J.S., Bandeira, L.G., Monte-Alto-Costa, A. 2016. Selective inhibition of COX-2 improves cutaneous wound healing of pressure ulcers in mice through reduction of iNOS expression. Life Sciences. 153:82-92.

Sanchez-Aguirre, O., Cruz-Navarro, A., Guevara-Valencia, M., Rengifo-Salgado, E., Vargas-Arana, G. Phytochemical screening, antioxidant activity and in vitro biological evaluation of leave extracts of *Hyptis suaveolens* (L.) from south of Mexico. S Afr J Bot. 128:62-66.

Santos, E.L., Freita, P.R., Araújo, A.C.J., Almeida, R.S., Tintino, S.R., Paulo, C.L.R., Silva A.C.A., Silva, L.E., do Amaral, W., Deschamps, C., Pinto, S.J.J., Barbosa, F.J.M., Ribeiro, Sousa, G., Ribeiro-Filhho, J., Coutinho, H.D.M. 2021. Enhanced antibacterial effect of antibiotics by the essential oil of *Aloysia gratissima* (Gillies & Hook.) Tronc. and its major constituent beta-caryophyllene. Phytomedicine Plus. 1:100100.

Santos, M.R.V., Carvalho, A.A., Medeiros, I.A., Alves, P.B., Marchioro, M., Antoniolli, A.R. 2007. Cardiovascular effects of *Hyptis frutiosa* essential oil in rats. Fitoterapia. 78:186-191.

Santos, O.P., Costa, M.J.C., Alves, J.A.B., Nascimento, P.F.C., de Melo, D.L.F.M., Barbosa, A.M., Tridade, R.C. 2008. Chemical composition and antimicrobial activity of the essential oil of *Hyptis pectinata* (L.) Poit. Quimica Nova. 31 (7):1648-1652.

Sathyanarayanan, S., Muniyandi, K., George, E., Sivaraj, D., Sasidharan, S. P., Thangaraj, P. 2017. Chemical profiling of *Pterolobium hexapetalum* leaves by HPLC analysis and its productive wound healing activities in rats. Biomed Pharmacother. 95:287-297.

Setiawati, A., Immanuel, H., Utami, M.T. 2016. The inhibition of *Typhonium flagelliforme* Lodd. Blume leaf extract on COX-2 expression of WiDr colon cancer cells. Asian Pac J Trop Biomed. 6 (3):251-255.

Sheng, L. J., Mak, K.K., Zhang, S., Rao, M. P., Marappan, P., Mohandas, K., Katyayani, B. K. 2021. In vitro methods used for discovering plant derived products as wound healing agents – An update on the cell types and rationale. Fitoterapia. 154:105026.

Shorky, A.A., El-Shiekh, R.A., Kamel, G., Bakr, A., Ramdan, A. 2022. Bioactive phenolics fraction of *Hedera helix* L. (Common Ivy Leaf) standardized extract ameliorates LPS-induced acute lung injury in the mouse model through the inhibition of proinflammatory cytokines and oxidative stress. Heliyon. 8 (5):e09477.

Silva, C. G., Raulino, R. J., Cequeira, D. M., Mannarino, S. C., Pereira, M. D., Panek, A. D. Silva, J. F. M., Menezes, F. S., Eleutherio, E. C. A. 2009. *In vitro* and *in vivo* determination of antioxidant activity and mode of action of isoquercitrin and *Hyptis fasciculata.* Phytomedicine. 16:761-767.

Silva, C.G., Herdeiro, R.S., Mathias, C.J., Panek, A.D., Silvaeira, C.S., Rodrigues, V.P. Renno, M.N., Falcao, D.Q., Cerqueira, D.M., Minto, A.B.M., Nogueire, F.L.P., Quaresma, C.H., Silva, J.F.M., Menezes, F.S., Eleutherio, E.C.A. 2005. Evaluación of antioxidant activity of Brazilian plants. Pharmacological Research. 52:229-233.

Silva, L.L., Garlet, Q.I., Benovit, S.C., Dolci, G., Mallmann, C.A., Bürger, M.E., Baldisserotto, B., Longhi, S.J., Heinzmann, B.M., 2013. Sedative and anesthetic activities of the essential oils of *Hyptis mutabilis* (Rich) Briq. and their isolated components in silver catfish (Rhamdia quelen). Braz J Med Biol Res. 46:771–779.

Singleton, V.L., Orthofer, R., Lamuela-Raventós, R.M. 1999. Analysis of total phenols and other oxidation substrates and antioxidants by means of Folin-Ciocalteu Reagent. Methods in Enzymology, 29:152–178.

Souza, F.K., Kato, N.N., Boareto, A.G., Weber, F.R.B.J.I., Macedo, A.F., Tasca, T., Macedo, A.J., Brenta, S.D., Carollo, C.A. 2019. *Nectandra* as a renewable source for (+)-α-bisabolol, an antibiofilm and anti-*Trichomonas vaginalis* compound. Fitoterapia. 136:104179.

Sujamol, M.S., Roy, J., James, K.M. (2021). Phytochemical screening and antimicrobial activity of Coleus aromaticus leaf extract. Materials Today Proceedings, 41, 569–599.

Sujamol, M.S., Roy, J., James, K.M. (2021). Phytochemical screening and antimicrobial activity of Coleus aromaticus leaf extract. Mater Today Proc, 41, 569–599.

Sun, Z., Williams, G.M. Chapter 18 - Skin wound healing: skin regeneration with pharmacological mobilized stem cells, Editor(s): Sang Jin Lee, James J. Yoo, Anthony Atala, In Situ Tissue regeneration. Academic Press. 2016. 345-368.

Süntar, I.P., Akkol, E.K., Yilmazer, D., Baykal, T., Kirmizibekmez, H., Alper, M., Yesilada, E. 2010. Wound healing potential of *Sambucus ebulus* L. leaves and isolation of an active component, quercetin 3-O-glucoside. J Ethnopharmacol. 127:468-477.

Swarup, V., Ghosh, S., Ghosh, a., Basu, A. 2007. Antiviral and anti-inflammatory effects of rosmarinic acid in an experimental murine model of Japanese encephalitis Antimicrob Agents Chemother. 51: 3367-3370.

Tchoumbougnang, F., Amvam Zollo, P.H., Fekam Boyom, F., Nyegue, M.A., Bessiere, J. M., Menut, C., 2005. Aromatic plants of tropical central africa. XLVIII. Comparative study of the essential oils of four *Hyptis* species from Cameroon: *H. lanceolata* Poit., *H. pectinata* (L.) Poit., *H. spicigera* Lam. and *H. suaveolens* Poit. Flavour Fragr J. 20:340–343.

Tesch, N.R., Yanez, R., Rojas, X.M., Rojas-Fermin, L., Carrillo, J.V., Diaz, T., Vivas, F.M., Colmenares, C.C., Gonzalez, P.M., 2015. Chemical composition and antibacterial activity of essential oil *Hyptis suaveolens* (L.) Poit. (Lamiaceae) from the Venezuelan plains. Rev Peru Biol. 22:103–107.

Tung, Y., Yen, P., Chang, S., Tung, Y., Yen, P. 2010. Anti-inflammatory activities of essential oils and their constituents from different provenances of indigenous cinnamon (*Cinnamomum osmophloeum*) leaves. Pharm Biol. 48:1130-1136.

Turner, B. L. 2011. Overview of the genus *Asterohyptis* (Lamiaceaee) and description of a new species from northern Mexico. Phytoneuron. 2:1-6.

Ud-Din, S., Foden, P., Mazhari, M., Al-Habba, S., Baguneid, M., Bulfone-Paus, S., McGeorge, D., Bayat, A. 2019. A double-blind, randomized trial shows the role of zonal priming and direct topical application of epigallocatechin-3-gallate in the modulation of cutaneous scarring in human skin. J Invest Dermatol. 139:1680-1690.

Urones, J.G., Marcos, I.S., Diez, D., Cubilla, R.L. 1997. Tricyclic diterpenes from Hyptis dilatata. Phytochemistry. 48(6):1035-1038.

Vasileva, L.V., Savova, M.S., Tews, D., Wabitsch, M., Georgiev, M.I. 2021. Rosmarinic acid attenuates obesity and obesity-related inflammation in human adipocytes. Food Chem Toxicol. 149:112002.

Vilasboas-Campos, D., Costa, M. D., Teixeira-Castro, A., Rios, R., Guimaraes, S. F., Bessa, C., Dias, A. C. P., Maciel, P. 2021. Neurotherapeutic effect of Hyptis spp. leaf extracts in *Caenorhabditis elegans* models of tauopathy and polyglutamine disease: Role of the glutathione redox cycle. Free Radical Bio Med. 162:202-215.

Violante, I.M.P., Hamerski, L., Silva, G.W., Batista, A.L., Rodrigues, C.M., Pott, V.J., Rodrigues, G.F. 2012. Antimicrobial activity of some medicinal plants from the cerrado of the central Western Region of Brazil. Braz J Microbiol. 43(4):1302-1308

Vishwakarma, R.K., Negi, A., Negi, D.S. 2022a. Anti-oxidant, COX inhibition activity of different extract of bark of *Betula utilis* and molecular docking analysis of its phytochemicals against COX-1 and COX-2 isoenzyme. Mater Today: Proc. 57(Part 1): 251-258.

Vishwakarma, R.K., Negi, A., Negi, D.S. 2022b. Development of potential COX inhibitor as anti-inflammatory agents from leaves of *Lantana camara* by *in-vitro* analysis, molecular docking and ADMET prediction. J Indian Chem Soc. 99 (10): 100694.

Wald-Dickler, N., Holtom, P., Spellberg, B. 2018. Busting the Myth of “Static vs Cidal”: A Systemic Literature Review. Clin Infect Dis. 66:1470-1474.

Wang, P.H., Huang, B.S., Horng, H.C., Yeh, C.C. y Chen, Y.J. 2018. Wound healing. J Chin Med Assoc. 81:94-101.

Wani, T.U., Raza, S.N., Khan, N.A. 2019. Rosmarinic acid loaded chitosan nanoparticles for wound healing in rats. IJPSR. 10:1138-1147.

Wu, X., Zhang, Q., Wang, Z., Xu, Y., Tao, Q., Wang, J., Kong, X., Sheng, K., & Wang, Y. 2022. Investigation of construction and characterization of carboxymethyl chitosan - sodium alginate nanoparticles to stabilize Pickering emulsion hydrogels for curcumin encapsulation and accelerating wound healing. Int J Biol Macromol, 209:1837–1847.

Xavier-Santos, J., Ramos Passos, J.G., Santos Gomes, J.A., Cavalcante Cruz, J.V., Ferreira Alves, J.S., Barreto Garcia, V., Moreira da Silva, R., Peporine Lopes, N., Araujo-Junior, R.F., Zucolotto, S.M., Suilva-Junior, A.A., Félix-Silva, J., Fernandes-Pedrosa, M.F. 2022. Topical gel containing phenolic-rich extract from Ipomoea pes-capre leaf (Convolvulaceae) has anti-inflammatory, wound healing, and antiophidic properties. Biomed Pharmacother. 149:112921.

Yan, Y., Liu, X., Zhuang, Y., Zhai, Y., Yang, X., Yang, Y., Wang, S., Hong, F., Chen, J. 2020. Pien Tze Huang accelerated wound healing by inhibition of abnormal fibroblast apoptosis in *Streptozotocin* induced diabetic mice. J Ethnorpharmacol. 261:113203.

Yazarlu, O., Iranshahi, M., Kashani, H.R.K., Reshadat, S. Habtemariam, S., Iranshanhy, M., Hasampour, M. 2021.Perspective on the application of medicinal plants and natural products in wound healing: A mechanistic review. Pharmacol Research. 174:105841.

Yunitasari, N., Swasono, R. T., Pranowo, H. D., Raharjo, T. J. 2022. Phytochemical screening and metabolomic approach based on Fourier transform infrared (FTIR): Identification of α-amylase inhibitor metabolites in *Vernonia amygdalina* leaves. J Saudi Chem Soc. 26:101540.

Zhao, R., Liang H., Clarke, E., Jackson, C., Xue, M. 2016. Inflammation in Chronic Wounds. International Journal of Molecular Sciences. 17: 2085.Liu, W. Y., Tzeng, T. F., Liu, I. M. 2017. Healing potential of zerumbone ointment on experimental full-thickness excision cutaneous wounds in rat. J Tissue Viability. 26:202-207.

Zhao, R., Liang H., Clarke, E., Jackson, C., Xue, M. 2016. Inflammation in Chronic Wounds. International J Mol Sci. 17: 2085.

Zhao-Fleming, H. Hand, A., Zhang, K., Polak, R., Northcut, A., Jacob, D., Dissanaike, S., Rumbaugh, K.P. 2018. Effect of non-steroidal anti-inflammatory drugs on post-surgical complications against the backdrop of the opioid crisis. Burns Trauma. 13:25.

Zhou, L., Cai, L., Ruan, H., Zhang, L., Wang, J., Jiang, H., Wu, Y., Feng, S., Chen, J. 2021. Electrospun chitosan oligosaccharide/polycaprolactone nanofibers loaded with wound-healing compounds of Rutin and Quercetin as antibacterial dressings. Int J Biol Macromol. 183:1145-1154.

Zhou, L., Xi, Y., Xue, Y., Wang, M., Liu, Y., Guo, Y., Lei, B. 2019. Injectable self-healing antibacterial bioactive polypeptide-based hybrid nanosystems for efficiently treating multidrug resistant infection, skin-tumor therapy, and enhancing wound healing. Adv Funct Mater. 29(22):1806883.

Zhou, L., Xu, T., Yan, J., Li, X., Xie, Y., Chen, H. 2020. Fabrication and characterization of matrine-loaded konjac glucomannan/fish gelatin composite hydrogel as antimicrobial wound dressing. Food Hydrocoll. 104:105702.

Zuo, A.R., Dong, H.H., Yu, Y.Y., Shu, Q.L., Zheng, L.X., Yu, X.Y., Cao, S.W. 2018. The antityrosinase and antioxidant activities of flavonoids dominated by the number and location of phenolic hydroxyl groups. Chin Med. 13:51.

ANEXO I. *Asterohyptis stellulata*: phytochemistry and wound healing activity (artículo de requisito.

Food Bioscience 50 (2022) 102150

Contents lists available at ScienceDirect

Food Bioscience

journal homepage: www.elsevier.com/locate/fbio

Asterohyptis stellulata: Phytochemistry and wound healing activity

Nallely Álvarez-Santos [a,b], Edgar Antonio Estrella-Parra [a], José del Carmen Benítez-Flores [c], Rocío Serrano-Parrales [d], Tomás Ernesto Villamar-Duque [e], Martha Angelica Santiago-Santiago [f], María del Rosario González-Valle [c], José Guillermo Avila-Acevedo [a], Ana María García-Bores [a,*]

[a] Phytochemistry Laboratory, UBIPRO, Superior Studies Faculty (FES)-Iztacala, National Autonomous University of Mexico (UNAM), Tlalnepantla de Baz, Mexico State, 54090, Mexico
[b] Postgraduate Biological Sciences, Postgraduate Studies Unit, National Autonomous University of Mexico (UNAM), Coyoacan, Mexico City, 04510, Mexico
[c] Histology Laboratory 1, UMF, Superior Studies Faculty (FES)-Iztacala, National Autonomous University of Mexico (UNAM), Tlalnepantla de Baz, Mexico State, 54090, Mexico
[d] Natural Products Bioactivity Laboratory, UBIPRO, Superior Studies Faculty (FES)-Iztacala, National Autonomous University of Mexico (UNAM), Tlalnepantla de Baz, Mexico State, 54090, Mexico
[e] Bioterium, Superior Studies Faculty (FES)-Iztacala, National Autonomous University of Mexico (UNAM), Tlalnepantla de Baz, Mexico State, 54090, Mexico
[f] Plant Physiology Laboratory, UBIPRO, FES-Iztacala, UNAM, Tlalnepantla de Baz, Mexico State, 54090, Mexico

ARTICLE INFO

Keywords:
Asterohyptis stellulata
Phytochemistry
Skin regeneration
Wound healing

ABSTRACT

Wound healing is a fast and efficient process. However, several factors can inhibit healing, causing scars and chronic wounds. This affects patients in their physical integrity, economic and emotional stability. Many plants that are used in wound healing treatment have antioxidant/anti-inflammatory activity through ROS regulation and antibacterial activity. *Asterohyptis stellulata* is used for wound treatment. Nonetheless, this activity has not been evaluated and its secondary metabolites are unknown. Therefore, the objective of this study was to analyze its phytochemical composition and evaluate the healing activity of *A. stellulata*. For the identification of secondary metabolites, the following were carried out: phytochemical screening, quantification of total phenols, and HPLC/MS analysis. The antibacterial and antioxidant activities were also determined. Next, to evaluate the healing activity of topical application of *A. stellulata*, the extract was mixed with the Beeler base to form an emulsion and an irritability test was performed. The emulsion was evaluated on incisional wounds of CD1 et/et mice, with tests of tensile strength, total re-epithelialization time, wound closure speed, and histological analysis. The phytochemical analysis showed that *A. stellulata* has phenolic compounds, two quercetin derivatives and a glycoside rosmarinic acid as main compounds. The extract exhibited medium antibacterial and antioxidant activities. *A. stellulata* emulsion was non-irritating, promoted closure speed of wound (1.479 ± 0.043 mm/day), increased tensile strength (980 ± 89.44 g), and histological analysis showed it promoted mice skin regeneration, compared to the controls (Recoveron® and Beeler base). This study confirms the traditional use of the *A. stellulata*.

1. Introduction

The skin is the largest organ in the human body, it helps maintain homeostasis and protects internal organs (Rognoni & Watt, 2018). The skin frequently suffers damage known as wounds. The healing allows for integral restoration, and function of the tissue is recovered to the greatest extent possible (Gurtner et al., 2008) Wound healing process has four phases: a) hemostasis, provides a temporary fibrin clot and inhibit the loss of blood; b) inflammation, debridement of the wound through production of reactive oxygen species (ROS) by neutrophils and macrophages; c) proliferation, synthesize extracellular matrix (ECM), re-epithelialization, and wound contraction; d) remodeling, it begins with maturation of collagen type III which changes to a more resistant type I, and ends with the formation of scar or with restoration of tissue (Kamarazaman et al., 2022; Mi et al., 2022).

Under normal physiological conditions, the healing process is fast

* Corresponding author. Phytochemistry Laboratory, UBIPRO, Superior Studies Faculty (FES)-Iztacala, National Autonomous University of Mexico (UNAM), Av. de Los Barrios No.1, Los Reyes Iztacala, Tlalnepantla de Baz, Estado de México, 54090, Mexico.
E-mail address: boresana@iztacala.unam.mx (A.M. García-Bores).

https://doi.org/10.1016/j.fbio.2022.102150
Received 30 August 2022; Received in revised form 9 October 2022; Accepted 25 October 2022
Available online 4 November 2022

and efficient. However, aging, chronic diseases such as diabetes, vascular disease, and cancer can decrease the capacity of healing of tissue (Bao et al., 2022). Consequently, this promotes chronicity in wounds, characterized by factors such as exacerbate oxidative stress (increase of ROS), excessive inflammation, and sometimes infection (Sathyanarayanan et al., 2017). Likewise, excessive production of ROS causes cell and tissue damage (Süntar et al., 2012). Furthermore, the inflammatory phase may be prolonged by ROS-mediated activation of the NF-κB, AKT and MAPK pathways (Romo-Rico et al., 2022). When anti-inflammatory drugs are used, corticosteroids (Wang et al., 2013) and non-steroidal medicaments (Zhao-Fleming et al., 2018) can delay wound healing.

Another factor that obstructs healing is infection which could potentially lead to bacteremia and septicemia. *Staphylococcus aureus*, *S. epidermidis*, *Pseudomonas aeruginosa*, and *Escherichia coli* are some pathogens associated with wound infection (Rajoo et al., 2021). In addition, the use of antibiotics in non-infected wounds is associated with bacterial resistance (Caldwell, 2020).

Consequently, skin injuries affect many patients worldwide and cost billions of dollars to the public and private sectors (Nussbaum et al., 2018). Therefore, searching for new drugs with healing activity and fewer side effects is important.

Many plants that are used in wound healing treatment. *Aloe vera* enhances the wound healing with activities such as antioxidant, antibacterial, and anti-inflammatory properties, and increased synthesis of ECM (Yazarlu et al., 2021). Likewise, the topical application of *Verbesina crocata* promotes the regeneration of tissue, this is due to the secondary metabolites they produce (García-Bores et al., 2020). Phenolic compounds rutin, and quercetin have wound healing activity, act as an anti-inflammatory, antioxidant, and antimicrobial (Mssillou et al., 2022). Therefore, plants are the main source of research for drug formulation (Shedoeva et al., 2019).

Asterohyptis stellulata (Benth.) Epling is a Lamiaceae distributed from Mexico to Central America (Turner, 2011). It is used to treat wounds in the community of 'Los Amates', Tonatico, Mexico State. Aerial parts are boiled in water and locally applied on lavage in humans and animals, but there are no studies on it. Therefore, the aim of this research was to evaluate wound healing activity of the topical application of the crude methanolic extract of *A. stellulata* (ASM) in emulsion (ASME) with Beeler base and identify the secondary metabolites present in the extract.

2. Materials and methods

2.1. Chemicals

Methanol (MeOH 9063), hexane (9262), ethanol (EtOH 8006), chloroform (9175-03), $FeCl_3$ (1996), $K_3Fe(CN)_6$ (3114), acetonitrile (9017-03), H_3PO_4 (5854), H_2S0_4 (5642), ethyl acetate (9278) CH_3COOH (9511), HCl (9539), triethanolamine (9468) J.T. Baker (USA). 1,1-diphenyl-2-picrylhydrazyl (DPPH D9132), 2,2′-azino-bis-(3-ethylbenzothiazoline-6-sulphonic acid) radical cation (ABTS A1888), 2,4,6-Tris(2-pyridyl)-s-triazine (T1253), trolox (238813), alfa naphthol (N0875), sodium acetate trihydrate (236500), catechin (C1251), DMSO (D4540), Dragendorff reagent (44578), eosin (E4382), Folin-Ciocalteu's phenol reagent (F9252), gallic acid (G7384), hematoxylin (H3136), paraformaldehyde (P6148), quercetin (337951), shikimic acid (S5375), Biebrich's Scarlet Ponceau BS (B6008), acid fuchsin (F8129), phosphomolybdic acid (79560), aniline blue (415049), NA_2HPO_4 (7558-79-4) Sigma Aldrich (USA). Mayer reagent (36048) Fluka, Honeywell (USA). NaOH (1823), acetic anhydride (30188), sodium carbonate (103501N), NAH_2PO_4 (510012) Merck (Germany). Vainillin (2655) Meyer (Mexico). Picric acid (327) Laboratories FARQUINAL (Mexico). Paraffin Golden Bell, Mexico. Xylene (917-19) Hycel (Mexico). Mueller Hinton Agar (211667) Bioxon, BD (USA). Mueller Hinton Broth (275730) Difco, MD (USA). Recoveron® (C+) (sodium acexamate cream 5%) Armstrong (Mexico). Isoflurane PiSA (Mexico). Glycerin USP La Corona (Mexico).

2.2. Vegetable material

A. stellulata was collected in September 2019 at 'Los Amates', Tonatico, Mexico. The plant was deposited in the Izta Herbarium at the Superior Studies Faculty (FES)-Iztacala (UNAM), where a specimen was registered as No. 3303-IZTA. The plant name has been checked with "The World Flora online" (WFO, 2022).

2.3. Preparation of methanolic extract

The aerial parts of *A. stellulata* were dried at room temperature and in the shade. Subsequently, it was cut into small pieces (1176.5 g) and was then extracted by maceration with methanol (99.99% purity), 1:10 ratio, at room temperature for one week. This process was repeated three times. ASM was filtered, then concentrated under vacuum at 60 °C in rotary evaporator Laborota 4000 Heidolph Instruments (Germany). The obtained dried crude extract was stored in the dark before use. The yield was calculated using the following equation.

% Yield = (weight of dried crude extract (g)/weight of dried plant sample (g)) x 100

2.4. Phytochemical analysis

2.4.1. Phytochemical screening

ASM preliminary phytochemical screening was carried out with standard techniques to identify the groups of secondary metabolites. Tubes with 1 mg/mL of ASM/methanol were added to 3–5 drops of reactive. Precipitates indicates presence of alkaloids (Dragendorff and Mayer); blue or dark green coloration for phenols (ferric chloride test); purple halo for glycosides (Molisch test), bluish green color for steroids (Lieberman-Burchard test), orange color indicates lactones such as sesquiterpene lactones and coumarins (Baljet test), and saponins were identified by formation of foam (Guillén-Meléndez et al., 2022; Sujamol et al., 2021; Yunitasari et al., 2022). Terpenoids were identified by a thin-layer chromatography with mobile phase hexane and ethyl acetate (8:2), sprinkled with vanillin-sulfuric acid and incubated 5 min at 100 °C (Ali et al., 2021).

2.4.2. Total phenols

The Folin-Ciocalteu method was used to determine total phenolic content (Rajhi et al., 2022) with modifications in consideration of Singleton et al. (1999). Briefly, 75 μL of ASM (1 mg/mL of MeOH) were mixed with 1150 μL of distilled water, 250 μL of Folin-Ciocalteu reagent, and 1500 μL of 2% sodium carbonate. The absorbance was measured to 760 nm in the Spectrophotometer Lambda 2S UV/Vis PerkinElmer (USA). The experiments were performed in triplicate.

Considering the extract obtained is a mixture of secondary metabolites (Butnariu, 2014), an HPLC analysis was performed to identify the main phenolic compounds present in ASM.

2.4.3. HPLC-DAD-ESI-MS/MS

The phytochemical analysis of ASM (40 μL −1 mg/mL-) was performed using the method of Estrella-Parra et al. (2019) with HPLC-DAD (Thermo Dionex Ultimate 3000 HPLC, UV-ESI-MS Thermo Fischer Scientific, USA, Chromeleon software) using a Nucleodex β-OH column (200 mm × 4 mm, 5 μm; 720, 124, Macherey-Nagel, Germany). The sample was analyzed using a gradient of 0.1% formic acid in water (v/v) (A), 0.1% formic acid in acetonitrile (v/v) (B), and 0.1% formic acid in methanol (v/v) (C), starting with 95% A, 2% B and 3% C, switching to 54% A, 23% B and 23% C after 20 min, and ending with 95% A, 2% B and 3% C after 30 min. The flow rate was 0.6 mL/min. ESI/MS/MS

(Orbitrap Fusion Tri-hybrid system, Xcalibur software, Thermo Scientific Xcalibur V. 4.1.5.0, USA) was used for this procedure. The following compounds were used as standard to compare their UV spectrums and fragmentation patterns with the experimental patterns: catechin, quercetin, gallic acid, and shikimic acid. Furthermore, the experimental spectra were compared with the MassBank, PubChem, and a previously published report of *A. mociniana* (Synonym: *Hyptis mociniana*) (Espinosa-González et al., 2021).

2.5. Antioxidant activity by DPPH and FRAP assay

Phenolic compounds are known for their antioxidant activities and enhance the healing process (Mssillou et al., 2022). Therefore, the activity as a scavenger was evaluated.

The antioxidant activity of ASM was determined using the free radical 2,2-diphenyl-1-picrylhydrazyl (DPPH 250 μM) (Kamarazaman et al., 2022) with modification of MeOH as diluent. ASM was evaluated at different concentrations (10–300 μg/mL), the standards used were quercetin (1–10 μg/mL) and Trolox (10–45 μg/mL). The absorbance was measured to 515 nm with Multiscan FC Thermo Scientific (USA). The experiments were performed in triplicate. The antioxidant activity were expressed as IC_{50} value (μg/mL) and mg Trolox equivalents (TE)/g of extract.

The ferric reduction antioxidant power (FRAP) was determined using the FRAP reagent (Benzie & Devaki, 2018). ASM was evaluated at concentration of 100 μg/mL, and the standards used were quercetin (10–50 μg/mL) and Trolox (10–45 μg/mL). Each test was run in triplicate (593 nm). The antioxidant activity was expressed as mg quercetin equivalents (QE)/g of extract and mg ET/g of extract.

2.6. Antibacterial assay

The antibacterial susceptibility tests were made with bacterial strains associated with wound infection (Abbas et al., 2015; Caldwell, 2020). These were *Staphylococcus aureus* 23 MR, *S. aureus* ATCC 2913, *S. aureus* CC, *S. aureus* clinic, *S. epidermidis* ATCC 12228, *S. epidermidis* clinic, *Micrococcus luteus* ATCC 10240, *Pseudomonas aeruginosa* ATCC27853, *Escherichia coli* 82 MR, *Enterobacter aerogenes* ATCC 13048, and *Salmonella typhi* ATCC 19430. The microorganisms were obtained from the Natural Products Bioactivity Laboratory, FES-Iztacala, UNAM.

Antibacterial activity of ASM was evaluated according to the Clinical and Laboratory Standard Institute guideline M100 (CLSI, 2020). For the diffusion test, ASM was evaluated at a concentration of 2 mg per disk, measuring the inhibition halo. Chloramphenicol (30 μg/mL) was used as a positive control, and DMSO (10 μL) as a negative control. To determine the minimum inhibitory concentration (MIC), the microdilution test was done with half serial dilution (1/2) from 4 to 0.125 mg/mL. The experiments were performed in triplicate.

2.7. Skin irritation and wound healing assays

2.7.1. Experimental animals

Male CD-1 et/et mice (*Mus musculus*) aged 6–8 weeks in the FES-Iztacala Bioterium, UNAM, were employed and kept in a climate-controlled environment with a 12 h light/dark cycle. Five mice per cage were housed for the wound healing assay and three for the skin irritation test. All were acclimatized for one week before starting the experiment. The Bioethical Committee/FES Iztacala, UNAM approved all animal protocols (CE/FESI/092017/1200, 9, 27, 2017), which were developed according to NOM-062-ZOO-1999.

2.7.2. Formulation of emulsion with A. stellulata and measure of its stability

Topical emulsion (ASME) containing ASM, and Beeler base was used. This base allows the penetration of polar molecules with a high molecular size into the stratum corneum with a homogeneous distribution both in epidermis and dermis of hairless mice (Boiy et al., 2007). The Beeler base was prepared as stipulated by the Spanish Agency of Medication and Sanitary Products (AEMPS, 2019) with minor modifications (glycerin substituting propylene glycol). ASM at different concentrations of 1, 5 and 10% (w/w) were resuspended in Beeler base and homogeneously mixed, to obtain the emulsion ASME. The developed formulations were evaluated for appearance, color, and odor after 24 h of their preparation and for 6 months (Xavier-Santos et al., 2022).

The formulations were subjected to a centrifugation test (12000 rpm) for 30 min (Wu et al., 2022; Xavier-Santos et al., 2022) with Centrifuge 5418 Eppendorf (Hamburg). Afterwards, the stability of ASM was measured for the creaming index (CI) and analyzed by emulsification method (Wu et al., 2022)., which is calculated by the formula:

$$CI\ (\%) = (Hs/Ht)\ x\ 100$$

Where CI = creaming index, Hs = height of the upper emulsion layer, Ht = height of total emulsion.

After centrifugation, the occurrence of changes in the visual aspect of the formulation was observed (Xavier-Santos et al., 2022).

To determine the stability of ASM in the emulsion, this was demulsified using methanol (32 μg/mL of MeOH) and ASM to the same concentration. UV scanning (200–400 nm) was then performed using methanol as a blank (Butnariu, 2014; Wu et al., 2022).

2.7.3. ASME skin irritation test

The irritation test was based on the method established by the OECD guideline (2015) for testing chemicals 404, with modification of the use of mice as model. Three healthy male mice CD1 et/et were used as test animals. The vehicle (Beeler base without extract) and ASME at different concentrations (1, 5 and 10%) were applied topically (0.5 mL) once. At the application sites, the skin was observed and photographed for signs of erythema and edema, the first time 60 min after application and then every 24 h for three days.

2.8. Wound healing assay

The ASME (5%) was select to evaluate healing activity for the results of stability and irritation tests, as well as the previous studies (Chiocchio et al., 2018; Kamarazaman et al., 2022). Moreover, the reference drug Recoveron® sodium acexamate cream (C+) was used as a positive control and the Beeler base vehicle as a negative control (C-).

The parameters used to assess the ASME wound healing activity were based on a previous publication by the research team (García-Bores et al., 2020) with slight modifications. The physical evaluations were as follows: a) wound closure speed (WCS, mm/day); b) total re-epithelialization time (TRT, day); c) skin resistance to tensile strength (TS) necessary to open the wound. Additionally, the histological parameters were as follows: a) re-epithelialization; b) size of the healed wound (SHW) measurements were obtained with the NIS-Elements BR software -version 3.2- provided by Nikon Instruments (USA); c) thickness, disposition and maturation of collagen and granulation tissue; d) the stage of the healing process of the samples. The photomicroscope DM 5000 Leica Biosystems (Switzerland) was used for the histological analysis and photographic images.

2.9. Statistical analysis

The data were analyzed with Shapiro-Wilk and Kolmogorov-Smirnov normality tests to select the appropriate statistic. Subsequently, the data of WCS, TRT, TS and SHW were subjected to a one-way analysis of variance (ANOVA) $p < 0.05$ and linear regression to determine WCS. Statistical analysis was performed with GraphPad Prism 9 software.

3. Results and discussion

3.1. Phytochemical analysis

3.1.1. Phytochemical screening

The yield of ASM was 121.42 g (10.32% w/w). The preliminary phytochemical analysis indicated that ASM contains phenolic, terpene, lactone, steroidal, and glycosides compounds.

The genus *Asterohyptis* has been barely studied, including its phytochemical aspect (Frezza et al., 2019). The only studied species is *A. mociniana* (Synonym: *Hyptis mociniana*), for which phenolic compounds were determined in its methanolic extract. (Espinosa-González et al., 2021). Moreover, *Hyptis* species have phenolic compounds, flavonoids, terpenes, lactones (Bridi et al., 2021; Sedano-Partida et al., 2020) and alkaloids (Picking et al., 2013). These reports coincide with the phytochemical screening of *A. stellulata*.

Secondary metabolites present in plants are responsible for their biological activities. Since phenolic compounds have provided evidence on their therapeutic activity in wound healing (Mssillou et al., 2022; Xavier-Santos et al., 2022), the quantification of total phenols present in ASM was performed.

3.1.2. Total phenols

ASM had a phenol concentration of 133 ± 0.04 mg of GAE/g of extract. So far, there are no reports of total phenols of the genus *Asterohyptis*. However, in reported species of *Hyptis* the concentration of phenols is higher than in *A. stellulata*, such as *H. suaveolens* with 336.469 ± 0.005 mg GAE/g of extract (Sanchez-Aguirre et al., 2020), *H. fruticosa* had 360.51 ± 16.29 mg GAE/g of extract (de Lima et al., 2013), and *H. spicigera* with 280 ± 0.71 mg GAE/g of extract (Adamu et al., 2020). In comparison with the species of *Hyptis*; *A. stellulata* has a lower content of total phenols.

Phenolic compounds are widely known as antioxidants, anti-inflammatories (Khan et al., 2019) and antimicrobials (Ivanov et al., 2022). Thus, the presence of these compounds in the extract ASM could be associated with wound healing, which is consistent with the compounds identified by the HPLC analysis, described below.

3.1.3. HPLC-DAD-ESI-MS/MS

In the HPLC-DAD-ESI-MS/MS analysis, three compounds were identified (Fig. 1): 2-(3,4-dihydroxyphenyl)-5,7-dihydroxy-3-[2,3,4-trihydroxy-5-(hydroxymethyl) cyclohexoxy] chromen-4-one (**I**), quercetin-3-O-glycoside (**II**) and 2-O-(4-hydroxy-cinnamoyl), 4′-O-D-glicopyranoside a rosmarinic acid glycoside (**III**). Quercetin-derived compounds were identified using the quercetin fragmentation pattern and UV spectrum (Fig. S1), MassBank spectral databases and the *A. mociniana* report by Espinosa-González et al. (2021).

3.1.4. Mass analysis of quercetin compounds derivatives

Two quercetin compound derivatives (**I** and **II**) were identified (Fig. 1). The aglycone quercetin presented an intense fragment ion of 303 *m/z* [M+H] (>15). Ions present in compounds and standard quercetin were 80, 156, 212, 280, and 303 m/z [M+H] (Fig. S1).

Compound **I** (RT: 12.42 min) had a molecular ion of 463.07 m/z [M+H]. The cyclitol fragmentation showed the loss of four hydroxyl groups (68 u) corresponding to the fragment with 395.13 *m/z* [M+H]. Furthermore, the fragment ion 303 *m/z* [M+H] corresponded to the aglycone. This ion is present in the standard quercetin (Fig. S2) at the spectra reported in PubChem (2022), and Espinosa-González et al. (2021).

Compound **II** (RT: 14.58 min) had a molecular ion of 465.23 *m/z* [M+H]. The glycoside region showed the loss of four hydroxyl groups (68 u) corresponding to the fragment ion 397.17 *m/z* [M+H] and has an oxygen heteroatom in the fragment ion 329 *m/z* [M+H]. Then, fragmentation of the ether bond generated a fragment ion of 303 *m/z* [M+H] to the quercetin aglycone. Moreover, the fragment ion 303 *m/z* [M+H] corresponds to standard quercetin, according to the reports in MassBank (2022), to the study made by Espinosa-González et al. (2021), and UV spectrum coincides with the rutin (255 nm and 353 nm) and isoquercetin (260 nm and 354 nm) spectrums reported for *Morus nigra* (Alves et al., 2018). Finally, the ion fragment 153 *m/z* [M+H] was formed by Diels-Alder retro-reaction on the C-ring of quercetin aglycone (Fig. S3).

The compound **I** had not been identified in *Asterohyptis* species, *Hyptis* or any other genus of the Lamiaceae family. However, quercetin glycosides such as compound **II** were identified in *A. mociniana* in its methanolic extract: rutin, isoquercitroside, and boehemerin (Espinosa-González et al., 2021). Some species of the genus *Hyptis* also have these compounds: *H. suaveolens* has quercetin-3-O-glucoside and quercetin; *H. atrorubens* contains isoquercetin and hyperoside; *H. rhomboidea* has quercetin; and *H. salzmannii* contains hyperoside (Bridi et al., 2021; Turner, 2011).

3.1.5. Mass analysis of glycoside rosmarinic acid

Glycoside rosmarinic acid **III** (RT: 18.13 min) has a molecular ion 507.37 *m/z* [M+H]. The glycopyranoside region showed loss of hydroxyl groups (68 u) producing a fragment ion 439.17 *m/z* [M+H]. Subsequently, a water molecule (18 u) was released by a double transposition of hydrogen to oxygen of ether bond, breaking the heterocyclic ring, and releasing an aliphatic chain of C_6H_5, forming a fragment ion 344 *m/z* [M+H], which corresponds to aglycone. This, by a hydrogen transposition and ester bond breakage, resulted in a fragment ion

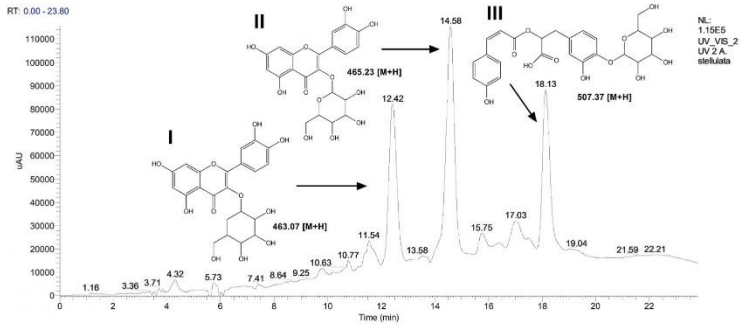

Fig. 1. ASM chromatogram. **I.** 2-(3,4-dihydroxyphenyl)-5,7-dihydroxy-3-[2,3,4-trihydroxy-5-(hydroxymethyl) cyclohexoxy] chromen-4-one (463.07 m/z [M+H]), **II.** quercetin-3-O-glycoside (465.23 m/z [M+H]), **III.** 2-O-(4-hydroxy-cinnamoyl),4′-O-D-glucopyranoside (507.37 [M+H]). UV: 254 nm.

148.97 *m/z* [M+H]. Moreover, the aglycone lost an acid group in addition to methine, forming a more abundant fragment ion 287 m/z [M+H]. Consequently, there was a loss of oxygen (16 u) that formed a more abundant fragment ion 271 m/z [M+H], and 148.97 *m/z* [M+H]. This two-oxygen loss (32 u) combined with the McLafferty rearrangement formed a tropylium group (Fig. S4). Meanwhile, spectroscopy studies revealed the presence of two absorbance peaks in the 229 nm and 328 nm region, respectively. This coincides with previous reports: rosmarinic acid (RA) present in *Rosmarinus officinalis* extracts showed UV absorbance (Olah et al., 2016) similar to our results (233 and 328). Likewise, compound III has been reported in *A. mociniana*, which presents a fragmentation pattern and UV absorbance (219 and 328 nm) that are also similar to ours (Espinosa-González et al., 2021).

RA and its derivatives are specific to the Lamiaceae family (Olah et al., 2016). In the genus *Hyptis* (Bridi et al., 2021), many species have the polyphenol RA such as *H. pectinata*, *H. suaveolens*, *H. capitata*, *H. atrorubens*, *H. verticillata*, and *H. salzmannii*.

Quercetin and RA are widely known for their antioxidant activity by free radical scavengers, chelating metals, and modulating endogenous antioxidant systems (Ferraz et al., 2021; Kumar et al., 2021). This activity is related to the pharmacological action in wound healing. Therefore, the antioxidant activity of ASM was evaluated.

3.2. Antioxidant activity DPPH and FRAP

The scavenger activity of ASM on the DPPH radical was CA_{50} = 112.84 ± 3.71 μg/mL and CA_{50} = 230 mg ET/g of extract. Standards quercetin had a CA_{50} = 5.01 ± 0.1 μg/mL and Trolox had a CA_{50} = 20.63 ± 5.75 μg/mL. *A. mociniana* had a better scavenger activity on DPPH radical with a CA_{50} = 29.06 ± 2.69 μg/mL (Espinosa-González et al., 2021). In the case of *Hyptis*, antioxidant activity on DPPH is variable per specie (126 ± 4.16–350.14 ± 13.67 mg ET/g of extract), but some of them were similar to ASM such as *H. lacustris* 265.63 ± 29.55 mg ET/g of extract, *H. meridionalis* 266.28 ± 29.55 mg ET/g of extract, and *H. multibracteata* 214.35 ± 4.99 mg ET/g of extract (Pereira et al., 2018).

In the FRAP assay, ASM presented a ferric reduction of 181.6 ± 0.05 mg of QE/g of extract and 353.14 ± 35.31 mg ET/g of extract. *Hyptis* species showed variable activity in the FRAP assay (149.15–852.76 mg TE/g of extract); the most similar to ASM were *H. lacustris* 366.96 ± 9.59 mg ET/g of extract, *H. meridionalis* 388.08 ± 17.48 mg ET/g of extract, and *H. multibracteata* 357.59 ± 6.27 mg ET/g of extract (Pereira et al., 2018).

Secondary metabolites in ASM were glycosides of quercetin and RA. The glycosylation decreases their antioxidant activity for the substitution of hydroxyl group (Ferraz et al., 2021). This could be the possible reason for the medium activity of ASM, compared to *A. mociniana* and some species of *Hyptis*. However, moderate activity in wound healing can be beneficial. For example, *Sedum album* with IC_{50} = 171.88 ± 10.02 μg/mL (DPPH) increases the percentage of wound healing (*in vitro* assay), in comparison with other species of *Sedum* more antioxidant (Chiocchio et al., 2018).

It is also worth noting that moderate antioxidant activity could modulate the inflammatory phase without inhibiting it. Antioxidants can promote healing by scavenging ROS, inhibiting lipid peroxidation, protecting tissues from oxidative damage, and modulating the inflammatory phase (Yazarlu et al., 2021). However, it is important that ROS are not completely inhibited, since they are signaling molecules that play a meaningful role in pathways such as Nrf2 -mediated cellular homeostasis/antioxidant defense- and TGF-β1 -extra-cellular matrix production, as well as fibroblast/myofibroblast-differentiation (Yazaki et al., 2021).

3.3. Antibacterial activity

ASM had moderate antibacterial activity against *S. aureus* clinical strain (inhibition halo 5.96 ± 0.06 mm; MIC > 4 mg/mL) and *S. epidermidis* clinical strain (inhibition halo 6.66 ± 0.26 mm MIC >4 mg/mL). MIC with a concentration greater than 4 mg/mL is considered a bacteriostatic agent (Wald-Dickler et al., 2018).

These results were similar to those found in some species of *Hyptis*, which are used for the treatment of skin infections and wound healing. *H. albida*, *H. pectinate*, *H. suaveolens* and *H. verticillate* exhibited an inhibition halo of 6 mm with a concentration of 20 mg/mL, but MIC was not evaluated (Rojas et al., 1992). Bacteriostatic activity in some cases is better than bactericidal (Wald-Dickler et al., 2018). This was observed in other plants that enhanced wound healing. *Elaeis guineensis* is used for the treatment of wounds, and the crude extract has a MIC of 6.25 mg/mL against *S. aureus*: when applied topically promotes tissue regeneration (Rajoo et al., 2021). One possible reason as to why moderate antibacterial activity aids the healing process could be that if it maintains a slow rate of bacterial growth, then the immune system will be able to eliminate any remaining pathogens more efficiently.

3.4. Irritation and wound healing assays

3.4.1. ASME stability

ASMEs were homogeneous, physically stable as the concentration increased (1, 5 and 10%). Likewise, color, odor, and appearance remained without changes during 6 months of observation and after the centrifugation test. Additionally, results of CI were 100% in all concentrations because they did not show separation of phases (centrifugation). UV scanning showed that ASM and ASME had the same absorption, hence the qualities of the extract were preserved (Fig. S5).

3.4.2. Skin irritation test

The irritability test of topical application at different concentrations (1, 5 and 10%) of ASME showed no signs of edema or erythema on the dorsal skin of mice (Fig. S6). Therefore, it is inferred that topical application of the ASME is non-irritating and can be used for *in vivo* evaluations.

ASME to 5% was selected for healing tests. This decision was based on previous studies where were observed that the application of extracts at higher concentrations (250, 500 and 1000 μg/mL) not necessarily have a more favorable effect *in vitro* wound healing assay (Kamarazaman et al., 2022). Furthermore, a high concentration of polyphenols in the extract (90.22 ± 1.03 μg GAE/mg of dry extract) reduces migration and proliferation in HaCaT in scratch assay, when applied in high doses −100 μg/mL- and promotes migration and proliferation to low doses −10 and 50 μg/mL- (Chiocchio et al., 2018). This could be related to the decreased production of inflammatory elements that are essential to the scarring process, thus a higher concentration may reduce its healing property (Chiocchio et al., 2018; Kamarazaman et al., 2022).

3.4.3. Wound closure speed (WCS) and total re-epithelialization time (TRT)

At the beginning of the experiment (day 0), the incisional wound size in CD-1 et/et mice was 17.06 ± 1.70 mm. On day nine, 50% of the mice in the ASME group had a total wound closure, in comparison with the controls. TRT of 100% in all groups was observed after 13 days (Fig. 2a and Fig. S7). There were no significant differences between treatments ($p > 0.05$).

WCS was higher in the group treated with Recoveron®, followed by those treated with ASM, and finally the mice treated with the vehicle (Fig. 2a). There were not significant differences between treatments ($p > 0.05$). ASME is better than other plants (13 days-17 mm). *Diospyros mespiliformis* crude methanol extract promotes healing at 13 days (15 mm) (Ebbo et al., 2022), methanolic extract of *Dodonaea viscosa* in 12 days (10 mm) (Nayeem et al., 2021), and hydroalcoholic extract of *Moringa oleifera* in 13 days (10 mm) (Ali et al., 2022).

Topical application of ASME suggests enhanced wound healing, given that WCS is similar to Recoveron®, and other plants with healing

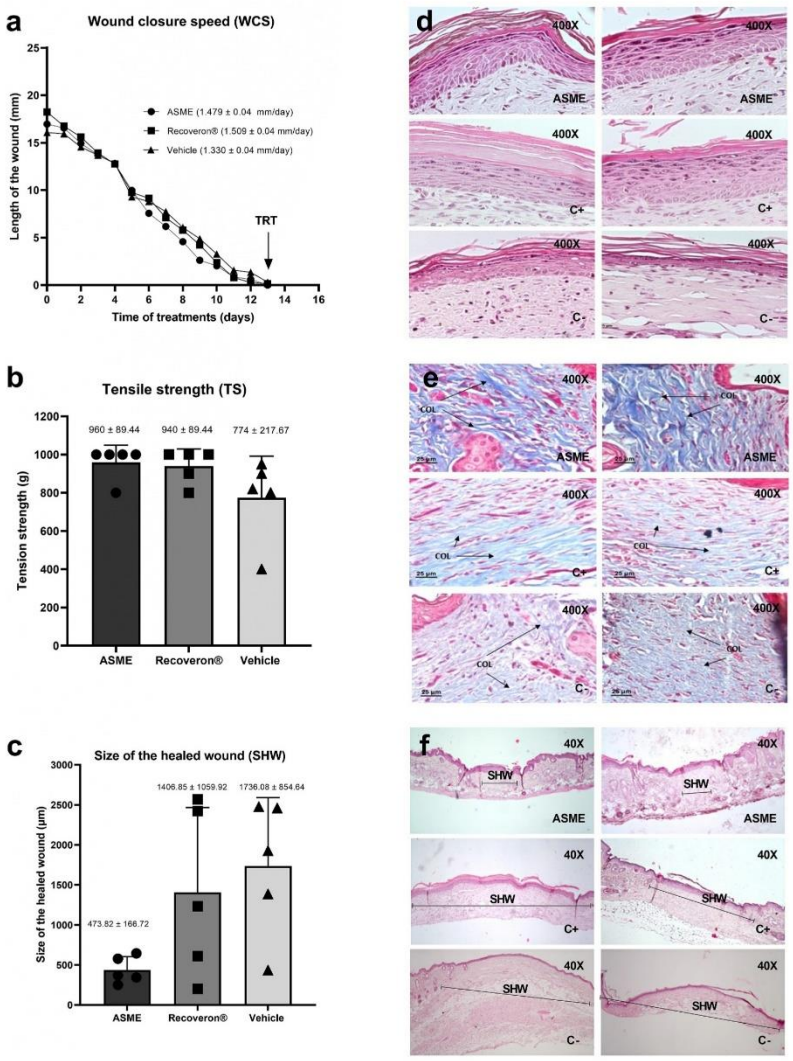

Fig. 2. Wound healing activity in the physical tests and histological analysis for topical application of ASME, Recoveron® (C+), and vehicle (C-) in incisional wounds in mice CD-1 et/et. a) Wound closure speed (WCS) and total re-epithelialization time (TRT); b) Tensile strength (TS); c) Size of the healed wound (SHW); d) Epidermis of new-formation H&E stain; e) Collagen Masson's trichrome stain; f) Size of healed wound (SHW) H&E stain. COL: collagen, SHW: size of the healed wound, ASME: Emulsion of *A. stellulata* methanolic extract.

activity. Quick re-epithelialization in wound healing is essential because it is a temporary repair mechanism that provides a barrier (Low et al., 2021). Therefore, a good treatment for healing should promote re-epithelialization and decrease the time of wound closure, with the topical application of ASME.

In addition to wound closure and re-epithelialization, the synthesis of the ECM is essential in the healing process. This matrix is mainly made up of collagen type I, which increases tensile strength. Therefore, it was the next property to be evaluated.

3.4.4. *Tensile strength (TS)*

The evaluation of the wound healing activity considering TS (g) gave the following results (Fig. 2b): the individuals treated with ASME required greater force to open the skin, followed by those treated with Recoveron®, and lastly those treated with the vehicle. There were no significant differences between treatments ($p < 0.05$). Observing a

trend, the topical application of ASME increases the TS necessary to open the healed wound, which is slightly higher than that recorded with Recoveron®. Moreover, TS in other plants was lesser than that shown by ASME (960 ± 89.44 g), such as methanolic extract of *D. viscosa* which showed TS 568.83 ± 7.77 g (Nayeem et al., 2021), hydroalcoholic extract of *M. oleifera* had 243 g (Ali et al., 2021), and methanol:methylene chloride extract of *Ceiba pentandra* showed a TS of ~800 g (Osifo et al., 2022).

TS is related to synthesis, deposition, and maturation of collagen. In the remodeling phase, the gradual degradation of immature type III collagen synthesized in the proliferation phase is fundamental, alongside the formation of mature type I collagen (Wang et al., 2018). Since type III collagen is weak and type I collagen is stronger, this step is critical to scar formation (Alhajj & Goyal, 2022). Hence, the increased TS in animals treated with ASME indicates an increase in deposition, maturation, and organization of type I collagen and possibly a better progress in the remodeling phase, compared to the controls. These results were confirmed by the histological analysis.

3.4.5. Histological analysis

3.4.5.1. Re-epithelialization and size of the healed wound (SHW). Epidermal neoformation showed differences between treatments (Fig. 2d). However, all individuals had 100% wound closure by day 13 (Fig. 2a). Mice treated with ASME and Recoveron® showed an epidermis similar to normal skin, while the vehicle group showed a visibly thinner epidermis. Additionally, SHW was lower in ASME group compared to controls, and it also presents less SHW variation in the individuals (Fig. 2c and f). In addition, plants with good healing activities promote the formation of moderately thick epidermis, similar to normal skin, such as *Cycas thouarsii* (Binsuwaidan et al., 2022), *A. vera* (Movaffagh et al., 2022), *Dalbergia tsoi* (Zhang et al., 2022). These results were similar to those observed for ASME.

Re-epithelialization and wound contraction are characteristic of the proliferative phase (Low et al., 2021). Therefore, ASME promotes the progression from proliferative phase to remodeling phase.

3.4.5.2. Thickness, disposition, and maturation of collagen. The ASME group showed the best performance in the distribution and maturation of collagen (Fig. 2e), forming dense and organized fibers, similar to the Recoveron® group, while the skin treated with the vehicle had less.

Plants with healing activity promote the maturation and synthesis of collagen, similar to ASME. For example, hydroalcoholic extract of *Amphipterygium adstringens* promoted maturation of collagen and showed regular fibers throughout the wound area (Pérez-Contreras et al., 2022); ethanolic extract of *Polygonatum kingianum* had dense and abundant collagen (Pan-Yue et al., 2022); and methanolic extract of *V. crocata* promoted synthesis and maturation of collagen (García-Bores et al., 2020).

The ECM has collagen as its main component, an adequate proportion is essential during the formation of connective tissue and the wound healing process (Pérez-Contreras et al., 2022). This related to the tensile strength reported for the different treatments, confirming that the topical application of ASME accelerates progress towards the remodeling phase.

3.4.5.3. Granulation tissue and phase of the wound healing process. The histological study of granulation tissue -middle part of healed wound- (Fig. S8) is consistent with the previous results. The sections of the ASME group had a lower number of fibroblasts/myofibroblasts, abundant blood vessels and inflammatory infiltrate was not observed. Meanwhile, the Recoveron® group had profuse reactive fibroblasts, few blood vessels and did not show inflammatory infiltrate. Finally, the vehicle group had an intermediate number of fibroblasts, few blood vessels and neutrophils. The histological, WCP, and TS results allowed us to determine the phase of healing.

Mice treated with ASME showed myofibroblasts, abundant new blood vessels, absent neutrophils, a normal new epidermis, smaller mature collagen, and minor SHW -contraction of wound- (Table 1). This implies that they are in the remodeling phase. Moreover, there are signs of regeneration, because the healed wound zone is small and there is a tendency to developed layers just like normal skin -muscle, hypodermis, dermis-, neoformation of pilose follicles, and sebaceous glands (Fig. 3d–f).

The Recoveron® group was between the proliferation and remodeling phases (Fig. 3c and Table 1). It has abundant fibroblasts, few myofibroblasts, new blood vessels, absent neutrophils, mature collagen, and better resistance to TS. Proliferation is characterized by angiogenesis, proliferation of fibroblasts (new ECM/type III collagen), keratinocytes (re-epithelialization) and endothelial cells (blood vessels) (Low et al., 2021; Yazarlu et al., 2021). Ultimately, fibroblasts and keratinocytes produce TGF-β leaning to myofibroblasts differentiation, regulating wound closure (Yazarlu et al., 2021) and beginning the remodeling phase.

The vehicle group was transitioning from inflammation to proliferation (Fig. 3b and Table 1), due to the presence of neutrophils, few fibroblasts, immature collagen, smaller resistance of TS and large SHW (null contraction). During inflammation, phagocytic cells, including neutrophils and macrophages, prevent infection and remove cell debris (Yazarlu et al., 2021). They also release cytokines, chemokines, and growth factors, involved in the recruitment and activation of fibroblast and epithelial cells for the proliferative stage (Low et al., 2021).

Wound healing may be implicated in tissue regeneration and return to the original condition (Akita, 2019). Several conditions allow tissue regeneration. *Acomys* spp. mice can completely regenerate wounded tissue due to the presence of blastema, but mice CD-1 only present scarring (Gawriluk et al., 2016). In general, skin wounds do not regenerate completely, they produce disorganized ECM, commonly known as scar (Castaño et al., 2018). Variable dermal fibrosis, effaced epidermis, limited or absent sebaceous glands and follicles can be observed in such scars, resulting in a loss of structure and function (Sun & Williams, 2016). However, the topical application of ASME in mice CD-1 et/et decreases scar formation and promotes skin regeneration, but more studies are needed to verify this.

ASM has quercetin glycoside (**II**), and these compounds have been reported in plants to improve wound healing. *Euphorbia characias* subsp. *wulfenii* (methanolic extract) showed healing functions with inhibitory activities on collagenase, elastase, and hyaluronidase; in fractions containing quercitrin, hyperoside, and guaijaverin, but fractions had no better activity (Özbilgin et al., 2018). *Sambucus ebulus* has quercetin 3-O-glucoside, an isolate of its fraction, but the healing activity was lower than that of the initial methanolic extract (Süntar et al., 2010). In addition, quercetin, kaempferol and hyperoside (43% w/w) were identified in the ethyl acetate extract from *Eugenia pruniformis*, and this extract accelerates wound healing and dermal remodeling (de Albuquerque et al., 2016). Carvalho et al. (2021), described the role of

Table 1
Parameters to define the transition of phases of the wound healing process.

Groups	E	D	Granulation Tissue				Phases (transition)
			F	M	N	V	
ASME	R	R	+	++	-	+++	Remodeling/ Regeneration
Recoveron®	R	NR	+++	+	-	++	Proliferation/ Remodeling
Vehicle	T	NR	++	-	+	+	Inflammation/ Proliferation

E: epidermis, D: dermis, R: regeneration, NR: no regeneration, T: thin, F: fibroblast, M: myofibroblast, N: neutrophil, V: new blood vessel, -: absent, +: few, ++: regular, +++: many, ASME: Emulsion of *A. stellulata* methanolic extract.

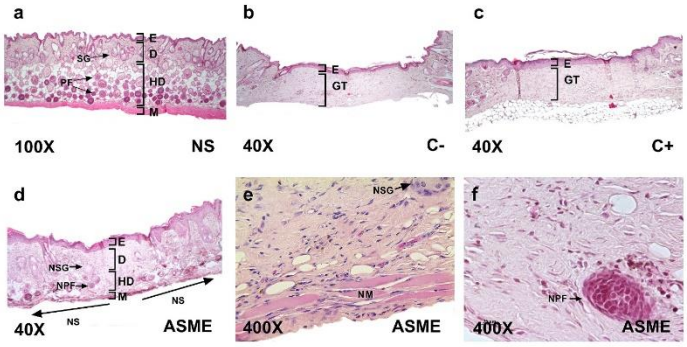

Fig. 3. Comparison of normal skin to healed tissue that underwent treatment with vehicle (C-), Recoveron® (C+), and ASME, of mice CD-1 et/et. a) Normal skin of CD-1 et/et; b) SHW treatment with vehicle; c) SHW treatment with Recoveron®; d) SHW treatment with ASME; e) Neoformation of muscle and sebaceous glands in healed wound; f) Neoformation of pilose follicle in healed wound. E: epidermis, D: dermis, GT: granulation tissue, IID: Hypodermis, M: muscle, NM: neoformation of muscle, NS: normal skin, NPF: neoformation of pilose follicle, PF: pilose follicle, SG: sebaceous gland, NSG: neoformation of sebaceous gland.

flavonoids in wound healing and tissue regeneration through different mechanisms: antioxidant, anti-inflammatory, acting on a group of cells modulating the release cytokines and growth factors, and regulating pathways involved in healing. Quercetin is a compound that promotes the healing process in mice with excisional wounds (Choudhary et al., 2020; Fu et al., 2020). Hence, the presence of these compounds in ASM could promote wound healing and regeneration.

The other metabolite present in ASM was the glycoside RA (**III**). To date, no reports from the activities of that metabolite have been found. Nonetheless, the aglycone RA is a wound healing agent. The topical application of RA cream (10%) reduced the size of the wound and resulted in less scarring, but the healing time was prolonged, and epithelialization was reduced (Küba et al., 2021). Furthermore, the application of RA in nanoparticles and gel has antibacterial, antioxidant and wound healing activities, which can decrease scar formation and promote tissue regeneration (Chhabra et al., 2020; Wani et al., 2019).

ASM is a mix of different secondary metabolites, including derived quercetin and glycoside RA. These compounds could enhance wound healing activity. However, it is possible that other unidentified metabolites have healing qualities. Some reports indicate that doing subfractions decreases the activity of the extract, given that synergy exists between the different compounds (Süntar et al., 2010; Özbilgin et al., 2018).

4. Conclusion

A. stelullata contains phenolic, terpene, lactone, steroidal, and glycoside compounds. It also has a medium content of total phenols, some of which are quercetin derivatives and rosmarinic acid glycoside. These secondary metabolites are probably responsible for the scavenger activity, reducing the concentration of ROS and modulating its function with activators of signaling pathways related to inflammation. It may also be related to the bacteriostatic activity of *A. stellulata* against *S. aureus* and *S. epidermidis* clinical strains.

Topical application of ASME to 5% in incisional wound reduced closure time and re-epithelialization. Additionally, increased collagen synthesis and maturation, consequently the tensile strength. Furthermore, it promoted advancement towards the maturation phase. This fact was confirmed by the granulation tissue with few cell groups representing the prior phases. It even showed signs of regeneration, since the healed wound zone is small and has developed layers as normal skin -muscle, hypodermis, dermis-, hair follicle, and sebaceous glands.

Therefore, topical application of *A. stellulata* promotes skin regeneration in mice CD-1 et/et, reducing the possibility of infection due to its bacteriostatic activity and regulating inflammation through antioxidant activity. These results confirm the traditional use of *A. stellulata* as a wound healing agent. However, it is necessary to do more research on the mechanism of action and its possible pharmacologic applications.

Author statement

Nallely Álvarez-Santos (Conceptualization, Methodology, Formal Analysis, Investigation, Writing-Original Draft and Visualization).

Edgar Antonio Estrella-Parra (Methodology, Visualization, Validation).

José del Carmen Benítez-Flores (Validation, Resources).

Rocío Serrano-Parrales (Methodology).

Martha A. Santiago-Santiago (Methodology, Visualization).

Tomás E. Villamar-Duque (Methodology).

María del Rosario González-Valle (Methodology).

José Guillermo Avila-Acevedo (Supervision, Resources, Review & Editing).

Ana María García-Bores (Project administration, Supervision, Writing-Review & Editing, Conceptualization, Resources and Funding Acquisition).

Declaration of competing interest

The authors confirm that they have no conflicts of interest with respect to the work described in this manuscript.

Data availability

Data will be made available on request.

Acknowledgements

This work was supported by DGAPA, PAPIIT-UNAM [IN220920], COMECyT [FICDTEM-2021-20]; Biological Sciences Postgraduate Studies Unit-UNAM, and Doctorate's Scholarship-CONACYT [CVU 775307].

We express our gratitude to Juan Antonio Reyes García, Lt. Col. José Cruz Rivera Cabrera, Chief Department of Pharmacology, Unit of LC-MS, Military Physician School, México. Dra. Claudia Tzasná Hernández-Delgado from FES-Iztacala, UNAM Natural Products Bioactivity Laboratory, Leticia Flores Sánchez from FES-Iztacala, UNAM Bioterium. M. en C. María Patricia Jácquez-Ríos from FES-Iztacala, UNAM Herbarium IZTA.

Appendix A. Supplementary data

Supplementary data to this article can be found online at https://doi.org/10.1016/j.fbio.2022.102150.

References

Abbas, M., Uçkay, I., & Lipsky, B. A. (2015). In diabetic foot infections antibiotics are to treat infection, no to heal wounds. *Expert Opinion on Pharmacotherapy, 16*, 821–832. https://doi.org/10.1517/14656566.2015.1021780

Adamu, K., Adamu, F. U., Ibrahim, R., Rabilu, S. A., Abdu, A., & Danazumi, I. B. (2020). Antifungal and phytochemical constituents of aqueous leaves extract of *Hyptis spicigera* Lam. on *Aspergillus* and *Fusarium* species. *FUW Trends in Science & Technology Journal, 5*, 520–524.

AEMPS. (2019). Monografías, excipientes. In R. B. Tarno, F. L. Escribano,T., Vara, & P. I. Alcaraz (Eds.), *Formulario nacional. Madrid:Ministerio de Sanidad, consumo y bienestar social* (p. 277). https://www.boe.es/biblioteca_juridica/abrir_pdf.php?id=PUB-NT-2019-112. (Accessed 23 June 2022).

Akita, S. (2019). Wound repair and regeneration: Mechanisms, signaling. *International Journal of Molecular Sciences, 20*, 6328. https://doi.org/10.3390/ijms20246328

de Albuquerque, R. D. D. G., Perini, J. A., Machado, D. E., Angell Gamba, T., Esteves, R. S., Santos, M. G., Passos Oliveira, A., & Rocha, L. (2016). Wound healing activity and chemical standardization of *Eugenia pruniformis* Cambess. *Pharmacognosy Magazine, 12*, 288–294. https://doi.org/10.4103/0973-1296.192206

Alhajj, M., & Goyal, A. (2022). Physiology, granulation tissue [Updated 2021 Oct 30]. In: StatPearls [Internet]. Treasure Island (FL): StatPearls Publishing. Available from: https://www.ncbi.nlm.nih.gov/books/NBK554402/. (Accessed 15 May 2022).

Ali, A. M. A., El-Nour, M. E., Yagi, S. M., Qahtan, Alatar, A. A., Abdel-Salam, E. M., & Sengin, G. (2021). Cytotoxicity, phytochemical screening and genetics analysis of ginger (*Zingiber officinale* Rosc.) callus and rhizome. *South African Journal of Botany*. https://doi.org/10.1016/j.sajb.2021.11.011 (in press).

Ali, A., Garg, P., Goyal, R., Khan, A., Negi, P., Li, X., & Kulshrestha, S. (2022). An efficient wound healing hydrogel based on a hydroalcoholic extract of *Moringa oleifera* seeds. *South African Journal of Botany, 145*, 192–198. https://doi.org/10.1016/j.sajb.2021.05.003

Alves, S. P., Rocha, S. G., Sousa, S. P. G., Carlvalho, S. A., Teixeria, A. F. J. M., Rolim-Neto, P. J., Guedes, S. A. J. R., & Araújo, R. L. (2018). Development and validation of a high performance liquid chromatography-diode array detection (HPLCDAD) method for the quantification of rutin and isoquercetin in *Morus nigra* L. (Moraceae). *African Journal of Biotechnology, 17*, 2018.

Bao, L., Cai, X., Zhang, M., Xiao, Y., Jin, J., Qin, T., & Li, Y. (2022). Bovine collagen oligopeptides accelerate wound healing by promoting fibroblast migration via PI3K/Akt/mTOR signaling pathway. *Journal of Functional Foods, 90*, Article 104981. https://doi.org/10.1016/j.jff.2022.104981

Benzie, I. F. F., & Devaki, M. (2018). The ferric reducing/antioxidant power (FRAP) assay for non-enzymatic antioxidant capacity: Concepts, procedures, limitations and applications. In R. Apak, E. Capanoglu, & F. Shahidi (Eds.), *Measurement of antioxidant activity & capacity: Recent trends and applications* (pp. 77–106). Wiley Online Library, ISBN 9781119135388. https://doi.org/10.1002/9781119135388.ch5.

Binsuwaidan, R., Elekhnawy, E., Elseady, W. S., Keshk, W. A., Shoeib, N. A., Attallah, N. G. M., Mokhtar, F. A., Abd El Hadi, S., Ahmen, E., Magdelhin, S., & Negm, W. A. (2022). Antibacterial activity and wound healing potential of *Cycas thouarsii* R. Br n-butanol fraction in diabetic rats supported with phytochemical profiling. *Biomedicine & Pharmacotherapy, 155*, Article 113763. https://doi.org/10.1016/j.biopha.2022.113763

Boiy, A., Roelandts, R., Roskams, T., & de Witte, P. A. M. (2007). Effects of vehicles and esterification on the penetration and distribution of hypericin in the skin of hairless mice. *Photodiagnosis and Photodynamic Therapy, 4*, 130–139. https://doi.org/10.1016/j.pdpdt.2007.02.002

Bridi, H., Carvalho, M. G., & Lino, V. P. G. (2021). Subtribe lyptidinae (Lamiaceae): A promising source of bioactive metabolites. *Journal of Ethnopharmacology, 264*, Article 113225. https://doi.org/10.1016/j.jep.2020.113225

Butnariu, M. (2014). Detection of the polyphenolic components in *Ribes nigrum* L. *Annals of Agricultural and Environmental Medicine, 21*, 11–14.

Caldwell, M. D. (2020). *Bacteria and antibiotics in wound healing* (Vol. 100, pp. 757–776). Surgical Clinics of North America. https://doi.org/10.1016/j.suc.2020.05.007

Carvalho, M. T. B., Araújo-Filho, H. G., Barreto, A. S., Quintana Júnior, L. J., Quintans, J. S. S., & Barreto, R. S. S. (2021). Wound healing properties of flavonoids: A systematic review highlighting the mechanisms of action. *Phytomedicine, 90*, Article 153636. https://doi.org/10.1016/j.phymed.2021.153636

Castaño, O., Pérez-Amodio, S., Navarro-Requena, C., Mateos-Timoneda, M. A., & Engel, E. (2018). Instructive microenvironments in skin wound healing: Biomaterials as signal releasing platforms. *Advanced Drug Delivery Reviews, 129*, 95–117. https://doi.org/10.1016/j.addr.2018.03.012

Chhabra, P., Chauhan, G., & Kumar, A. (2020). Augmented healing of full thickness chronic excision wound by rosmarinic acid loaded chitosan encapsulated graphene nanopockets. *Drug Development and Industrial Pharmacy, 46*, 878–888. https://doi.org/10.1080/03639045.2020.1762200

Chiocchio, I., Poli, F., Governa, P., Biagi, M., & Lianza, M. (2018). Wound healing and *in vitro* antiradical activity of five *Sedum* species grown within two sites of community importance in Emilia-Romagna (Italy). *Plant Biosystems - An International Journal Dealing with all Aspects of Plant Biology, 15*, 610–615. https://doi.org/10.1080/11263504.2018.1549611

Choudhary, A., Kant, V., Jangir, B. L., & Joshi, V. G. (2020). Quercetin loaded chitosan tripolyphosphate nanoparticles accelerated cutaneous wound healing in Wistar rats. *European Journal of Pharmacology, 880*, Article 173172. https://doi.org/10.1016/j.ejphar.2020.173172

CLSI. (2020). *Performance standards for antimicrobial susceptibility testing*. Wayne, Pennsylvania: CLSI supplement M100, ISBN 978 1 68440 135 2.

Ebbo, A. A., Sani, D., Suleiman, M. M., Ahmand, A., & Hassan, A. Z. (2022). Assessment of antioxidant and wound healing activity of the crude methanolic extract of *Diospyros mespiliformis* Hochst ex a. Dc (Ebenaceae) and its fractions in Wistar rats. *South African Journal of Botany, 150*, 305–312. https://doi.org/10.1016/j.sajb.2022.07.034

Espinosa-González, A. M., Estrella-Parra, E. A., Nolasco-Ontiveros, E., García-Bores, A. M., García-Hernández, R., López-Urrutia, E., Campos-Contreras, J. E., González-Valle, M. R., Benítez-Flores, J. C., Céspedes-Acuña, C. L., Alarcón Enos, J., Rivera-Cabrera, J. C., & Avila-Acevedo, J. G. (2021). *Hyptis mociniana*: Phytochemical fingerprint and photochemoprotective effect against UV-B radiation-induced erythema and skin carcinogenesis. *Food and Chemical Toxicology, 151*, Article 112095. https://doi.org/10.1016/j.fct.2021.112095

Estrella Parra, E. A., Espinosa González, A. M., García Bores, A. M., Zamora Salas, S. X., Benítez Flores, J. C., González Valle, M. R., Hernandez Delgado, C. T., Peñalosa Castro, I., & Avila Acevedo, J. G. (2019). Flavonol glycosides in *Dyssodia tagetiflora* and its temporal variation, chemoprotective and ameliorating activities. *Food and Chemical Toxicology, 124*, 411–422. https://doi.org/10.1016/j.fct.2018.12.024

Ferraz, C. R., Franciosi, A., Braga, E. N., Rasquel-Oliveria, F. S., Manchope, T. T., Carvalho, T. T., Artero, N. A., Fattori, V., Vicentini, F. T. M. C., Casagrande, R., & Verri, W. A., Jr. (2021). Quercetin as an anti inflammatory analgesic. In M. Mushtaq, & F. Anwar (Eds.), *A centum of valuable plant bioactives* (pp. 319–347). Academic Press, ISBN 9780128229231. https://doi.org/10.1016/B978-0-12-822923-1.00023-6.

Frezza, C., Venditti, A., Serafini, M., & Bianco, A. (2019). Phytochemistry, chemotaxonomy, ethnopharmacology, and nutraceutics of Lamiaceae. *Studies in Natural Products Chemistry, 62*, 125–178. https://doi.org/10.1016/B978-0-444-64185-4.00004-6

Fu, J., Huang, J., Lin, M., Xie, T., & You, T. (2020). Quercetin promotes diabetic wound healing via switching macrophages from M1 to M2. *Journal of Surgical Research, 246*, 213–223. https://doi.org/10.1016/j.jss.2019.09.011

García Bores, A. M., Álvarez Santos, N., López Villafranco, M. E., Jácquez Ríos, M. P., Aguilar-Rodríguez, S., Grego-Valencia, D., Espinosa-González, A. M., Estrella-Parra, E. A., Hernández-Delgado, C. T., Serrano-Parrales, R., González-Valle, M. R., & Benítez-Flores, J. C. (2020). *Verbesina crocata*: A pharmacognostic study for the treatment of wound healing. *Saudi Journal of Biological Sciences, 27*, 3113–3124. https://doi.org/10.1016/j.sjbs.2020.08.038

Gawriluk, T. R., Simkin, J., Thompson, K. L., Biswas, S. K., Clare Salzler, Z., Kimani, J. M., Kiama, S. G., Smith, J. J., Ezenwa, V. O., & Seifert, A. W. (2016). Comparative analysis of ear-hole closure identifies epimorphic regeneration as a discrete trait in mammals. *Nature Communications, 7*, Article 11164. https://doi.org/10.1038/ncomms11164

Guillén-Meléndez, G. A., Soto-Domínguez, A., Loera-Arias, M. J., Castillo-Velázquez, U., Villa-Cedillo, S., Piña-Mendoza, E. I., Estrada-Castillón, E., Chávez-Montes, A., González-Alcocer, A., Becerra-Verdín, E. M., Castañeda-Martínez, A., Pérez-Hernández, R. A., & Salas-Treviño, D. (2022). Effect of methanolic extract of *Mimosa malacophylla* A. Gray in vero and HEK-293 cell lines, and in the morphology of kidney and bladder of rats with induced urolithiasis. *Journal of Ethnopharmacology, 297*, Article 115552. https://doi.org/10.1016/j.jep.2022.115552

Gurtner, G. C., Werner, S., Barrandon, Y., & Longaker, M. T. (2008). Wound repair and regeneration. *Nature, 453*, 314–321. https://doi.org/10.1038/nature07039

Ivanov, M., Kostic, M., Stojkovic, D., & Sokovic, M. (2022). Rosmarinic acid-Modes of antimicrobial and antibiofilm activities of common plant polyphenol. *South African Journal of Botany, 146*, 521–527. https://doi.org/10.1016/j.sajb.2021.11.050

Kamarazaman, I. S., Ali, N. A. M., Abdullah, F., Saad, N. C., Ali, A. A., Ramli, S., Rojsitthisak, P., & Halim, H. (2022). *In vitro* wound healing evaluation, antioxidant, and chemical profiling of *Baeckea frutescens* leaves ethanolic extract. *Arabian Journal of Chemistry, 15*, Article 103871. https://doi.org/10.1016/j.arabjc.2022.103871

Khan, H., Sureda, A., Belwal, T., Cetinkaya, S., Süntar, I., Tejada, S., Devkota, H. P., Ullah, H., & Aschener, M. (2019). Polyphenols in the treatment of autoimmune diseases. *Autoimmunity Reviews, 18*, 647–657. https://doi.org/10.1016/j.autrev.2019.05.001

Küba, M. C., Türkoglu, A., Oguz, A., Tuncer, M. C., Kaya, S., Basol, Ö., Bilge, H., & Tatli, F. (2021). Comparison of local rosmarinic acid and topical dexpanthenol applications on wound healing in a rat experimental wound model. *Folia Morphologica, 80*, 618–624. https://doi.org/10.5603/FM.a2020.0097

Kumar, K. A., Kumar, V. A., Chayanika, G., Bhoomika, S., Rahul, B. K., & Kumar, A. (2021). Rosmarinic acid and mitochondria. In M. R. de Oliveira (Ed.), *Mitochondrial physiology and vegetal molecules* (pp. 209–231). Academic Press, ISBN 9780128215623. https://doi.org/10.1016/B978-0-12-821562-3.00030-7.

de Lima, A. C., Paixão, M. S., Melo, M., de Santana, M. T., Damascena, N. P., Dias, A. S., Porto, Y. C. B. S., Fernandes, X. A., Santos, C. S., Lima, C. A., Quintans Júnior, L. J., Estevam, C. D., & Araújo, B. S. (2013). Orofacial antinociceptive effect and antioxidant properties of the hydroethanol extract of *Hyptis fruticosa* salmz ex Benth. *Journal of Ethnopharmacology, 146*, 192–197. https://doi.org/10.1016/j.jep.2012.12.031

Low, J. S., Mak, K. K., Zhang, S., Pichika, M. R., Marappan, P., Mohandas, K., & Balijepalli, M. K. (2021). *In vitro* methods used for discovering plant derived products as wound healing agents – an update on the cell types and rationale. *Fitoterapia, 154*, Article 105026. https://doi.org/10.1016/j.fitote.2021.105026

MassBank. (2022). *Isoquercetin and quercetin*. https://massbank.eu/MassBank/RecordDisplay?id=RP017101. https://massbank.eu/MassBank/RecordDisplay?id=RP017102. https://massbank.eu/MassBank/RecordDisplay?id=RP012401. (Accessed 18 January 2022).

Mi, Y., Zhong, L., Lu, S., Hu, P., Pan, Y., Ma, X., Yan, B., Wei, Z., & Yang, G. (2022). Quercetin promotes cutaneous wound healing in mice through Wnt/β-catenin

signaling pathway. *Journal of Ethnopharmacology, 290*, Article 15066. https://doi.org/10.1016/j.jep.2022.115066

Movaffagh, J., Khatib, M., Fasly, B. B. S., Taherzadeh, Z., Hashemi, M., Seyedian, M. A., Abbas, T. S., Azizzadeh, M., & Jirofti, N. (2022). Evaluation of wound-healing efficiency of a functional Chitosan/*Aloe vera* hydrogel on the improvement of re-epithelialization in full thickness wound model of rat. *Journal of Tissue Viability*. https://doi.org/10.1016/j.jtv.2022.07.009 (in press).

Mssillou, I., Bakour, M., Slighoaua, M., Laaroussi, H., Saghrouchni, H., Amrati, F. E., Lyoussi, B., & Derwich, E. (2022). Investigation on wound healing effect of mediterranean medicinal plants and some related phenolic compounds: A review. *Journal of Ethnopharmacology, 298*, Article 115663. https://doi.org/10.1016/j.jep.2022.115663

Nayeem, N., Basheeruddin, A. S. M., Alamri, A. S., Alsanie, W. F., Alhomrani, M., Monhzari, Y., Alrashed, A. A., Alotaibi, N., Aalhathal, A. S., Alharbim, M. A., Aldhawyan, N. N., Asad, M., Abdalla, M. A., & Najmi, S. Y. (2021). Wound healing potential of *Dodonaea viscosa* extract formulation in experimental animals. *Journal of King Saud University Science, 33*, Article 101476. https://doi.org/10.1016/j.jksus.2021.101476

Nussbaum, S. R., Carter, M. J., Fife, C. E., DaVanzo, J., Haught, R., Nusgart, M., & Cartwright, D. (2018). An economic evaluation of the impact, cost, and medicare policy implications of chronic nonhealing wounds. *Value in Health, 21*, 27–32. https://doi.org/10.1016/j.jval.2017.07.007

OECD. (2015). In *Test No. 404 acute: Dermal irritation/corrosion. OECD* (pp. 1–8). https://doi.org/10.1787/9789264070622-en. Paris.

Olah, N. K., Gyongyi, O., Ramona, F. C., Pripon, F. F., Benede, D., Lorena, F., Raita, O., & Hanganu, D. (2016). The study of polyphenolic compounds profile of some *Rosmarinus officinalis* L. extracts. *Pakistan journal of pharmaceutical sciences, 29*, 2355–2361.

Osifo, M., Amarachi, I. S., Ani, N., Sylvester, N. C., & Akah, P. (2022). Wound healing and anti-inflammatory activities of *Ceiba pentendra* (L.) Gaertn. *Pharmacological Research - Modern Chinese Medicine, 3*, Article 100077. https://doi.org/10.1016/j.prmcm.2022.100077

Özbilgin, S., Acikara, Ö. B., Akkol, E. K., Süntar, I., Keles, H., & Iscan, G. S. (2018). *In vivo* wound-healing activity of *Euphorbia characias* subsp. *wulfenii*: Isolation and quantification of quercetin glycosides as bioactive compounds. *Journal of Ethnopharmacology, 224*, 400–408. https://doi.org/10.1016/j.jep.2018.06.015

Pan Yue, Q., Ya Jing, X., Xiang Duo, Z., Jun Hua, D., Bin, Q., Xue Fang, L., Jing Ping, L., & Jie, Y. (2022). Effect and mechanisms of *Polygonatum kingianum* (polygonati rhizome) on wound healing in diabetic rats. *Journal of Ethnopharmacology, 298*, Article 115612. https://doi.org/10.1016/j.jep.2022.115612

Pereira, S. K., Sedano-Partida, M. D., Sala-Carvalho, W. R., Ortega, S. J. L. B., da Silva-Luz, C., & Furlan, C. M. (2018). Biological activity of *Hyptis* Jacq. (Lamiaceae) is determined by the environment. *Industrial Crops and Products, 112*, 705–715. https://doi.org/10.1016/j.indcrop.2017.12.065

Pérez-Contreras, C. V., Alvarado-Flores, J., Orono-Ortiz, A., Balderas-López, J. K., Salgado, R. M., Zcaula-Juarez, N., Krötzsch, E., & Navarrete, A. (2022). Wound healing activity of the hydroalcoholic extract and the main metabolites of *Amphipterygium adstringens* (cuachalalate) in a rat excision model. *Journal of Ethnopharmacology, 293*, Article 115313. https://doi.org/10.1016/j.jep.2022.115313

Picking, D., Delgoda, R., Boulogne, I., & Mitchell, S. (2013). *Hyptis verticillata* jacq: A review of its traditional uses, phytochemistry, pharmacology and toxicology. *Journal of Ethnopharmacology, 147*, 16–41. https://doi.org/10.1016/j.jep.2013.01.039

PubChem. (2022). 2 (3,4 dihydroxyphenyl) 5,7 dihydroxy 3 [2,3,4 trihydroxy 5 (hydroxymethyl) cyclohexoxy] chromen 4 one. https://pubchem.ncbi.nlm.nih.gov/compound/15959354. (Accessed 5 March 2022).

Rajhi, I., Boulaaba, M., Baccouri, B., Rajhi, F., Hammami, J., Barhoumi, F., Flamini, G., & Mhadhbi, H. (2022). Assessment of dehulling effect on volatiles, phenolic compounds and antioxidant activities of faba bean seeds and flours. *South African Journal of Botany, 147*, 741–753. https://doi.org/10.1016/j.sajb.2022.03.010

Rajoo, A., Ramanathan, S., Mansor, S. M., & Sasidharan, S. (2021). Formulation and evaluation of wound healing activity of *Elaeis guineensis* Jacq leaves in a *Staphylococcus aures* infected Sprague Dawley rat model. *Journal of Ethnopharmacology, 266*, Article 113414. https://doi.org/10.1016/j.jep.2020.113414

Rognoni, E., & Watt, F. M. (2018). Skin cell heterogeneity in development, wound healing, and cancer. *Trends in Cell Biology, 28*, 709–722. https://doi.org/10.1016/j.tcb.2018.05.002

Rojas, A., Hernandez, L., Pereda-Miranda, R., & Mata, R. (1992). Screening for antimicrobial activity of crude drug extracts and pure natural products from Mexican medicinal plants. *Journal of Ethnopharmacology, 35*, 275–283. https://doi.org/10.1016/0378-8741(92)90025-M

Romo-Rico, J., Krishna, S. M., Bazaka, K., Golledge, J., & Jacob, M. V. (2022). Potential of plant secondary metabolite-based polymers to enhance wound healing. *Acta Biomaterialia, 147*, 34–49. https://doi.org/10.1016/j.actbio.2022.05.043

Sanchez-Aguirre, O., Cruz-Navarro, A., Guevara-Valencia, M., Rengifo-Salgado, E., & Vargas Arana, G. (2020). Phytochemical screening, antioxidant activity and *in vitro* biological evaluation of leave extracts of *Hyptis suaveolens* (L.) from south of Mexico. *South African Journal of Botany, 128*, 62–66. https://doi.org/10.1016/j.sajb.2019.10.016

Sathyanarayanan, S., Muniyandi, K., George, E., Sivaraj, D., Sasidharan, S. P., & Thangaraj, P. (2017). Chemical profiling of *Pterolobium hexapetalum* leaves by HPLC analysis and its productive wound healing activities in rats. *Biomedicine & Pharmacotherapy, 95*, 287–297. https://doi.org/10.1016/j.biopha.2017.08.062

Sedano-Partida, M. D., Santos, K. P., Sala-Carvalho, W. R., Silva-Luz, C. L., & Furlan, C. M. (2020). A review of the phytochemical profiling and biological activities of *Hyptis* jacq.: A Brazilian native genus of Lamiaceae. *Revita Brasileira de Botanica, 43*, 1–16. https://doi.org/10.1007/s40415-020-00582-y

Shedoeva, A., Leavesley, D., Upton, Z., & Fan, C. (2019). Wound healing and the use of medicinal plants. *Evidence-based Complementary and Alternative Medicine.* , Article 2684108. https://doi.org/10.1155/2019/2684108

Singleton, V. L., Orthofer, R., & Lamuela Raventós, R. M. (1999). Analysis of total phenols and other oxidation substrates and antioxidants by means of Folin Ciocalteu Reagent. *Methods in Enzymology, 29*, 152–178.

Sujamol, M. S., Roy, J., & James, K. M. (2021). Phytochemical screening and antimicrobial activity of *Coleus aromaticus* leaf extract. *Materials Today Proceedings, 41*, 569–599. https://doi.org/10.1016/j.matpr.2020.05.255

Süntar, I. P., Akkol, E. K., Yilmazer, D., Baykal, T., Kirmizibekmez, H., Alper, M., & Yesilada, E. (2010). Wound healing potential of *Sambucus ebulus* L. leaves and isolation of an active component, quercetin 3-O glucoside. *Journal of Ethnopharmacology, 127*, 468–477. https://doi.org/10.1016/j.jep.2010.01.051

Süntar, I., Küpeli, A. E., Nahar, L., & Sarker, S. D. (2012). Wound healing and antioxidant properties: Do they coexist in plants? *Free Radicals and Antioxidants, 2*, 1–7. https://doi.org/10.5530/ax.2012.2.2.1

Sun, Z., & Williams, G. M. (2016). Skin wound healing: Skin regeneration with pharmacological mobilized stem cells. In S. J. Lee, J. J. Yoo, & A. Atala (Eds.), *Tissue regeneration* (pp. 345–368). Academic Press, ISBN 9780128022252. https://doi.org/10.1016/B978-0-12-802225-2.00018-0.

Turner, B. L. (2011). Overview of the genus *Asterohyptis* (Lamiaceae) and description of a new species from northern Mexico. *Phyton, 1–6*. http://www.phytoneuron.net/PhytoN Asterohyptis.pdf. (Accessed 11 November 2021).

Wald-Dickler, N., Holtom, P., & Spellberg, B. (2018). Busting the myth of "static vs cidal": A systemic literature review. *Clinical Infectious Diseases, 66*, 1470–1474. https://doi.org/10.1093/cid/cix1127

Wang, A. S., Armstrong, E. J., & Armstrong, A. W. (2013). Corticosteroids and wound healing: Clinical considerations in the perioperative period. *The American Journal of Surgery, 206*, 410–417. https://doi.org/10.1016/j.amjsurg.2012.11.018

Wang, P. H., Huang, B. S., Horng, H. C., Yeh, C. C., & Chen, Y. J. (2018). Wound healing. *Journal of the Chinese Medical Association, 81*, 94–101. https://doi.org/10.1016/j.jcma.2017.11.002

Wani, T. U., Raza, S. N., & Khan, N. A. (2019). Rosmarinic acid loaded chitosan nanoparticles for wound healing in rats. *International Journal of Pharmaceutical Sciences and Research, 10*, 1138–1147. https://doi.org/10.13040/IJPSR.0975-8232.10(3).1138-47

WFO. (2022). The World Flora online. http://www.worldfloraonline.org/search?query=Asterohyptis+stellulata. (Accessed 7 July 2022).

Wu, X., Zhang, Q., Wang, Z., Xu, Y., Tao, Q., Wang, J., Kong, X., Sheng, K., & Wang, Y. (2022). Investigation of construction and characterization of carboxymethyl chitosan – sodium alginate nanoparticles to stabilize Pickering emulsion hydrogels for curcumin encapsulation and accelerating wound healing. *International Journal of Biological Macromolecules, 209*, 1837–1847.

Xavier-Santos, J. B., Ramos Passos, J. G., Santos Gomes, J. A., Cavalcante Cruz, J. V., Ferreira Alves, J. S., Barreto Garcia, V., Moreira da Silva, R., Peporine Lopes, N., Araujo Junior, R. F., Zucolotto, S. M., Silva-Junior, A. A., Félix Silva, J., & Fernandes-Pedrosa, M. F. (2022). Topical gel containing phenolic-rich extract from *Ipomoea* pes-capre leaf (Convolvulaceae) has anti-inflammatory, wound healing, and antiophidic properties. *Biomedicine & Pharmacotherapy, 149*, Article 112921. https://doi.org/10.1016/j.biopha.2022.112921

Yazaki, K., Matsuno, Y., Yoshida, K., Sherpa, M., Nakajima, M., Matsuyama, M., Kiwamoto, T., Morishima, Y., Ishii, Y., & Hizawa, N. (2021). ROS-Nrf2 pathway mediates the development of TGF β1 induced epithelial mesenchymal transition through the activation of Notch signaling. *European Journal of Cell Biology, 100*, Article 151181. https://doi.org/10.1016/j.ejcb.2021.151181

Yazarlu, O., Iranshahi, M., Kashani, H. R. K., Reshadat, S., Habtemariam, S., Iranshanhy, M., & Hasanpour, M. (2021). Perspective on the application of medicinal plants and natural products in wound healing: A mechanistic review. *Pharmacological Research, 174*, Article 105841. https://doi.org/10.1016/j.phrs.2021.105841

Yunitasari, N., Swasono, R. T., Pranowo, H. D., & Raharjo, T. J. (2022). Phytochemical screening and metabolomic approach based on Fourier transform infrared (FTIR): Identification of α-amylase inhibitor metabolites in *Vernonia amygdalina* leaves. *Journal of Saudi Chemical Society, 26*, Article 101540.

Zhang, H., Li, W., Zhang, Q., Zhong, R., Li, C., Chen, Y., Xia, T., Peng, M., Ren, Z., Zhao, H., Wang, Y., & Shu, Z. (2022). Identification of active compounds and molecular mechanisms of *Dalbergia tsoi* Merr.et Chun to accelerate wound healing. *Biomedicine & Pharmacotherapy, 150*, Article 112990. https://doi.org/10.1016/j.biopha.2022.112990

Zhao-Fleming, H., Hand, A., Zhang, K., Polak, R., Northcut, A., Jacob, D., Dissanaike, S., & Rumbaugh, K. P. (2018). Effect of non-steroidal anti-inflammatory drugs on post-surgical complications against the backdrop of the opioid crisis. *Burns & Trauma, 13*, 1–9. https://doi.org/10.1186/s41038-018-0128-x

ANEXO II. Secondary metabolites in wound healing: a review of their mechanisms of action (Capítulo de libro)

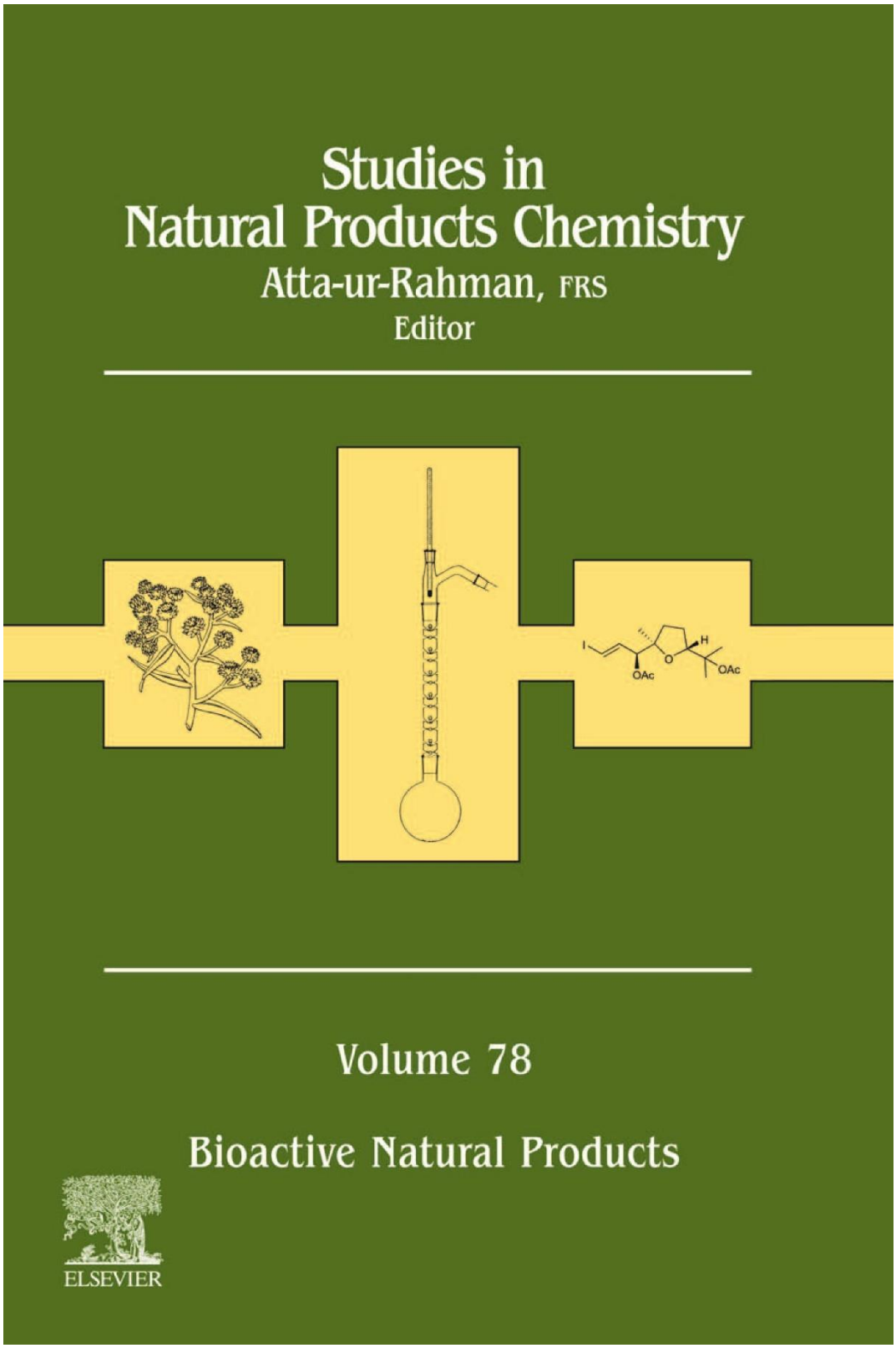

Elsevier
Radarweg 29, PO Box 211, 1000 AE Amsterdam, Netherlands
The Boulevard, Langford Lane, Kidlington, Oxford OX5 1GB, United Kingdom
50 Hampshire Street, 5th Floor, Cambridge, MA 02139, United States

Notices

Knowledge and best practice in this field are constantly changing. As new research and experience broaden our understanding, changes in research methods, professional practices, or medical treatment may become necessary.

Practitioners and researchers must always rely on their own experience and knowledge in evaluating and using any information, methods, compounds, or experiments described herein. In using such information or methods they should be mindful of their own safety and the safety of others, including parties for whom they have a professional responsibility.

To the fullest extent of the law, neither the Publisher, nor the authors, contributors, or editors, assume any liability for any injury and/or damage to persons or property as a matter of products liability, negligence or otherwise, or from any use or operation of any methods, products, instructions, or ideas contained in the material herein.

ISBN: 978-0-323-91253-2
ISSN: 1572-5995

Publisher: Candice G Janco
Acquisitions Editor: Gabriela D Capille
Editorial Project Manager: Czarina Mae S. Osuyos
Production Project Manager: Kumar Anbazhagan
Cover Designer: Christian Bilbow

Typeset by TNQ Technologies

Studies in Natural Products Chemistry

Bioactive Natural Products

Volume 78

Edited by

Atta-ur-Rahman, FRS
International Center for Chemical and Biological Sciences
(H.E.J. Research Institute of Chemistry)
University of Karachi
Karachi, Pakistan

ELSEVIER

Chapter 10

Secondary metabolites in wound healing: a review of their mechanisms of action

Nallely Álvarez-Santos,[1,2] Ana María García-Bores,[1] Diana Barrera-Oviedo,[3] Claudia Tzasná Hernández-Delgado,[4] Edgar Antonio Estrella-Parra[1] and José Guillermo Avila-Acevedo[1,*]

[1]*Laboratorio de Fitoquímica, UBIPRO, FES-Iztacala, UNAM, Estado de México, Mexico;* [2]*Posgrado de Ciencias Biológicas, UNAM, Ciudad de México, Mexico;* [3]*Laboratorio de Farmacología y Bioquímica Clínica Experimental, Facultad de Medicina, UNAM, Ciudad de México, Mexico;* [4]*Laboratorio de Bioactividad de Productos Naturales, UBIPRO, FES-Iztacala, UNAM, Estado de México, Mexico*

[*]*Corresponding author: E-mail:* tuncomadrosio2000@yahoo.com.mx.

Introduction

The skin is composed of two main layers: The epidermis and dermis [1]. It is the largest organ in the human body and helps maintain homeostasis and protects internal organs [2]. The skin is prone to damage from the formation of lesions known as wounds. The healing process allows these damages to be restored, and the original homeostatic properties, integrity, and function of the tissue are recovered to the greatest extent possible [3].

Skin lesions affect many patients worldwide and are among the most critical medical problems [4]. Trauma, surgical wounds, aging, chronic diseases such as diabetes and cancer, and infections can complicate the healing process [5]. Skin lesions represent a significant economic impact on the health systems and patients; in the US, this cost can reach billions of dollars [6]. Patients with chronic wounds experience financial instability and emotional issues such as depression and social isolation [7].

Plants are a source of natural products that form the basis for the treatment of various diseases and pathologies. Their use dates back thousands of years, and plants continue to be essential in primary healthcare in developed/developing countries [8]. A considerable amount of current research on drug

Studies in Natural Products Chemistry. https://doi.org/10.1016/B978-0-323-91253-2.00012-1

formulations is based on the information obtained from different studies of natural products and their derivatives obtained from traditional medicine [9].

Secondary metabolites synthesized by plants improve the wound-healing process [8]. Some phytoconstituents belong to the main group of metabolites, including phenols, terpenes, and alkaloids. However, there are diverse compounds that can improve the healing process.

This study is aimed to describe the healing process and the associated mechanisms of action of secondary metabolites such as phenolic compounds, terpenes, and alkaloids.

Physiopathology of the healing process

Wounds are classified as acute or chronic based on their duration and pathophysiological differences during the healing process. Acute wounds are injuries that recover completely with minimal scarring and within the expected time frame, whereas chronic wounds are injuries that heal slowly, do not heal, or have tissue loss [10] (Fig. 10.1).

Acute wounds

In acute wounds, the four overlapping phases of the healing process, including hemostasis, inflammation, proliferation, and remodeling, exhibit a normal duration and intensity [11].

The first response to injury is hemostasis (min) [9,12]. Hemostasis is a set of mechanisms that prevents blood loss after vascular rupture. Vasoconstriction and clot formation prevent bleeding and provide a temporary barrier to the external environment [13]. This process is regulated by coagulation [14]. After skin injury, the exposed subendothelium, collagen, and tissue factors activate platelet aggregation, which leads to degranulation and the release of growth and chemotactic factors, such as PDGF, EGF, PF4, and TGF-β. Factor XIII promotes clot formation through fibrin cross-linking at the site of injury [15]. Mast cells release histamine, which increases vascular permeability [16] in conjunction with the appearance of PAMPs and DAMPs and the activation of the complement system [3], favoring the migration of inflammatory cells, such as neutrophils and monocytes, to the wound site [17].

Inflammation is the second phase of the wound healing process, which lasts from hours to four to 6 days and involves the release of proteolytic enzymes and proinflammatory cytokines that attract cells from the immune system [12]. Subsequently, neutrophils initiate the phagocytosis of microorganisms and damaged tissues, producing ROS, antimicrobial peptides, eicosanoids, proteases, MPOs, and MMPs. The Nrf2 signaling pathway maintains redox homeostasis during the inflammatory process by removing ROS through the regulation of antioxidant enzymes [18]. M1 are present at the wound site during the inflammatory stage and secrete proinflammatory factors (IL-6,

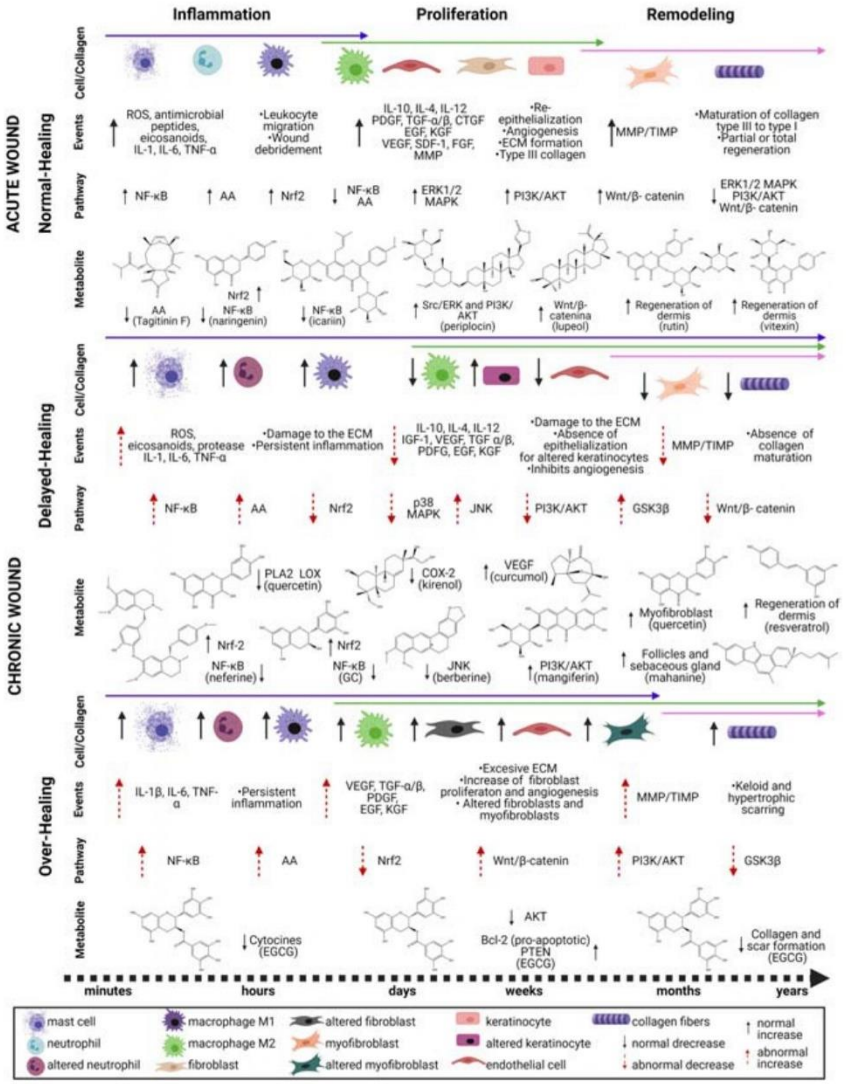

FIGURE 10.1 Physiopathology of the healing process in acute and chronic wounds. The secondary metabolites enhance the normal-healing, delayed-healing and overhealing processes, through the regulation of signaling pathways, modulating the cell groups and the events characteristic of the inflammation, proliferation, and remodeling phases. *Created with www.BioRender.com*

IL-1β, and TNF-α) [19]. This response is regulated by the NF-κB pathway [18]. M2 modulate the inflammatory to proliferative phase transition and secrete antiinflammatory factors (IL-4, IL-10, and IL-12) and growth factors (IGF-1, VEGF, and TGF-α/β) [19]. The debrided wound allows the tissue to cover the area of injury.

In the proliferative phase, the processes of reepithelialization, angiogenesis, and granulation tissue formation occur over days to weeks [9]. The pathways that regulate these events during the cell proliferation phase are PI3/AKT [20] and Wnt/β-catenin [21]. Fibroblasts migrate to the wound bed and help synthesize type III collagen and other components to create a new ECM [22]. This step is regulated by cytokines and growth factors, such as PDGF, TGF-α/β, and CTGF. Keratinocytes initiate reepithelialization stimulated by EGF and KGF, while endothelial and stromal cells initiate angiogenesis with the help of VEGF, SDF-1, PDGF, FGF, MMP, and thrombin [17]. At the end of this process, fibroblasts differentiate into myofibroblasts, which are regulated by Wnt/β-catenin [21], allowing contraction of the granulation tissue and initiating the remodeling phase [17].

Remodeling is characterized by changes in the ECM and is the longest phase, lasting weeks or months [9]. At this stage, type III collagen is replaced by type I collagen, which gives the skin greater tensile strength [23]. This process is accomplished by MMPs secreted by fibroblasts, macrophages, and endothelial cells [3]. The catalytic activity of MMPs is regulated by TIMPs, and the balance between the two is essential for wound remodeling and repair. The population of dermal fibroblasts is progressively reduced by apoptosis [9]. Partial or total regeneration was achieved at the end of this phase.

The wound healing process may involve the regeneration of tissues that contribute to the restoration of the original condition of the damaged organ or tissue [24]. In general, skin wounds do not completely regenerate or heal. A disorganized ECM is commonly known as a scar [25]. In scars, variable dermal fibrosis, effaced epidermis, limited or absent hair follicles and glands can be observed, which cause a loss of structure and function [26]. Additionally, if the healing process fails, it is very likely that a chronic wound will develop.

Chronic wounds

Wounds that do not heal within 6 weeks and do not progress through the healing phases are considered chronic wounds. This period primarily involves the inflammatory and remodeling phases, which can last a year [9]. Chronic lesions are characterized by persistent inflammation, impaired angiogenesis, difficult reepithelialization, dysregulated cytokine and growth factor levels, and increased protease activity [27]. These events are associated with the elevated activation of NF-κB [18] and Nrf2 deficiency [28]. Additionally, phenotypic alterations in neutrophils and macrophages maintain their

inflammatory states. Neutrophils show changes that produce less infiltration and greater permanence in the wound [27], which induces overproduction of ROS, dysregulation between MMP and TIMP, and damage to the ECM [29]. In addition, there is an imbalance between M1/M2 that maintains the inflammatory state, inhibits angiogenesis, and causes a lack of oxygen and nutrients in the wound [30]. This process is related to the inactivation of p38 MAPK and autophagy since the epidermis shows significant inhibition of this pathway in diabetic wounds [31].

Severe burns with exacerbated inflammation, delayed reepithelialization, and impaired angiogenesis exhibit excessive healing and are considered hypertrophic [17] and chronic wounds. Hypertrophic and keloid scars present exacerbated inflammation and increased production of connective tissue and myofibroblasts [32]. There is an alteration in the signaling of PI3K/AKT, ERK1/2 [33], and Wnt/β-catenin [21], increasing cell migration and survival.

Other factors that contribute to the development of chronic wounds include genetic factors such as syndromes where there is an alteration in collagen genes, preexisting patient diseases, aging, and microbial infection due to wound contamination and/or immunosuppression [34–36].

Finally, loss of tissue function, mobility, and even psychological damage is noted in chronic, hypertrophic, and keloid wounds.

Secondary metabolites in wound healing

The study of medicinal plants in the wound healing process, mainly using in vivo (murine) and/or in vitro (cell culture) evaluations, has allowed the identification of pure compounds that act in one or more phases of the healing process. It is important to identify the active compounds, pharmacological activities, mechanisms of action, and define parameters for the standardization of the extracts to produce pharmacological formulations.

Further, sections will be presented with the main groups of secondary metabolites: phenols, terpenes, and alkaloids, which have wound healing effects, and their possible mechanisms of action (Figs. 10.1 and 10.2).

Phenols in wound healing

Phenolic compounds have one or more aromatic rings and hydroxyl groups, which are classified as phenolic acids, flavonoids, tannins, and stilbenes and are recognized for their antioxidant and antiinflammatory activities [37]. These compounds participate in wound healing and tissue regeneration, favoring the formation of the neo-dermis with associated structures such as hair follicles, sweat, and sebaceous glands [38] (Figs. 10.1 and 10.2, Table 10.1).

Modulation of inflammation is important for the healing process in acute or chronic wounds. Consequently, it is a potential therapeutic target for the treatment of wounds. Phenolic compounds are antiinflammatory because they

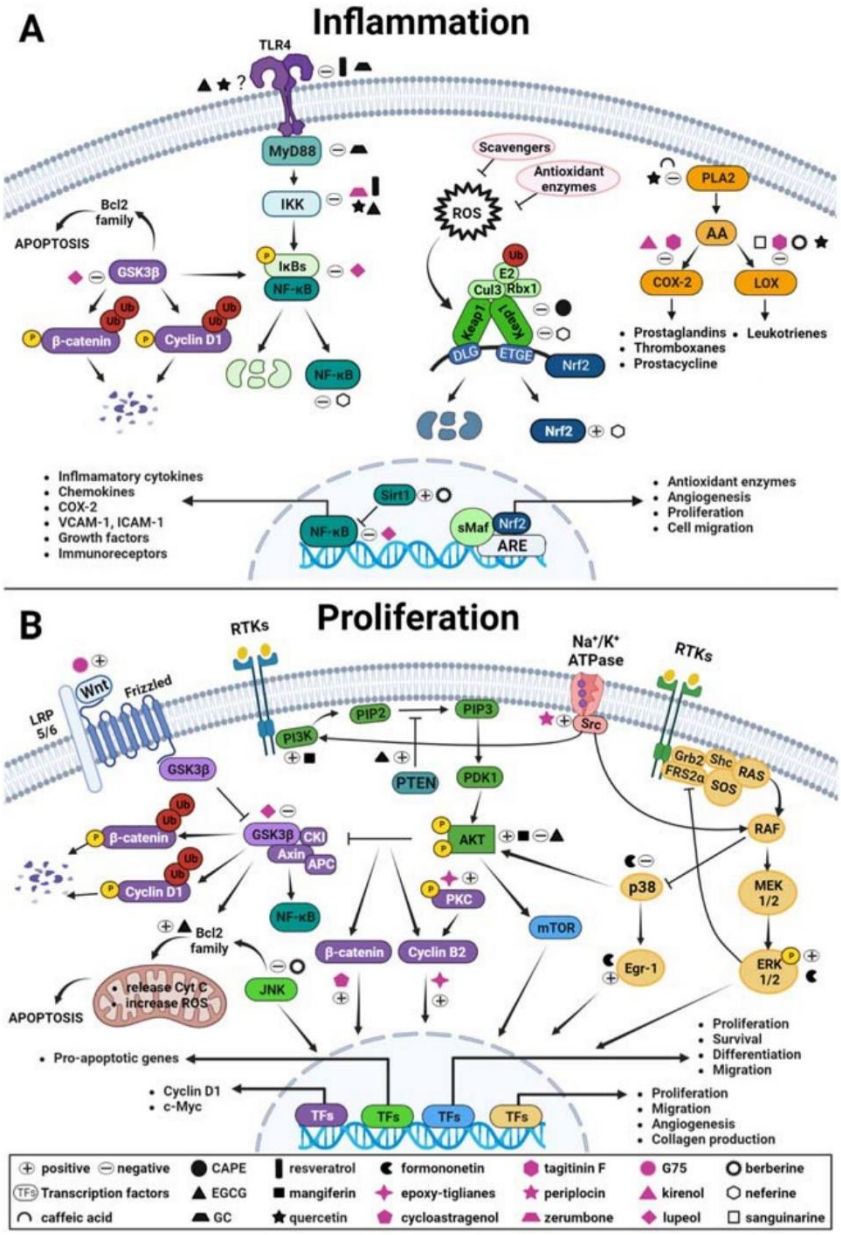

FIGURE 10.2 Signaling pathways involved in the wound healing process and the action mechanisms of the secondary metabolites. (A) Inflammation: action mechanisms of secondary metabolites in the signaling pathways NF-κB, Nrf2, and AA; (B) Proliferation: action mechanisms of secondary metabolites in the signaling pathways PI3K/AKT, MEK/ERK1/2, Wnt/β-catenin, and others. *Created with* www.BioRender.com

TABLE 10.1 Phenolic compounds in wound healing.

Secondary metabolite-Type-Source	Model	Administration/dose	Closure time	Effects	Phase	Signaling pathway	References
Phenolic compounds							
Apigenin Flavone (*Morus alba*)	Excisional and dead space wounds in diabetic Wistar rats	NR	18 days	↑ collagen production ↑ granulation tissue ↑ SOD, GSH, CAT	Inflammation Proliferation	NR	[39]
Caffeic acid Hydroxycinnamic acid (Sigma)	Incisional wound in mouse BALB/c	Oral 10 mg/kg daily	NR	↓ neutrophils ↑ activity of PLA2 ↓ liberation of histamine ↑ collagen	Inflammation Proliferation	AA	[40]
CAPE Hydroxycinnamic acid (Sigma-Aldrich)	Incision wound in Wistar rats	Intraperitoneally 10 μmol/kg^{-}	7 days	↑ GSH, SOD ↓ MDA ↑ regenerate a dermis like that of intact skin	Inflammation Proliferation Remodeling	NR	[41]
CAPE Hydroxycinnamic acid (Sigma-Aldrich)	Pressure ulcers in Swiss mice	Intraperitoneally 5×10^{-6} mol/kg	12 days	3 days ↑ NO/NOS2 ↑ lipoperoxidation ↑ NF-κB ↑ migration	Inflammation Proliferation	NO/NOS2 Nrf2 NF-κB	[42]

Continued

TABLE 10.1 Phenolic compounds in wound healing.—cont'd

Secondary metabolite-Type-Source	Model	Administration/ dose	Closure time	Effects	Phase	Signaling pathway	References
				macrophages ↓ Nrf2 7 days ↑ Nrf2 ↓ NO/NOS2 ↓ lipoperoxidation ↓ migration macrophages ↓ NF-κB ↑myofibroblast 12 days ↓ myofibroblast ↑ collagen, reepithelialization			
Mix: **Curcumin** Diketone derives from a ferulic acid. **Chrysin** Flavone (Sigma-Aldrich)	Excisional wound in Wistar rats	Topical alone: 5, 10, 15% combination: 5:10, 10:5, 7.5:7.5	15 (15% chrysin and 15% curcumin)	alone and combination ↑ IL-6 ↑ MMP-2, ↓ iNOS ↑ TIMP-1, TIMP-2	Inflammation	NR	[43]

EGCG Flavanol (Sigma-Aldrich)	Keloid explants humans	100 μg/mL	4 weeks (Reduced keloid volume)	↑ healing of keloid wounds ↓ cell proliferation ↓ synthesis of collagen I and III ↓ mast cells associated with keloids ↓ blood vessels ↑ epidermal contraction ↑ apoptosis ↓ CTGF, VEGF, TGF-β2, ↓ MMP-2, MMP-9	Proliferation Remodeling	NR	[44]
EGCG Flavanol (NR)	Ex vivo human scar model	NR	6 weeks	↑ differentiation of the M1 to M2 phenotype ↓ angiogenesis ↑ skin elasticity ↓ scar formation/ thickness in both fresh and old epithelialized wounds	Remodeling	NR	[45]

Continued

TABLE 10.1 Phenolic compounds in wound healing.—cont'd

Secondary metabolite-Type-Source	Model	Administration/dose	Closure time	Effects	Phase	Signaling pathway	References
Formononetin Isoflavone (*Astragalus membranaceus*)	Incisional wound in athymic nude mice HUVEC scratch test	50 μM injected in three sites (50 μL) Direct 1 μM, 50 μM, 50 ng/mL	10 days 18 h	↑ TGF, VEGF, PDGF, bFGF ↑ expression of Egr-1 ↑ phosphorylation of ERK ⊤ slightly the phosphorylation of MAPK	Proliferation	ERK1/2 p38 MAPK	[46]
GC Flavanol (Sigma-Aldrich)	Excisional wound in diabetic Sprague Dawley rats	Topical 13.06 μM, 26.12 μM	18 days	↑ SOD, CAT, GPx ↓ lipoperoxidation ↑ Nrf2, NQO-1, HO-1 ↓ Keap-1, TLR4, MyD88, NFκB, TNF-α, IL-6 ↑ IκB-α ↑ VEGF, EGF, TGF-β, FGF-2 ↓ MMP-2 ↑ regeneration of dermis, hair follicles, sweat and sebaceous glands	Inflammation Proliferation Remodeling	Nrf2/HO-1 TLR4/MyD88/NF-κB	[38]

Glycitin and 4′,6,7-trimehoxy isoflavone Isoflavone (*Glycine* max and *Amphimas pterocarpoides*)	Excision wound in ICR mouse and burn wound in C57BL/6 mouse HaCaT and fibroblast scratch test	Topical 200 μL of a 1:1 (200 μM:200 μM) Direct 1:1 (10 μM: 10 μM) 1:2 (6.7 μM:13.3 μM) 2:1 (13.3 μM:6.7 μM)	14 days 24 h (partial close)	↑ differentiation and migration of keratinocytes, ↑ proliferation and differentiation fibroblast ↑ secretion of TGF-β ↑ skin regeneration	Proliferation Remodeling	NR	[47]
Icariin Prenylated flavonol (Sigma-Aldrich)	Excisional wound in Wistar rats	0.5%	14 days (95%)	↑ IL-10, ↑ angiogenesis ↓ NF-κB and TNF-α ↓ MMP-2 and MMP-9 activity	Inflammation	NF-κB	[48]
Quercetin Flavonol (NR)	Excisional wound in diabetic Sprague-Dawley rats	10, 20, 40 mg/mL	14 days (40 mg/mL)	↓ TNFα, IL-1β, IL-6 ↑ IL-10 levels ↑ expression VEGF, TGF-α/β. ↑ differentiation M1 to M2	Inflammation Proliferation	NR	[19]
Quercetin Flavonol (Sigma-Aldrich)	Excisional wound in Wistar rats	0.3% quercetin 0.03, 0.2 y 0.3% nanoparticles	21 days	↑ IL-10, VEGF, TGF-β ↓ TNF-α, ↑ conversion of fibroblasts to myofibroblasts ↓ inflammatory cells	Inflammation Proliferation	NR	[49]

Continued

TABLE 10.1 Phenolic compounds in wound healing.—cont'd

Secondary metabolite-Type-Source	Model	Administration/ dose	Closure time	Effects	Phase	Signaling pathway	References
Mangiferin C-Glycosyl Xanthone (*Mangifera indica*)	Excisional wound in diabetic rats (NR)	Topical 1%, 2%	21 days	↑ expression of EGF, FGF, TGF, VEGF, PI3K, MMP-2 y Nrf2 ↓ TNF-α, NF-κB ↑ epidermal thickness	Inflammation Proliferation	Nrf2 NF-κB PI3K/AKT	[50]
Naringenin Flavanone (Sigma-Aldrich)	Burns in Wistar rats	Oral 25, 50, 100 mg/ kg/day	7 days	↑ SOD, CAT, GST, GPx ↓ IL-6, IL-1β, TNF-α, LTB4, NO, PGE2, NF-κB	Inflammation	NF-κB	[51]
Naringin Flavanone glycoside (Sigma chemical)	Excisional wound in diabetic Sprague-Dawley rats	Oral 20, 40, 80 mg/kg	16 days (80 mg)	↑SOD ↓ lipoperoxidation ↓MPO ↑IGF-1, TGF-β, VEGF-c, ↑ Ang-1, collagen-1 ↓ TNF-α, IL-1β, IL-6 ↑ angiogenesis ↑ regeneration of dermis	Inflammation Remodeling	NR	[52]

Resveratrol Stilbene (Sigma-Aldrich)	Burns in diabetic Sprague-Dawley rats HUVECs scratch test	Topical NR Direct 100 nM for 3 h	14 days 24 h (almost complete closure)	↑ protect against H_2O_2 ↑ proliferation and migration ↑ expression Mn-SOD and Nrf2 ↑ regeneration of dermis	Inflammation Remodeling	Nrf2	[53]
Rutin Flavonol glycoside (Kahira pharmaceuticals and chemical industries co.)	Excisional wound in Wistar rats	Topical Excision wound 0.5 mL-0.025%	10 days	↓ lipoperoxidation ↑GSH, CAT ↑ regeneration of dermis	Inflammation Remodeling	NR	[54]
Vitexin Flavone glycoside (Sigma-Aldrich)	Excisional wound in Sprague-Dawley rats HaCaT and NIH-3T3 scratch test	Topical 10 mg/mL Direct 1 μg	21 days 72 h	↑ migration of keratinocytes and fibroblast ↑ regeneration of dermis	Remodeling	NR	[55]

↑, increase; ↓, decrease; ⊤, inhibition; NR, not reported.

regulate oxidative stress via scavengers and increase the expression or activity of antioxidant enzymes [38,39,51,52,54], probably due to the activation of Nrf2 [38,42,50,53].

Nrf2 is a redox-sensitive transcription factor that modulates cellular stress and redox homeostasis through gene regulation [56]. Although several substances have been investigated to modify the expression of Nrf2, as is the case with CAPE [42], a pharmacological target of phenolic compounds in this signaling pathway has not yet been recognised.

One proposed mechanism of action of the secondary metabolites is through the inactivation of Keap 1 by promoting the modification of cysteines. This promotes the release of Nrf2, promoting the expression of antioxidant enzymes and factors related to angiogenesis, cell proliferation, and migration [28].

Phenolic compounds influence inflammation and promote wound healing by modulating cytokines [19,48,51], growth factors [19], MMPs [48], TIMPs, iNOS [43], and NF-κB [38,48,50,51,53]. In the cytoplasm, NF-κB is inactive and is associated with IκB. Following activation, it is translocated to the nucleus to induce the expression of genes involved in the inflammatory response [38]. Investigations of phenolic compounds in wounds indicate that their application decreased NF-κB expression [38,42,48,50]. For example, GC improves wound healing by inactivating NF-κB through the TLR4 and MyD88 receptors [38]. Khan et al. [37] reported that polyphenols, such as resveratrol, quercetin, and epigallocatechin-3-gallate (EGCG), can alter the NF-κB pathway, thereby avoiding IKK activation.

The AA-dependent pathway is another therapeutic target for controlling inflammation. Metabolites such as CAPE accelerate wound healing by inhibiting PLA2 and preventing AA release [40]. Quercetin, kaempferol, and anthocyanidins inhibit PLA_2 and LOX [37]. Kim et al. [57] established a structure-activity relationship of phenolic compounds, with flavones being the chief inhibitors of COX and flavonols of LOX.

The modulation of the signaling pathways associated with inflammation allows progression to the next phase of the healing process, proliferation. This step is regulated by the transition of M1 to M2 phenotype, which is a critical point at the start of proliferation. Natural products such as EGCG [45] and quercetin [19] promote the differentiation of M2. Macrophage polarization occurs through the activation or inhibition of TLRs and inflammasomes (NLRP3), which are activated by DAMPS, PAMP, ROS, cytokines, metabolites, etc. [58]. Therefore, a possible mechanism of action of these phenolic compounds could be their interaction with TLRs, leading to their possible inactivation; for example, resveratrol inhibits the dimerization of TLR4 and therefore NF-κB activation. TLR4 inhibition promotes M2 polarization and enhances wound healing [59].

Phenols act in the proliferation phase through the activation of signaling pathways such as PI3K/AKT, ERK1/2, and p38 MAPK. ERK1/2 regulates cellular functions such as proliferation, differentiation, and transformation

[60]. For example, formononetin accelerates wound closure by overexpressing Egr-1, promoting phosphorylation of ERK1/2, and inhibiting p38 MAPK [46]. However, it has been reported that activation of p38 MAPK stimulates wound closure in human fibroblasts [61]. p38 MAPK has two roles: stress-activated enhancement of apoptosis and, in the wound healing process, promotion of migration and cell proliferation, which are dependent upon extracellular stimuli [62].

PI3K/AKT signaling regulates the inhibition of GSK3β and activation of mTOR, thereby promoting tissue restoration [20]. Regulation of this pathway allows the closure of chronic wounds and prevents the formation of keloids. Secondary metabolites such as mangiferin increase the expression of PI3K and phosphorylate AKT, thereby promoting the closure of diabetic wounds [50]. Excessive PI3K/AKT activation is associated with cancer [63] and keloids [33]. EGCG is a polyphenol well known for its therapeutic effects in different pathologies, including cancer, by inhibition of AKT-mediated signaling, regulation of Bcl-2 family proteins, increase in PTEN, and promotion of apoptosis [64]. Therefore, it is not surprising that EGCG improves keloid wound healing by decreasing cell proliferation and increasing apoptosis [44], probably by regulating the PI3K/AKT pathway. Therefore, the investigation of secondary metabolites with anticancer activity and their possible application in keloid scars is required.

One of the features of scars is the present variable dermal fibrosis with limited or absent hair follicles and accessory glands, which result in the loss of function and aesthetic, physical, and even psychological damage [26]. Some reports have shown that phytochemicals induce regenerative effects by decreasing scar formation and restoring the skin to a near-normal state. Thus, EGCG [45], CAPE [41], naringin [52], rutin [54], and vitexin [55] promote skin regeneration. Ouyang et al. [65] reported that controlling excessive inflammatory responses by regulating ROS/MAPK/NF-κB promotes wound healing and tissue repair. Therefore, the regeneration process of phenolic compounds may be related to their activity in these pathways.

As described above, phenolic compounds help improve the healing process, promote tissue regeneration, and restore function.

Terpenoids in wound healing

Monoterpenes, sesquiterpenes, diterpenes, and triterpenes have been studied in different biological models of wound-healing processes. Some terpenes exhibit antiinflammatory activity through mechanisms related to the regulation of oxidative stress, although very few exhibit antioxidant activity. In many cases, mechanisms of action have been established during the proliferation phase (Figs. 10.1 and 10.2, Table 10.2).

Some terpenes act as scavengers, reducing free radicals [66], decreasing lipoperoxidation [67], modulating the response of antioxidant enzymes

TABLE 10.2 Terpenic compounds in wound healing.

Secondary metabolite-Type-Source	Model	Administration/dose	Closure time	Effects	Phase	Signaling pathway	References
α-Phellandrene Terpinolene Monoterpenes (Sigma-Aldrich)	L929 cell line scratch test	Direct 10, 100 and 200 μM	16 h (partial close)	↑ migration and proliferation of fibroblasts ↓ $ABTS^{\bullet+}$, $NO^{\bullet}$, $O_2^{\bullet-}$ ↓ IL-6, TNF-α, NO ⊤ NF-κB	Inflammation Proliferation	NF-κB	[66]
β-Caryophyllene Sesquiterpene (Sigma-Aldrich)	Excisional wound in Wistar rats	Topical 15 μL (10% w/w)	12 days	↓ IL-1, TNF-α ↓ MPO ↓ lipoperoxidation ↑ fibroblast, collagen, epidermal cells, angiogenesis, reepithelization	Inflammation Proliferation	NR	[67]
Astragaloside IV Triterpenoid saponin (Zhejiang Institute of Food and drug Control)	Excisional wound in Sprague–Dawley rats HaCaT cells	Topical 0.5% Direct 50, 100, 150 μmol/L	18 days 96 h (almost complete closure, 100 μmol/L)	↑ migration of keratinocytes ↑ tensile strength ↑ angiogenesis, collagen synthesis ↑ relation collagen type III and I ↓ TGF-β1 ↓ scar	Proliferation Remodeling	NR	[68]

Bacoside A Mixed triterpenoid saponins (*Bacopa monnieri*)	Excisional, incisional infected and uninfected wounds (*S. aureus*), and dead space wounds in Wistar rats	Topical 0.2% Oral 4 mg/mL	18.30 days	↑ epithelialization ↑ tensile strength ↑ granulation tissue ↑ fibroblasts ↑ cross-linking of collagen fibers ↓ monocytes ⊤ MMP's	Inflammation proliferation	NR	[69]
Curcumol Sesquiterpene (Chinese materials Research Center)	Excisional wound in diabetic Sprague-Dawley rats	0.5, 1 mg/kg	24 days	↑ VEGF ↑rates of wound closure	Proliferation	NR	[70]
Cycloastragenol Triterpenoid (*Astragali radix*)	EpSC cells scratch test	Direct 0, 0.03, 0.3, 1, 10 μM	72 h	↑ viability, proliferation, and migration ↑ expression levels of TERT, β-catenin, c-Myc	Proliferation	Wnt/β-catenin	[71]
Epoxy-tiglianes Diterpene esters (*Fontainea picrosperma*)	HaCaT cells	Direct 0 a 15.1 μM	48 h (almost complete closure)	↑ proliferation and migration keratinocytes ↑ progression through G0/G1-S and S-G2/M phases ↑ genes of	Proliferation	PKC	[72]

Continued

TABLE 10.2 Terpenic compounds in wound healing.—cont'd

Secondary metabolite-Type-Source	Model	Administration/dose	Closure time	Effects	Phase	Signaling pathway	References
				proliferation and migration keratinocytes ↑ expression of cyclin B2 ↓ CDKN1A ↓ MMP-1, MMP-7, MMP-10 ↑ KRT13, KRT15 ↓ KRT6, KRT16m KRT17 ↓ IL-1α, Il-6, IL-8, TNF-α, CCL2, CCL5, CXCL1, CXCL10 ↑ PKC phosphorylation			
G75 Triterpenoid saponin (*Panax ginseng*)	Excisional wound in mouse HaCaT cells and fibroblasts scratch test	Topical 5 μM Direct 5, 10 μM	9 days 24 h (partial close)	↑ proliferation and migration of keratinocytes and fibroblasts ↑ CTGF ↑ inducing genes of signaling pathways related to growth factors ↑ bound to GR and translocated into the nucleus	Proliferation	Glucocorticoid receptor Wnt	[73]

Kirenol Diterpenoid (*Siegesbeckia orientalis*)	Excisional wound in diabetic Wistar rats L929 cell line scratch test	Topical 15%, 30% Direct 10, 25 μg	14 days 24 h (partial close)	↓ NF-κB, COX-2, iNOS, MMP-2 and MMP-9 ↓ MDA ↑ SOD, CAT, GPx, GST ↑ migration fibroblasts ↑ fibroblasts, new blood vessels, displacement of collagen	Inflammation Proliferation Remodeling	NF-κB AA	[74]
Lupeol Triterpenoid (*Celastrus paniculatus*)	Excisional, incisional, and dead space wounds animals NR	Topical 0.2% w/v Oral (dead space) 1% w/v	17 days	↑ breaking strength ↑ granulation tissue ↓ macrophages ⊤ GSK3-β	Proliferation	GSK3-β/β-catenin	[75]
Nerolidol Sesquiterpene (Sigma-Aldrich)	Excisional wound in mice	Topical 2%, 4%	14 days (2%)	↑ fibroblast proliferation, angiogenesis, collagen ↑ restructuring of connective matrix ↑number of dermal papillae ↓ inflammation (2%)	Inflammation Proliferation Remodeling	NR	[76]

Continued

TABLE 10.2 Terpenic compounds in wound healing.—cont'd

Secondary metabolite-Type-Source	Model	Administration/dose	Closure time	Effects	Phase	Signaling pathway	References
Periplocin Cardiotonic steroid (*Periploca forrestii*)	Excisional wound in Sprague-Dawley rats L929 cell line scratch test	Topical 50 μL (20 μg/mL) Direct 5, 10, 20 μM	9 days 48 h (partial close)	↑ proliferation and migration fibroblast ↓ IL-1β, TNF-α ↑ Src bind to Na/KATPase α1 ↑ phosphorylation of Src, ERK, PI3K and AKT ↑ angiogenesis, fibroblasts, collagen accumulation	Inflammation Proliferation	Src/ERK PI3K/AKT by Na/K-ATPase	[77]
Tagitinin F Sesquiterpene derivative (NR)	Excisional wound in BALB/c mouse	Topical 200 μL (0.5%, 1%)	NR	↓ 5-LOX, COX-1, COX-2 ↓ MMP-1, MMP-2 ↓ PGE2, LTB4, TNF-α ↓ MPO, ↓ neutrophils, macrophages ↑ type III collagen	Inflammation Proliferation	AA	[78]

Zerumbone Sesquiterpene (*Zingiber zerumbet*)	Excisional wound in Wistar rats	Topical 100 mg (1% w/w)	15 days	↑ SOD, CAT, GSH ↑ VEGF, TGF-β1 ↑ type IV collagen ↑ reepithelization, fibroblasts, angiogenesis	Inflammation Proliferation	NR	[79]

↑, increase; ↓, decrease; ⊤, inhibition; NR, Not reported.

[74,79], and regulating proinflammatory cytokines [72,77]. Further, some compounds act by inhibiting [66] or modifying the expression of NF-κB [74].

The transcription factor NF-κB is considered a pivotal mediator of the inflammatory process, and its inhibition is a therapeutic strategy for wound healing [66]. The activity of terpenes in the inhibition of the NF-κB pathway is mediated by IκBs phosphorylation, IKK inhibition, DNA binding, and p65 translocation [80]. For example, zerumbone enhances the wound healing process [79] and blocks the IKK complex because of a decrease in protein phosphorylation [81]. Lupeol promotes wound healing by inhibiting the GSK3-β protein that activates the NF-κB pathway [75,80]. Other studies have reported that lupeol inhibits IκBα phosphorylation and prevents the binding of NF-κB to DNA [80,81].

Terpene compounds possess antiinflammatory properties by modulating the AA pathway and three enzymes involved in the AA pathway: PLA2, COX, and LOX. The natural product tagitinin F inhibits COX-2 and 5-LOX [78], and kirenol prevents COX-2 gene expression [74].

Terpenes play a role in the proliferative phase of wound healing by stimulating the proliferation and migration of fibroblasts [66,73,77], promoting the proliferation of keratinocytes [65], and enhancing the expression of growth factors [70,73,79]. The signaling pathways activated by some terpenoids that promote the proliferative phase have also been studied.

The Wnt/β-catenin pathway is also involved in cell adhesion, proliferation, differentiation, and growth. This pathway regulates wound healing, and enhances angiogenesis, and epithelial remodeling [82]. Furthermore, β-catenin is involved in the transition of fibroblasts to myofibroblasts [21]. Patients with diabetes can get ulcers, which have been reported to be related to alterations in the Wnt/β-catenin pathway [82]. Terpenes act through this pathway, such as cycloastragenol, which induces cell proliferation and migration through TERT, β-catenin, c-Myc expression, and Wnt/β-catenin activation [71]. Lupeol increases epithelialization and wound contraction by inhibiting GSK3-β [75]. G75 terpenoid binding to GR increases their translocation into the nucleus and induces the expression of Wnt signaling pathway genes [73].

Terpene compounds also activate other signaling pathways associated with cell proliferation. Periplocin activates the MEK/ERK and PI3K/AKT pathways through the Na/K-ATPase/Src complex and Src activation [77]. In addition, epoxy-tigliane compounds promote PKC phosphorylation and activation, cyclin B2 expression, and cell cycle progression in keratinocytes [72]. However, it does not specify which isoforms are activated. PKCs are a group of enzymes that participate in the regulation of different pathways related to proliferation [83].

Some terpenoids also act in the remodeling phase by regulating metalloproteinases [69,74,78] and changing from type III to type I collagen [68]. Moreover, nerolidol improves the appearance of connective tissue and

increases the number of dermal papillae [76], whereas astragaloside IV decreases scar formation [68].

In summary, terpenes act in different phases of the wound healing process, mainly in terms of proliferation, but their role in the reduction of scar formation should be further studied.

Alkaloids in wound healing

Alkaloids are chemically heterogeneous but have common characteristics, such as the presence of one or more nitrogen atoms derived from amino acids in a heterocycle [84]. However, some compounds that do not meet all the characteristics are also included in this group. Alkaloids act in different phases of the healing process; however, some reports suggest that the anticancer or cytotoxic properties of alkaloids that prevent wound healing [85–87]. Current studies have sought to evaluate the effect of phytochemicals, including alkaloids, using biological markers of different signaling pathways and the different processes in wound repair (Figs. 10.1 and 10.2, Table 10.3).

Alkaloids can modulate inflammation and accelerate progression to the proliferative phase by decreasing inflammatory cytokines and increasing growth factors [88,90,92]. In addition, some alkaloids decrease lipoperoxidation, reduce iNOS, and balance M1 and M2 levels [92]. Furthermore, modulating inflammation through the Nrf-2, NF-κB, and AA pathways, such as neferine, improved wound healing in diabetic rats by regulating oxidative stress and the transition of M1 to M2 by increasing the expression of Nrf-2, decreasing Keap-1, and reducing the expression of NF-κB [92]. Berberine inhibits the NF-κB pathway, activating SIRT 11 [88] and the activity of 12-lipoxygenase derived from the AA pathway [96]. Other alkaloids with wound-healing activity act in the AA pathway, such as sanguinarine, which inhibits 5-LOX [96].

Some alkaloids act in the proliferation phase of the healing process, such as berberine, which activates TrxR1 and suppresses downstream JNK pathway signaling, promotes cell proliferation, and enhances extracellular matrix synthesis [89]. JNK activation upregulates proapoptotic Bim and promotes apoptosis [97]. Berberine is an example of a compound that can act in different pathways and regulate inflammation and proliferation phases. Therefore, this molecule has high pharmacological potential for the treatment of wounds and other diseases associated with inflammation.

Alkaloids act in the remodeling phase, regulating MMPs [93], increasing the expression of type 1 collagen [92] and promoting tissue regeneration. Some carbazole derivative alkaloids, such as mahanimbicine, increase the formation of sebaceous glands and hair follicles and promote dermal regeneration [91]. Berberine [88] and neferine [92], promote regeneration of the dermis, indicating the possibility of tissue regeneration and recuperation of function (regulation of temperature, defense, etc.). Neferin acts on Nrf2 and

TABLE 10.3 Alkaloids in wound healing.

Secondary metabolite-Type-Source	Model	Administration/ dose	Closure time	Effects	Phase	Signaling pathway	References
Berberine Isoquinoline alkaloids (Sigma chemical)	Excisional wound in diabetic Sprague Dawley rats HFF-1, HaCaT cells scratch wound assay	Topical 0.01 g/10 mL Direct 100 μg/mL	13 days 12 h (Almost total closure)	↑ proliferation and migration cellular ↑ VEGF ↑ CD31 ↑ α- SMA myofibroblast ↑ regeneration of dermis ↑ SIRT 11 ↓ NF-κB ↓ TNF-α, IL-6 ↓ MMP-9	Inflammation Proliferation	SIRT 11/ NFκB	[88]
Berberine Isoquinoline alkaloids (*Coptis*)	Excisional wound in diabetic Sprague Dawley rats	Topical 0.06 mg/mL	15 days	↓ apoptosis ↑ SOD, GSH ↑ total antioxidant capacity ↓ lipoperoxidation ↓ caspasa-3 ↓ ROS ↓ 8-OHdG	Inflammation Proliferation	TrxR1/JNK	[89]

				↓ MMP 9 ↑ TGF-β1 ↑ TIMP1 ↓ JNK ↑ TrxR1 ↑ proliferation and cell viability in keratinocyte ↑ collagen			
Hypaphorine Indole alkaloid (*Erythrina velutina*)	Excisional wound in diabetic Sprague Dawley rats	Topical 10 mg/50 mL	12 days	↓ TNF-α, IL-1β ↓ inflammatory cells ↑ vascular regeneration ↑ fibroblast	Inflammation Proliferation	NR	[90]
Mahanine **Mahanimbicine** **Mahanimbine** Indole alkaloids	Excisional wound in Sprague Dawley rats	Topical 50 mg	18 days	↓ inflammatory cells ↑ restructuring of collagen ↑ hair follicles and sebaceous glands ↑ regeneration of dermis	Inflammation Proliferation Remodeling	NR	[91]
Neferine Isoquinoline alkaloid (*Nelumbo nucifera*)	Excisional wound in diabetic Wistar rats	Topical 10%, 20%	14 days (almost total closure)	↑SOD, CAT, GST, GPx ↓ lipoperoxidation ↑ Nrf-2	Inflammation Proliferation	Nrf-2 NF-κB	[92]

Continued

TABLE 10.3 Alkaloids in wound healing.—cont'd

Secondary metabolite-Type-Source	Model	Administration/dose	Closure time	Effects	Phase	Signaling pathway	References
				↑ type 1 collagen ↑ TGF-β ↑ α-SMA ↓ Keap-1 ↓ NF-κB ↓TNF-α, IL-1β, IL-6, iNOS = M1 a M2 ↑ regeneration dermis			
Lily-derived Steroidal glycoalkaloid (*Lilium longiflorum*)	Primary human dermal fibroblast cells, scratch wound assay	Direct 5 μM	16 h (34%)	↑ migration fibroblast ↑ CXCL11, IL-10, IL-2, IL-4 ↑ CTSG, F13A1, FGA, MMP-9, PLG ↓ CSF3 ↓ CXCL2, CCL7, ↓ MMP-7, PLAT ↑ TGF-α ↑ type IV collagen, ITGB6	Inflammation Proliferation Remodeling	NR	[93]

Taspine hydrochloride Apophyllic alkaloids (*Paeonia*)	Excisional wound in Sprague Dawley rats	Topical 1 mg/mL (50 μL)	18 days	↑ hydroxyproline ↑ KGF ↑ fibroblast ↑ capillaries	Proliferation	NR	[94]
Sanguinarine Isoquinoline alkaloids (*Fumaria parviflora*) **N-methylstylopine** **Dihydrosanguinarine** **Protopine** **Dihydrofumariline** **α-Hydrastine** **Fumaramine** **Microcarpine**	Human fibroblast scratch wound assay	Direct 1 μg/mL	72 h 94% 92.4% 91% 90.5% 88.4% 85.4% 76.4% 75%	↑ migration rate and wound closure	Proliferation	NR	[95]

↑, increase; ↓, decrease; ⊤, inhibition; =, equal; NR, Not reported.

NF-κB by modulating inflammation [92], which enhances the regeneration process [65].

It is likely that some alkaloids can also promote the regeneration of injured tissue through various pathways; however, further studies are required.

Conclusions

Phytochemicals improve wound healing primarily during the proliferation and inflammation phases. They act at diverse levels through the regulation of different signaling pathways. Therefore, these compounds exert multiple therapeutic effects. These secondary metabolites can act as antioxidants and modulate inflammation and the succession of phases in the healing process. Furthermore, they have the potential to promote tissue regeneration and restore skin function, which is important in chronic wounds.

Natural products represent a reliable and important source for identifying treatments that promote healing. Thus, investigating secondary metabolites during the healing process remains a promising path.

List of abbreviations

8-OHdG	8-hydroxy-2′-deoxyguanosine
AA	Arachidonic acid
ABTS$^{\bullet+}$	2,2′-azino-bis-(3-ethylbenzothiazoline-6-sulfonic acid)
AKT	Serine/threonine protein kinase
Ang-1	Angiopoietin 1
APC	Adenomatous polyposis coli
ARE	Antioxidant response element
Bcl-2	B-cell lymphoma-2
bFGF	Basic fibroblast growth factor
Bim	Bcl-2 interacting mediator of cell death
c-Myc	Proto-oncogene protein
CAPE	Caffeic acid phenethyl ester
CAT	Catalase
CCL	C−C Motif chemokine ligand
CD31	Endothelial cell adhesion molecule
CDKN1A	Cyclin-dependent kinase inhibitor 1A
CKI	Casein kinase 1
COX	Cyclooxygenase
CSF3	Colony-stimulating factor 3
CTGF	Connective tissue growth factor
CTSG	Cathepsin G
Cul3	Cullin 3
CXCL	C-X-C Motif chemokine ligand
Cyt C	Cytochrome C
DAMP	Damage-associated molecular pattern
DLG	DLG motif

E2	Ubiquitin-protein ligase
ECM	Extracellular matrix
EGCG	Epigallocatechin-3-gallate
EGF	Epidermal growth factor
Egr-1	Early growth response gene 1
EpSCs	Human epidermal stem cells
ERK	Extracellular signal-regulated kinase
ETGE	ETGE motif
F13A1	Coagulation factor XIII A chain
Factor XIII	Fibrin stabilizing factor
FGA	Fibrinogen alpha chain
FGF	Fibroblast growth factor
FRS2α	Fibroblast growth factor receptor substrate 2
G75	Gypenoside LXXV
GC	Gallocatechin
GPx	Glutathione peroxidase
GR	glucocorticoid receptor
Grb2	Growth factor receptor-bound protein 2
GSH	Glutathione
GSK3-β	Glycogen synthase kinase 3 beta
GST	Glutathione S-transferase
H_2O_2	Hydrogen peroxide
HaCaT cells	Immortalized human skin keratinocytes
HFF-1	Human skin fibroblasts
HO-1	Haeme oxygenase 1
HUVEC	Human umbilical vein endothelial cell
ICAM-1	Intercellular adhesion molecule 1
IGF-1	Insulin-like growth factor 1
IKK	IkappaB kinase
IL	Interleukin
iNOS	Inducible nitric oxide synthase
ITGB6	Beta 6 subunit of αvβ6 integrin
IκB	Inhibitor of NF-κB
JNK	Jun N-terminal kinase
Keap-1	Kelch-like ECH associated protein 1
KGF	Keratinocyte growth factor
KRT	Gen keratin
L929	Mouse fibroblast cell line
LOX	Lipoxygenase
LRP	Low-density lipoprotein receptor-related protein
LTB4	Leukotriene B4
M1	Macrophage type 1
M2	Macrophage type 2
MAPK	Mitogen-activated protein kinase
MDA	Malondialdehyde
MEK	Membrane-bound GTPases
MMP	Matrix metalloproteinases
MPO	Myeloperoxidase

mTOR	Mammalian (mechanistic) target of rapamycin
MyD88	Myeloid differentiation factor 88
Na^+/K^+-ATPase	Sodium−potassium pump
NF-κB	Nuclear factor kappa B
NIH-3T3	Fibroblast cell line from mouse NIH/Swiss embryos
NLRP3	NLR Family pyrin domain containing 3
NO	Nitric oxide
NOS2	Nitric oxide synthase 2
$NO^{\bullet}$	Nitric oxide radical
NQO-1	NAD(P)H quinone 1
Nrf2	Nuclear factor erythroid 2−related factor 2
$O_2^{\bullet -}$	Superoxide anion
p38 MAPK	p38 group of the mitogen-activated protein kinase
p65	RELA
PAMP	Pathogen-associated molecular patterns
PDGF	Platelet-derived growth factor
PDK1	Protein serine/threonine kinase-3′-phosphoinositide-dependent kinase 1
PF4	Platelet factor 4
PGE2	Prostaglandin E2
PI3K	Phosphoinositide 3-kinase
PIP2	Phosphatidylinositol (4,5)-bisphosphate
PIP3	Phosphatidylinositol (3,4,5)-trisphosphate
PKC	Protein kinase C
PLA2	Phospholipase A2
PLAT	Plasminogen activator tissue
PLG	Plasminogen
PTEN	Phosphatase and tensin
RAF	Proto-oncogene serine/threonine-protein kinase
RAS	Small guanosine triphosphatases
Rbx1	Ring box 1
ROS	Reactive oxygen species
RTK	Receptor tyrosine kinases
SDF-1	Stromal cell-derived factor-1
Shc	Src homology and containing protein
SIRT 11	Sirtuin 1
sMaf	Small maf proteins
SOD	Superoxide dismutase
SOS	Son of sevenless
Src	protein-tyrosine kinase
TERT	Telomerase reverse transcriptase transforming growth factor
TGF	Transforming growth factor
TIMP	Tissue inhibitor of metalloproteinase
TLR	Toll-like receptor
TNF-α	Tumor necrosis factor-alpha
TrxR1	Selenoprotein thioredoxin reductase 1
Ub	Ubiquitin
VCAM-1	Vascular cell adhesion molecule 1

VEGF	Vascular endothelial growth factor
Wnt	Wingless/integrase-1
α-SMA	Alfa-smooth muscle actin.

Acknowledgments

We thank DGAPA-PAPIIT, UNAM (IN220920), COMECYT (FICDTEM-2021-20), CONACyT (CB-A1-S-14605) and CONACyT (CVU 775307) for the doctoral scholarship. Posgrado de Ciencias Biologicas, UNAM.

References

[1] S.A. Eming, P. Martin, M. Tomic-Canic, Wound repair and regeneration: mechanisms, signalling, and translation, Sci. Transl. Med. 6 (265) (2014) 265sr6, https://doi.org/10.1126/scitranslmed.3009337.

[2] H.S. Kim, X. Sun, J.H. Lee, H.W. Kim, X. Fu, K.W. Leong, Advanced drug delivery systems and artificial skin grafts for skin wound healing, Adv. Drug Deliv. Rev. 146 (2019) 209−239, https://doi.org/10.1016/j.addr.2018.12.014.

[3] G.C. Gurtner, S. Werner, Y. Barrandon, M.T. Longaker, Wound repair and regeneration, Nature 453 (7193) (2008) 314−321, https://doi.org/10.1038/nature07039.

[4] H. Taghiyar, B. Yadollahi, S.J. Moshtaghian, A. Talebi, A.A. Kajania, PMMA nanofibers containing keplerate-type polyoxometalate and metronidazole: preparation and wound-healing effect in a rat model, J. Drug Deliv. Sci. Technol. 69 (2022) 103140, https://doi.org/10.1016/j.jddst.2022.103140.

[5] L. Bao, X. Cai, M. Zhang, Y. Xiao, J. Jin, T. Qin, Y. Li, Bovine collagen oligopeptides accelerate wound healing by promoting fibroblast migration via PI3K/Akt/mTOR signalling pathway, J. Funct. Foods 90 (2022) 104981, https://doi.org/10.1016/j.jff.2022.104981.

[6] S.R. Nussbaum, M.J. Carter, C.E. Fife, J. DaVanzo, R. Haught, M. Nusgart, D. Cartwright, An economic evaluation of the impact, cost, and medicare policy implications of chronic nonhealing wounds, Value Health 21 (1) (2018) 27−32, https://doi.org/10.1016/j.jval.2017.07.007.

[7] Z. Meng, D. Zhou, Y. Gao, M. Zeng, W. Wang, miRNA delivery for skin wound healing, Adv. Drug Deliv. Rev. 129 (2018) 308−318, https://doi.org/10.1016/j.addr.2017.12.011.

[8] T. Maver, U. Maver, K. Stana Kleinschek, D.M. Smrke, S. Kreft, A review of herbal medicines in wound healing, Int. J. Dermatol. 54 (7) (2015) 740−751, https://doi.org/10.1111/ijd.12766.

[9] A. Shedoeva, D. Leavesley, Z. Upton, C. Fan, Wound healing and the use of medicinal plants, Evid Based Complement Alternat. Med. (2019) 2684108, https://doi.org/10.1155/2019/2684108.

[10] J. Boateng, O. Catanzano, Advanced therapeutic dressings for effective wound healing–a review, J. Pharmaceut. Sci. 104 (11) (2015) 3653−3680. https://doi.org/10.1002/jps.24610.

[11] M. Ali-Seyed, A. Siddiqua, Calotropis - a multi-potential plant to humankind: special focus on its wound healing efficacy, Biocatal. Agric. Biotechnol. 28 (2020) 101725. https://doi.org/10.1016/j.bcab.2020.101725.

[12] A. Moeini, P. Pedram, P. Makvandi, M. Malinconico, G. Gomez d'Ayala, Wound healing and antimicrobial effect of active secondary metabolites in chitosan-based wound dressings:

a review, Carbohydr. Polym. 233 (2020) 115839. https://doi.org/10.1016/j.carbpol.2020.115839.

[13] S.J. Chin, L. Madden, S.Y. Chew, D.L. Becker, Drug therapies and delivery mechanisms to treat perturbed skin wound healing, Adv. Drug Deliv. Rev. 149−150 (2019) 2−18. https://doi.org/10.1016/j.addr.2019.03.006.

[14] A. Blanco, G. Blanco, Chapter 31-Hemostasis, in: A. Blanco, G. Blanco (Eds.), Medical Biochemistry, Academic Press, 2018, pp. 781−789. https://doi.org/10.1016/B978-0-12-803550-4.00031-8.

[15] A. Opneja, S. Kapoor, E.X. Stavrou, Contribution of platelets, the coagulation, and fibrinolytic systems to cutaneous wound healing, Thromb. Res. 179 (2019) 56−63. https://doi.org/10.1016/j.thromres.2019.05.001.

[16] R. Zhao, H. Liang, E. Clarke, C. Jackson, M. Xue, Inflammation in chronic wounds, Int. J. Mol. Sci. 17 (12) (2016) 2085. https://doi.org/10.3390/ijms17122085.

[17] M. Xue, R. Zhao, H. Lin, C. Jackson, Delivery systems of current biologicals for the treatment of chronic cutaneous wounds and severe burns, Adv. Drug Deliv. Rev. 129 (2018) 219−241. https://doi.org/10.1016/j.addr.2018.03.002.

[18] X. Zhou, Y. Guo, K. Yang, P. Liu, J. Wang, The signaling pathways of traditional Chinese medicine in promoting diabetic wound healing, J. Ethnopharmacol. 282 (2022) 114662. https://doi.org/10.1016/j.jep.2021.114662.

[19] J. Fu, J. Huang, M. Lin, T. Xie, T. You, Quercetin promotes diabetic wound healing via switching macrophages from M1 to M2 polarization, J. Surg. Res. 246 (2020) 213−223. https://doi.org/10.1016/j.jss.2019.09.011.

[20] S.W. Jere, N.N. Houreld, H. Abrahamse, Role of the PI3K/AKT (mTOR and GSK3β) signalling pathway and photobiomodulation in diabetic wound healing, Cytokine Growth Factor Rev. 50 (2019) 52−59. https://doi.org/10.1016/j.cytogfr.2019.03.001.

[21] J. Liu, Y. Wang, Q. Pan, Y. Su, Z. Zhang, J. Han, X. Zhu, C. Tang, D. Hu, Wnt/β-catenin pathway forms a negative feedback loop during TGF-β1 induced human normal skin fibroblast-to-myofibroblast transition, J. Dermatol. Sci. 65 (2012) 38−49. https://doi.org/10.1016/j.jdermsci.2011.09.012.

[22] J.M. Reinke, H. Sorg, Wound repair and regeneration, Eur. Surg. Res. 49 (1) (2012) 35−43. https://doi.org/10.1159/000339613.

[23] E.A. Gantwerker, D.B. Hom, Skin: histology and physiology of wound healing, Clin. Plast. Surg. 39 (1) (2012) 85−97. https://doi.org/10.1016/j.cps.2011.09.005.

[24] S. Akita, Wound repair and regeneration: mechanisms, signalling, Int. J. Mol. Sci. 20 (24) (2019) 6328. https://doi.org/10.3390/ijms20246328.

[25] O. Castaño, S. Pérez-Amodio, C. Navarro-Requena, M.Á. Mateos-Timoneda, E. Engel, Instructive microenvironments in skin wound healing: biomaterials as signal releasing platforms, Adv. Drug Deliv. Rev. 129 (2018) 95−117. https://doi.org/10.1016/j.addr.2018.03.012.

[26] Z. Sun, G.M. Williams, Skin wound healing: skin regeneration with pharmacological mobilized stem cells, in: S.J. Lee, J.J. Yoo, A. Atala (Eds.), In Situ Tissue Regeneration Host Cell Recruitment and Biomaterial Design, Academic Press, London, 2016, pp. 345−368. https://doi.org/10.1016/B978-0-12-802225-2.00018-0.

[27] K. Las Heras, M. Igartua, E. Santos-Vizcaino, R.M. Hernandez, Chronic wounds: current status, available strategies and emerging therapeutic solutions, J. Contr. Release 328 (2020) 532−550. https://doi.org/10.1016/j.jconrel.2020.09.039.

[28] I. Süntar, S. Cetinkaya, E. Panieri, S. Saha, B. Buttari, E. Profumo, L. Saso, Regulatory role of Nrf2 signaling pathway in wound healing process, Molecules 26 (9) (2021) 2424. https://doi.org/10.3390/molecules26092424.

[29] Y. Yuan, D. Fan, S. Shen, X. Ma, An M2 macrophage-polarized anti-inflammatory hydrogel combined with mild heat stimulation for regulating chronic inflammation and impaired angiogenesis of diabetic wounds, Chem. Eng. J. 433 (3) (2022) 133859. https://doi.org/10.1016/j.cej.2021.133859.

[30] D. Baltzis, I. Eleftheriadou, A. Veves, Pathogenesis and treatment of impaired wound healing in diabetes mellitus: new insights, Adv. Ther. 31 (8) (2014) 817–836. https://doi.org/10.1007/s12325-014-0140-x.

[31] L. Li, J. Zhang, Q. Zhang, D. Zhang, F. Xiang, J. Jia, P. Wei, J. Zhang, J. Hu, Y. Huang, High glucose suppresses keratinocyte migration through the inhibition of p38 MAPK/autophagy pathway, Front Physiol. 10 (2019) 24.

[32] L. Nabai, A. Pourghadiri, A. Ghahary, Hypertrophic scarring: current knowledge of predisposing factors, cellular and molecular mechanisms, J. Burn Care Res. 41 (1) (2020) 48–56. https://doi.org/10.1093/jbcr/irz158.

[33] S. Tan, N. Khumalo, A. Bayat, Understanding keloid pathobiology from a quasi-neoplastic perspective: less of a scar and more of a chronic inflammatory disease with cancer-like tendencies, Front. Immunol. 10 (2019) 1810. https://doi.org/10.3389/fimmu.2019.01810.

[34] R.T. Beyene, S.L. Derryberry Jr., A. Barbul, The effect of comorbidities on wound healing, Surg. Clin. North Am. 100 (4) (2020) 695–705. https://doi.org/10.1016/j.suc.2020.05.002.

[35] M. Tomic-Canic, J.L. Burgess, K.E. O'Neill, N. Strbo, I. Pastar, Skin microbiota and its interplay with wound healing, Am. J. Clin. Dermatol. 21 (Suppl. 1) (2020) 36–43. https://doi.org/10.1007/s40257-020-00536-w.

[36] J.R. Stoll, S.J. Noor, S.W. Dusza, A. Markova, Skin substitutes for the treatment of chronic wounds in patients with cancer: a retrospective case series, J. Am. Acad. Dermatol. 85 (5) (2021) 1331–1333. https://doi.org/10.1016/j.jaad.2020.10.064.

[37] H. Khan, A. Sureda, T. Belwal, S. Cetinkaya, I. Süntar, S. Tejeda, H.P. Devkota, H. Ullah, M. Aschner, Polyphenols in the treatment of autoimmune diseases, Autoimmun. Rev. 18 (2019) 647–657. https://doi.org/10.1016/j.autrev.2019.05.001.

[38] N.R. Vendidandala, T.P. Yin, G. Nelli, V.R. Pasupuleti, S. Nyamathulla, S.I. Mokhtar, Gallocatechin-silver nanoparticle impregnated cotton gauze patches enhance wound healing in diabetic rats by suppressing oxidative stress and inflammation via modulating the Nrf2/HO-1 and TLR4/NF-κB pathways, Life Sci. 286 (2021) 120019. https://doi.org/10.1016/j.lfs.2021.120019.

[39] R. Shukla, S.K. Kashaw, A.P. Jain, S. Lodhi, Fabrication of apigenin loaded gellan gum-chitosan hydrogels (GGCH-HGs) for effective diabetic wound healing, Int. J. Biol. Macromol. 91 (2016) 1110–1119. https://doi.org/10.1016/j.ijbiomac.2016.06.075.

[40] H.S. Song, T.W. Park, U.D. Sohn, Y.K. Shin, B.C. Choi, C.J. Kim, S.S. Sim, The effect of caffeic acid on wound healing in skin-incised mice, Korean J. Physiol. Pharmacol. 12 (2008) 343–347. https://doi.org/10.4196/kjpp.2008.12.6.343.

[41] G. Serarslan, E. Altuğ, T. Kontas, E. Atik, G. Avci, Caffeic acid phenethyl ester accelerates cutaneous wound healing in a rat model and decreases oxidative stress, Clin. Exp. Dermatol. 32 (6) (2007) 709–715. https://doi.org/10.1111/j.1365-2230.2007.02470.x.

[42] B. Romana-Souza, J.S. Dos Santos, A. Monte-Alto-Costa, Caffeic acid phenethyl ester promotes wound healing of mice pressure ulcers affecting NF-κB, NOS2 and NRF2 expression, Life Sci. 207 (2018) 158–165. https://doi.org/10.1016/j.lfs.2018.05.057.

[43] Z. Mohammadi, M.S. Zak, H. Majdi, E. Mostafavi, M. Barati, H. Lotfimehr, K. Ghaseminasab, H. Pazoki-Toroudi, T.J. Webster, A. Akbarzadeh, The effect of chrysin-curcumin-loaded nanofibres on the wound-healing process in male rats, Artif. Cells Nanomed. Biotechnol. 47 (1) (2019) 1642−1652. https://doi.org/10.1080/21691401.2019.1594855.

[44] F. Syed, R.A. Bagabir, R. Paus, A. Bayat, Ex vivo evaluation of antifibrotic compounds in skin scarring: EGCG and silencing of PAI-1 independently inhibit growth and induce keloid shrinkage, Lab. Invest. 93 (8) (2013) 946−960. https://doi.org/10.1038/labinvest.2013.82.

[45] S. Ud-Din, P. Foden, M. Mazhari, S. Al-Habba, M. Baguneid, S. Bulfone-Paus, D. McGeorge, A. Bayat, A double-blind, randomized trial shows the role of zonal priming and direct topical application of epigallocatechin-3-gallate in the modulation of cutaneous scarring in human skin, J. Invest. Dermatol. 139 (8) (2019) 1680. https://doi.org/10.1016/j.jid.2019.01.030.

[46] J.E. Huh, D.W. Nam, Y.H. Baek, J.W. Kang, D.S. Park, D.Y. Choi, J.D. Lee, Formononetin accelerates wound repair by the regulation of early growth response factor-1 transcription factor through the phosphorylation of the ERK and p38 MAPK pathways, Int. Immunopharm. 11 (2011) 46−54.

[47] G.Y. Seo, Y. Lim, D. Koh, J.S. Huh, C. Hyun, Y.M. Kim, M. Cho, TMF and glycitin act synergistically on keratinocytes and fibroblasts to promote wound healing and anti-scarring activity, Exp. Mol. Med. 49 (3) (2017) e302. https://doi.org/10.1038/emm.2016.167.

[48] W.R. Singh, H.S. Devi, S. Kumawat, A. Sadam, A.V. Appukuttan, M.R. Patel, M.C. Lingaraju, T.U. Singh, D. Kumar, Angiogenic and MMPs modulatory effects of icariin improved cutaneous wound healing in rats, Eur. J. Pharmacol. 858 (2019) 172466. https://doi.org/10.1016/j.ejphar.2019.172466.

[49] A. Choudhary, V. Kant, B.L. Jangir, V.G. Joshi, Quercetin loaded chitosan tripolyphosphate nanoparticles accelerated cutaneous wound healing in Wistar rats, Eur. J. Pharmacol. 880 (2020) 173172. https://doi.org/10.1016/j.ejphar.2020.173172.

[50] O.M. Lwin, N. Giribabu, E.K. Kilari, N. Salleh, Topical administration of mangiferin promotes healing of the wound of streptozotocin-nicotinamide-induced type-2 diabetic male rats, J. Dermatol. Treat. 32 (8) (2021) 1039−1048. https://doi.org/10.1080/09546634.2020.1721419.

[51] A.S. Al-Roujayee, Naringenin improves the healing process of thermally-induced skin damage in rats, J. Int. Med. Res. 45 (2) (2017) 570−582. https://doi.org/10.1177/0300060517692483.

[52] A.D. Kandhare, P. Ghosh, S.L. Bodhankar, Naringin, a flavanone glycoside, promotes angiogenesis and inhibits endothelial apoptosis through modulation of inflammatory and growth factor expression in diabetic foot ulcer in rats, Chem. Biol. Interact. 219 (2014) 101−112. https://doi.org/10.1016/j.cbi.2014.05.012.

[53] X. Zhou, Q. Ruan, Z. Ye, Z. Chu, M. Xi, M. Li, W. Hu, X. Guo, P. Yao, W. Xie, Resveratrol accelerates wound healing by attenuating oxidative stress-induced impairment of cell proliferation and migration, Burns 47 (1) (2021) 133−139. https://doi.org/10.1016/j.burns.2020.10.016.

[54] M.H. Asfour, H. Elmotasem, D.M. Mostafa, A.A.A. Salama, Chitosan based pickering emulsion as a promising approach for topical application of rutin in a solubilized form intended for wound healing: in vitro and in vivo study, Int. J. Pharm. 534 (1−2) (2017) 325−338. https://doi.org/10.1016/j.ijpharm.2017.10.044.

[55] N. Bektas, B. Senel, E. Yenilmez, O. Özatik, R. Arslan, Evaluation of wound healing effect of chitosan-based gel formulation containing vitexin, Saudi Pharmaceut. J. 28 (2020) 87–94.

[56] P. Hiebert, S. Werner, Regulation of wound healing by the Nrf2 transcription factor-more than cytoprotection, Int. J. Mol. Sci. 20 (2019) 3856. https://doi.org/10.3390/ijms20163856.

[57] H.P. Kim, K.H. Son, H.W. Chang, S.S. Kang, Anti-inflammatory plant flavonoids and cellular action mechanism, J. Pharmacol. Sci. 96 (2004) 229–245. https://doi.org/10.1254/jphs.crj04003x.

[58] H. Lee, M.B. Fessler, P. Qu, J. Heymann, J.B. Kopp, Macrophage polarization in innate immune responses contributing to pathogenesis of chronic kidney disease, BMC Nephrol. 21 (2020) 270. https://doi.org/10.1186/s12882-020-01921-7.

[59] W. Zhu, R. Xu, J. Du, Y. Fu, S. Li, P. Zhang, L. Liu, H. Jiang, Zoledronic acid promotes TLR-4-mediated M1 macrophage polarization in bisphosphonate-related osteonecrosis of the jaw, FASEB. J. 33 (2019) 5208–5219. https://doi.org/10.1096/fj.201801791RR.

[60] D. Lake, S.A.L. Correa, J. Müller, Negative feedback regulation of the ERK1/2 MAPK pathway, Cell. Mol. Life Sci. 73 (2016) 4397–4413. https://doi.org/10.1007/s00018-016-2297-8.

[61] N. Bulat, G. Waeber, C. Widmann, LDLs stimulate p38 MAPKs and wound healing through SR-BI independently of Ras and PI3 kinase, J. Lipid Res. 50 (2009) 81–89. https://doi.org/10.1194/jlr.M800119-JLR200.

[62] D.T. Loughlin, C.M. Artlett, Modification of collagen by 3-deoxyglucosone alters wound healing through differential regulation of p38 MAP kinase, PLoS One 6 (2011) e18676. https://doi.org/10.1371/journal.pone.0018676.

[63] M.R. Khezri, R. Jafari, K. Yousefi, N.M. Zolbanin, The PI3K/AKT signaling pathway in cancer: molecular mechanisms and possible therapeutic interventions, Exp. Mol. Pathol. 127 (2022) 104787. https://doi.org/10.1016/j.yexmp.2022.104787.

[64] M. Alam, S. Ali, G. Md Ashraf, A.L. Bilgrami, D.K. Yadav, Md.I. Hassan, Epigallocatechin 3-gallate: from green tea to cancer therapeutics, Food Chem. 379 (2022) 132135. https://doi.org/10.1016/j.foodchem.2022.132135.

[65] T. Ouyang, H. Yin, J. Yang, Y. Liu, S. Ma, Tissue regeneration effect of betulin via inhibition of ROS/MAPKs/NF-κB axis using zebrafish model, Biomed. Pharmacother. 153 (2022) 113420. https://doi.org/10.1016/j.biopha.2022.113420.

[66] M.M. de Christo Scherer, F.M. Marques, M.M. Figueira, M.C.O. Peisino, E.F.P. Schmitt, T.P. Kondratyuk, D.C. Endringer, R. Scherer, M. Fronza, Wound healing activity of terpinolene and α-phellandrene by attenuating inflammation and oxidative stress in vitro, J. Tissue Viability 28 (2) (2019) 94–99. https://doi.org/10.1016/j.jtv.2019.02.003.

[67] J. Parisotto-Peterle, J. Bidone, L.G. Lucca, G.M.S. Araújo, M.C. Falkembach, M. da Silva Marques, A.P. Horn, M.K. Dos Santos, V.F. da Veiga Jr., R.P. Limberger, H.F. Teixeira, C.L. Dora, L.S. Koester, Healing activity of hydrogel containing nanoemulsified β-caryophyllene, Eur. J. Pharmaceut. Sci. 148 (2020) 105318. https://doi.org/10.1016/j.ejps.2020.105318.

[68] X. Chen, L.H. Peng, N. Li, Q.M. Li, P. Li, K.P. Fung, P.C. Leung, J.Q. Gao, The healing and anti-scar effects of astragaloside IV on the wound repair in vitro and in vivo, J. Ethnopharmacol. 139 (3) (2012) 721–727. https://doi.org/10.1016/j.jep.2011.11.035.

[69] R. Sharath, B.G. Harish, V. Krishna, B.N. Sathyanarayana, H.M. Swamy, Wound healing and protease inhibition activity of Bacoside-A, isolated from *Bacopa monnieri* wettest, Phytother Res. 24 (8) (2010) 1217–1222. https://doi.org/10.1002/ptr.3115.

[70] J. Zhou, M. Ni, X. Liu, Z. Ren, Z. Zheng, Curcumol promotes vascular endothelial growth factor (VEGF)-mediated diabetic wound healing in streptozotocin-induced hyperglycemic rats, Med. Sci. Mon. Int. Med. J. Exp. Clin. Res. 23 (2017) 555–562. https://doi.org/10.12659/msm.902859.

[71] Y. Cao, L. Xu, X. Yang, Y. Dong, H. Luo, F. Xing, Q. Ge, The potential role of cycloastragenol in promoting diabetic wound repair in vitro, BioMed Res. Int. 2019 (2019) 7023950. https://doi.org/10.1155/2019/7023950.

[72] R.L. Moses, G.M. Boyle, R.A. Howard-Jones, R.J. Errington, J.P. Johns, V. Gordon, P. Reddell, R. Steadman, R. Moseley, Novel epoxy-tiglianes stimulate skin keratinocyte wound healing responses and re-epithelialization via protein kinase C activation, Biochem. Pharmacol. 178 (2020) 114048. https://doi.org/10.1016/j.bcp.2020.114048.

[73] S. Park, E. Ko, J.H. Lee, Y. Song, C.H. Cui, J. Hou, B.M. Jeon, H.S. Kim, S.C. Kim, Gypenoside LXXV promotes cutaneous wound healing in vivo by enhancing connective tissue growth factor levels via the glucocorticoid receptor pathway, Molecules 24 (8) (2019) 1595. https://doi.org/10.3390/molecules24081595.

[74] J. Ren, M. Yang, J. Chen, S. Ma, N. Wang, Anti-inflammatory and wound healing potential of kirenol in diabetic rats through the suppression of inflammatory markers and matrix metalloproteinase expressions, Biomed. Pharmacother. 129 (2020) 110475. https://doi.org/10.1016/j.biopha.2020.110475.

[75] B.G. Harish, V. Krishna, H.S.S. Kumar, B.M.K. Ahamed, R. Sharath, H.M.K. Swamy, Wound healing activity and docking of glycogen-synthase-kinase-3-beta-protein with isolated triterpenoid lupeol in rats, Phytomedicine 15 (9) (2008) 763–767. https://doi.org/10.1016/j.phymed.2007.11.017.

[76] M.O.G. Ferreira, L.L.R. Leite, I.S. de Lima, H.M. Barreto, L.C.C. Nunes, A.B. Ribeiro, J.A. Osajima, E.C. da Silva Filho, Chitosan hydrogel in combination with nerolidol for healing wounds, Carbohydr. Polym. 152 (2016) 409–418. https://doi.org/10.1016/j.carbpol.2016.07.037.

[77] L. Chen, P. Jiang, J. Li, Z. Xie, Y. Xu, W. Qu, F. Feng, W. Liu, Periplocin promotes wound healing through the activation of Src/ERK and PI3K/Akt pathways mediated by Na/K-ATPase, Phytomedicine 57 (2019) 72–83. https://doi.org/10.1016/j.phymed.2018.12.015.

[78] L.P. Silva, E.C. Santos, B.A. Borges, M.P. Veloso, D.A. Chagas-Paula, R.V. Gonçalves, R.D. Novaes, Tagitinin F has anti-inflammatory, anti-nociceptive and anti-matrix metalloproteinase properties: an in silico, in vitro and in vivo study, Pharmacol. Res. 164 (2021) 105303. https://doi.org/10.1016/j.phrs.2020.105303.

[79] W.Y. Liu, T.F. Tzeng, I.M. Liu, Healing potential of zerumbone ointment on experimental full-thickness excision cutaneous wounds in rat, J. Tissue Viability 26 (3) (2017) 202–207. https://doi.org/10.1016/j.jtv.2017.04.002.

[80] H. jain, N. Dhingra, T. Narsinghani, R. Sharma, Insights into the mechanism of natural terpenoids as NF-κB inhibitors: an overview on their anticancer potential, Exp. Oncol. 38 (2016) 158–168.

[81] A. Salminen, M. Lehtonen, T. Suuronen, K. Kaarniranta, J. Huuskonen, Terpenoids: natural inhibitors of NF-kappa B signalling with anti-inflammatory and anticancer potential, Cell. Mol. Life Sci. 65 (19) (2008) 2979–2999. https://doi.org/10.1007/s00018-008-8103-5.

[82] H. Zhang, X. Nie, X. Shi, J. Zhao, Y. Chen, Q. Yao, C. Sun, J. Yang, Regulatory mechanisms of the Wnt/β-catenin pathway in diabetic cutaneous ulcers, Front. Pharmacol. 9 (2018) 1114. https://doi.org/10.3389/fphar.2018.01114.

[83] P.S. Lim, C.R. Sutton, S. Rao, Protein kinase C in the immune system: from signalling to chromatin regulation, Immunology 146 (2015) 508–522. https://doi.org/10.1111/imm.12510.

[84] B.R. Lichman, The scaffold-forming steps of plant alkaloid biosynthesis, Nat. Prod. Rep. 38 (1) (2021) 103–129. https://doi.org/10.1039/d0np00031k.

[85] N. Ojeh, O. Stojadinovic, I. Pastar, A. Sawaya, N. Yin, M. Tomic-Canic, The effects of caffeine on wound healing, Int. Wound J. 13 (2016) 605–613. https://doi.org/10.1111/iwj.12327.

[86] P.C. Wu, W.L. Hsu, C.L. Chen, C.F. Lam, Y.B. Huang, C.C. Huang, M.H. Lin, M.W. Lin, Morphine induces fibroblast activation through up-regulation of connexin 43 expression: implication of fibrosis in wound healing, Int. J. Med. Sci. 15 (2018) 875–882. https://doi.org/10.7150/ijms.23074.

[87] X. Wang, C.C. Decker, L. Zechmer, S. Krstin, M. Wink, In vitro wound healing of tumor cells: inhibition of cell migration by selected cytotoxic alkaloids, BMC Pharmacol. Toxicol. 20 (2019) 4. https://doi.org/10.1186/s40360-018-0284-4.

[88] P. Zhang, L. He, J. Zhang, X. Mei, Y. Zhang, H. Tian, Z. Chen, Preparation of novel berberine nano-colloids for improving wound healing of diabetic rats by acting Sirt1/NF-κB pathway, Coll. Surf. B Biointerf. 187 (2020) 110647. https://doi.org/10.1016/j.colsurfb.2019.110647.

[89] R. Zhou, C. Xiang, G. Cao, H. Xu, Y. Zhang, H. Yang, J. Zhang, Berberine accelerated wound healing by restoring TrxR1/JNK in diabetes, Clin. Sci. 135 (4) (2021) 613–627. https://doi.org/10.1042/CS20201145.

[90] M. Qi, X. Zhu, X. Yu, M. Ai, W. Cai, B. Du, B. Hou, L. Qiu, Preparation of W/O hypaphorine-chitosan nanoparticles and its application on promoting chronic wound healing via alleviating inflammation block, Nanomaterials 11 (11) (2021) 2830. https://doi.org/10.3390/nano11112830.

[91] T. Nagappan, T.C. Segaran, M.E. Wahid, P. Ramasamy, C.S. Vairappan, Efficacy of carbazole alkaloids, essential oil, and extract of *Murraya koenigii* in enhancing subcutaneous wound healing in rats, Molecules 17 (12) (2012) 14449–14463. https://doi.org/10.3390/molecules171214449.

[92] J. Li, H. Chou, L. Li, H. Li, Z. Cui, Wound healing activity of neferine in experimental diabetic rats through the inhibition of inflammatory cytokines and nrf-2 pathway, Artif. Cells, Nanomed. Biotechnol. 48 (1) (2020) 96–106. https://doi.org/10.1080/21691401.2019.1699814.

[93] R. Di, A.F. Murray, J. Xiong, D. Esposito, S. Komarnytsky, T.J. Gianfagna, J.P. Munafo Jr., Lily steroidal glycoalkaloid promotes early inflammatory resolution in wounded human fibroblasts, J. Ethnopharmacol. 258 (2020) 112766. https://doi.org/10.1016/j.jep.2020.112766.

[94] X. Wang, Y. Gao, X. Sun, Effect of taspine hydrochloride on the repair of rat skin wounds by regulating keratinocyte growth factor signal, Bioengineered 13 (1) (2020) 789–799. https://doi.org/10.1080/21655979.2021.2012920.

[95] M.B. Elsaid, D.M. Elnaggar, A.I. Owis, S.F. AbouZid, S. Eldahmy, Production of isoquinoline alkaloids from the in vitro conserved *Fumaria parviflora* and their in vitro wound healing activity, Nat. Prod. Res. 6 (2021) 1–8. https://doi.org/10.1080/14786419.2021.1904401.

[96] S. Chen, Natural products triggering biological targets–a review of the anti-inflammatory phytochemicals targeting the arachidonic acid pathway in allergy asthma and rheumatoid

arthritis, Curr. Drug Targets 12 (3) (2011) 288–301. https://doi.org/10.2174/138945011794815347.

[97] R. Jin, Y. Gao, S. Zhang, F. Teng, X. Xu, A. Aili, Y. Wang, X. Sun, X. Pang, Q. Ge, Y. Zhang, Trx1/TrxR1 system regulates post-selected DP thymocytes survival by modulating ASK1-JNK/p38 MAPK activities, Immunol. Cell Biol. 93 (2015) 744–752. https://doi.org/10.1038/icb.2015.36.


ELSEVIER
elsevier.com/books-and-journals
ISBN 978-0-323-91253-2
9 780323 912532

ANEXO III. Natural Products in Wound Regeneration (Capítulo de libro)

BENTHAM
SCIENCE
PUBLISHERS

Executive Suite Y – 2,
P.O. Box 7917, Saif
Zone, Sharjah,
U.A.E.
Tel: +971-6-5571132;
E-mail: mahmood@benthamscience.net

October 13, 2023

Israel Valencia Quiroz
Laboratorio de Fitoquímica, Unidad de Biotecnología y Prototipos (UBIPRO)
Facultad de Estudios Superiores Iztacala, Universidad Nacional Autónoma de México
Tlalnepantla de Baz, Estado de México
México

Certificate of Contribution

Bentham Science is an established international publisher of quality print and online journals and books covering varied disciplines of science, technology, medicine and social sciences. A number of journals published by Bentham carry impact factors and the Books are indexed in various indexing agencies like Web of Science, Scopus, EMBASE, Science Citation Index and Chemical Abstracts.

Selection of the editors/authors for Bentham Books is based on the expertise of scientists and their reputation in the area of research.

Bentham Books hereby declare that the book titled "**Biotechnology and Drug Development for Targeting Human Diseases",** edited by **Israel Valencia Quiroz** has been peer-reviewed by the neutral experts of the field. The final acceptance of the book was done on the recommendations of the reviewers/referees.

We are thankful for the editor's efforts and greatly look forward to having the same kind of cooperation in future as well.

With best regards,

Dr. Obaid Sadiq

OBAID SADIQ
Manager Publications
Bentham Science Publishers

CHAPTER 7

Natural Products in Wound Regeneration

[1]Laboratorio de Fitoquímica, FES-Iztacala, UNAM, Av. de los Barrios No. 1. Los Reyes Iztacala, Tlalnepantla, Estado de México, México, 54090. [2]Posgrado en Ciencias Biológicas, UNAM, Coyoacán, Ciudad de México, México, 04510. [3]Laboratorio de Bioactividad de Productos Naturales, FES-Iztacala, UNAM, Av. de los Barrios No. 1. Los Reyes Iztacala, Tlalnepantla, Estado de México, México, 54090. [4]Departamento de Ecología y Productos Naturales, Facultad de Ciencias, UNAM. México. Coyoacán, Ciudad de México, México, 04510.

Abstract: The skin is the largest organ in the body that provides protection. When a wound occurs, the skin structure and its function are damaged, and it can even compromise life. Damage repair can occur through two mechanisms: healing and regeneration. When a scar forms, fibrosis occurs in the area, and the skin appendages, which include the glands and hair follicles, are lost. In regeneration the functionality of the skin is partially or totally recovered. Medicinal plants and their active principles favor the regeneration of skin wounds because they have direct effects on the different phases of the process. They favor hemostasis, modulate inflammation, which allows the following stages of healing to occur in less time, such as proliferation and remodeling. They favor hemostasis, modulate inflammation, and that the following stages of healing to occur in less time (proliferation and remodeling). Natural products can also reduce the risk of wound infections by having antibacterial activity. However, the bioavailability of the extracts and their metabolites may be limited, and a solution to this problem is to integrate them into preparations such as hydrogels, nanoparticles, nanofibers, and nanoemulsions. Research on the therapeutic properties of various natural products and their integration into the formulations mentioned above for wound regeneration is described below according to their effect on epithelialization, regeneration of epidermal appendages, vascularization and in some cases their mechanism of action.

Keywords: Hair follicles, hydrogels, nanoemulsions, nanofibers, nanoparticles, natural products and, wound regeneration.

INTRODUCTION

The largest organ in the body is the skin; one of its main functions is to maintain the integrity of the individual. It has two main tissues: a) the outermost is the epidermis, a keratinized squamous epithelium composed mainly of keratinocytes, and the thickness varies from 0.04 to 1.6 mm depending on the location; b) the dermis is made up mainly of fibroblasts that synthesize and remodel the

extracellular matrix (ECM) such as type I collagen fibers, elastic fibers, and ground substance; this layer is thinner than the epidermis -15 to 40 times- epidermis [1, 2].

In the dermis there are two important compartments: a) the papillary dermis (PD) which is located below the epidermis, and is rich in papillary fibroblasts, with a high proliferative and synthetic capacity; and b) the reticular dermis (RD) which is much thicker with a parallel organization of connective tissue fibers to the surface of the skin, below the fatty layer called the hypodermis and later the fascia. In these layers, we find the radicular fibroblasts that oversee the synthesis of the ECM and participate in the generation of adipocytes. Through the epidermis and dermis are the hair follicle (HF) associated with sebaceous glands and the erector pili muscle, known as epidermal appendages [1]. It has been reported that papillary fibroblasts participate in the regulation of the maintenance and growth of the epidermis, as well as of the follicles. Mesenchymal stem cells are found in PD located at the base of the HF [2].

When the integrity of the skin is altered, a wound occurs. The damage repair process occurs through the formation of scars or fibrotic repair that do not present HF, sebaceous glands or sweat glands. The wound healing process comprises four interposed phases: a) hemostasis (generation of a clot), b) inflammation (debridement of the wound), c) proliferation (activation of fibroblasts with collagen III synthesis), and d) remodeling (restoring type I collagen), resulting in a scar [2].

The process of healing wounds on the skin occurs in several stages and there are no specific time limits between them, they overlap each other. This process is dynamic and highly regulated by cellular, humoral, and molecular mechanisms that participate in each of the phases. It begins immediately after the injury and can last for years. Closure of skin wounds can be achieved through scarring or regeneration. Healing occurs through a nonspecific form of healing through fibrosis and scar formation [3].

On the other hand, skin regeneration consists of the replacement and specific proliferation of tissues, such as the epidermis, and dermis with their annexes such as HFs [3, 4]. The role of papillary fibroblasts is crucial in skin regeneration by preventing fibrotic effects, and promoting the development of the epidermis, neoformation of HFs and blood vessels [2]. After injury, PD fibroblasts respond to Wnt/β-catenin and Sonic Hedgehog (Shh) signals. Transforming epidermal growth factor beta (TGF-β) stimulates DR fibroblasts to proliferate and secrete ECM in regeneration [5]. The epidermal Shh signaling pathway is involved in reseating dermal papillae with the regenerative niche that promotes hair follicle neogenesis

(HFN). The involvement of different pathways is complex and can lead to scarring or regeneration; for example, sustained Wnt expression is associated with fibrosis, but Shh signaling in Wnt-active cells promotes dermal papillae [6]. The temporal and spatial regulation of signals that can induce fibrotic scar formation or regeneration is complex and continues to be the subject of extensive research (Fig. **1**).

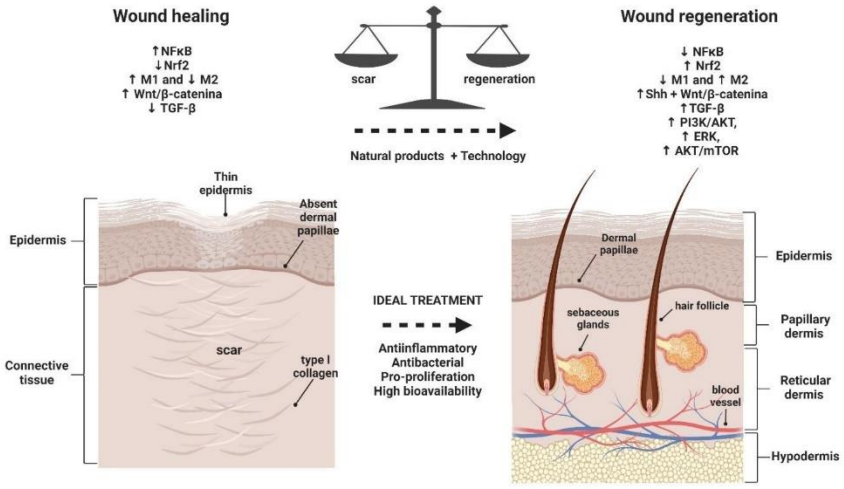

Figure 1: Differences between wound healing and wound regeneration. ↑: increase; ↓: decrease, M1: Macrophage type 1, M2: Macrophage type 2.

Natural products: extracts and secondary metabolites

Treatments for wound healing are diverse and with them the aim is to promote the healing phases and regeneration of tissue. In addition, it is recommended that treatments help maintain humidity around the wound, promote gas exchange, prevent infection, and be biocompatible, biodegradable, and nontoxic. In this sense, natural products have multiple mechanisms that can affect the different phases of healing, and can even induce regeneration by promoting re-epithelialization, de novo formation of HFs, and vascularization [7].

The extracts of several plant species, as well as compounds derived from their secondary metabolism, have been used for the treatment of wounds. Some have an effect in the early phases of tissue repair, favoring hemostasis, and reducing inflammation time, which allows the following stages of healing to occur in less time, such as proliferation and remodeling. Other compounds show an indirect beneficial effect; for example, there are active ingredients that have antioxidant, antimicrobial or anti-inflammatory activity [7].

Chronic diseases decrease the healing process and produce chronic wounds [8]. Diabetic patients with wounds are more susceptible to infection, which can cause amputation of members, bacteremia, and death [9]. Researchers are focusing on treatment in which wounds are closed quickly, infection is prevented, and tissue regeneration is promoted. One strategy is the application and use of technology tools.

The antimicrobial activity of an active principle favors healing by inhibiting the development of microorganisms, which prevents wounds from becoming infected, so that the tissue repair process can continue its course and culminate in an adequate time. As previously mentioned, inflammation is a stage of healing, and it must occur since growth factors are produced that allow the proliferation of keratinocytes and fibroblasts, as well as the production of collagen, ECM, and re-epithelialization. Growth factors involved in the formation of blood vessels, hair follicles, and sebaceous glands are also produced [7]. Another important point is the change in the phenotype of macrophages. M1 macrophages are a proinflammatory phenotype that produce cytokines and chemokines that maintain the inflammatory state, M2 macrophages are an antiinflammatory phenotype that produce cytokines/chemokines anti-inflammatory and growth factors, and higher expression of M2 plays a role in the resolution of inflammation, antifibrotic activity and regeneration of tissues [10]. Inflammation in wound healing is also regulated by nuclear factors such as NFκB (proinflammatory) and Nrf2 (homeostatic and antioxidant response), and the regulation of these factors modulates inflammation in the wound, which promotes tissue regeneration [11]. However, more research is still needed in this regard.

If an active principle has the property of decreasing the inflammation time, without inhibiting this process, growth factors are produced that allow the healing stages to occur in less time (Table **1**).

Table 1: Extracts of plant species with a wound regeneration effect.

Species	**Extract and plant structure**	**Biological model and method**	**Compounds**	**Mechanism of action**	**Reference**
Aloe vera Synonym *A. barbadensis*	Gel Leaves	Wistar rats (body weight 200-300 g) Excision wound model	Anthraquinones	In 21 days: re-epithelialized with a basal membrane ↑vascularized and well-organized collagen	[12]
A. vera Synonym *A. barbadensis*	Gel Leaves	Wistar rats (adult mature male, weighing 250 g) Excision wound model	Acemannan, maloyl glucans, aloine, emodin, anthrones, asarabinan, arabinorhamnogalactan, galactan, galactogalacturan, glucogalactomannan, galacto glucoarabinomannan, glucuronic acid, and lectins	modulated the inflammation, ↑rate and quality of fibroplasia, ↑remodeling stage, ↑ wound contraction, ↑epithelialization, ↑higher tissue alignment	[13]
Synonym *A. barbadensis*	Gel Leaves	Wistar male rats (250-300 g) Incision Wound Model	NR	↑regeneration epithelium ↑angiogenesis	[14]
Curcuma longa	Ethanolic Rhizome	Female rabbit *Oryctolagus cuniculus* (1500-2000 g) Incision Wound Model	Alkaloids, flavonoids, curcumin, essential oils, saponins, tannins, and terpenoids.	↓decreases length of wound	[15]
Panax gingseng	Aqueous Roots	Male Spraguee Dawley rats (200-250 g) Excision wound model	Ginsenoside	↑angiogenesis ↑epithelialization ↓ inflammatory cells ↑ number of fibroblasts ↑collagen	[16]
Artemisia montana	Essential oil Flowers	Human keratinocytes (HaCaT) Proliferation and migration Sprague-Daweley rats (200-220 g) Excision wound model	Major compounds in essential oil: β-caryophyllene (12.8%), germacrene D (9.9%), 1,8-cineole (7.9%), and camphor (6.2%)	↑proliferation ↑synthesis of collagen, ↑wound closure	[17]
Salvia officinalis	Hydroethanolic Leaves	White Wistar rats (200 g) Excision and incision wound models	Flavonoids and phenols	↑contraction and re-epithelialization in wound ↑new blood vessels and fibroblasts distribution	[18]

The active principles that present the mechanisms of action that have been mentioned produce a partial effect in tissue repair with the consequent formation of scars, while others may have regenerative properties through the proliferation of keratinocytes [17], of which epidermal appendages, as well as contraction and closure of the wound without the formation of an apparent scar. These effects are mainly because the extracts and/or active principles increase the expression of transformant growth factor-B (TGF-B) and vascular endothelial growth factor (VEGF), which have an important role in stimulating re-epithelialization, granulation tissue, angiogenesis, and the deposition of collagen fibers in incisional and excisional wounds [7], so such substances, whether extracts or pure compounds, can be considered to have a regenerative effect (Table **1**). Additionally, the PI3K/AKT, ERK, and AKT/mTOR pathways participate in wound healing by promoting cell proliferation differentiation and migration [23, 24]. Its role in the wound regeneration process has been reported, but its role in skin regeneration is still being investigated.

The diversity of species that produce active principles with healing properties is enormous and they are part of the flora with medicinal properties, which is used throughout the world. Of special importance are the plants used in the countries of Asia, Africa, and America, where species such as: *Aloe vera* and the synonym *A. barbadensis* [7, 25], *Centella asiatica* [26], *Curcuma longa* [15], *Panax gingseng* [16], *Salvia officinalis* [18], *Asterohyptis stellulata* [22], among others (Table **1**).

One of the most studied plants is *A. vera* (Synonym: *A. barbadensis*), which contains more than 200 active compounds such as anthraquinones -aloin, emodin, and chrysophanol-, anthrones, flavones, chromones, alkaloids, carbohydrates, amino acids, lipids, minerals, and vitamins, which may even act synergistically way. *A. vera* gel and extract promote skin repair in both *in vitro* and *in vivo* models [7, 21]. In addition, it has antioxidant, anti-inflammatory, antimicrobial and immunomodulatory properties [27]. These properties favor epithelialization, the organization of the ECM fibers, vascularization, the remodeling of the skin and epidermal appendage, which is why it favors skin regeneration [7, 12, 14, 27, 28].

The compounds with regenerative capacity are diverse among the different plant species, such as phenolic compounds, alkaloids, glycosides, and glycoproteins (Table **2**). Of these, phenolic compounds [29], glycosides and glycoproteins are especially relevant, which act by activating the growth factors involved in keratinocyte proliferation, angiogenesis, production and maturation of collagen, and wound closure [30, 31,32].

Whether they are crude extracts, mixtures of compounds and/or pure active principles, the concentrations in which they exert the regenerative effect play a fundamental role, since in several of them it has been observed that the effect is not always dependent on the concentration, of in such a way that in lower concentrations of natural products greater healing is observed, which is a hormetic effect. This effect occurs in processes related to cell keratinocyte proliferation, viability, migration, and collagen deposition in murine and human fibroblasts [33].

Asiaticoside and madecassoside are pentacyclic triterpene glycosides isolated from *Centella asiatica*. Glycosides and their aglycones -asiatic acid and madecassic acid- are recognized for their beneficial effects on the skin. These compounds favor skin regeneration because

they stimulate the synthesis of collagen, in addition to moisturizing the wound [34]. Madecassol®, which contains the following active ingredients: asiaticoside, asiatic acid and madecassic. These compounds improve tensile strength, collagen synthesis, re-epithelialization, and promote angiogenesis [35, 36, 37]. The activity of these compounds has been evaluated in different models that include burn [38] as well as excisional wounds [39]. Curcumin (diferuloylmethane) is the main curcuminoid in *Curcuma longa*. This compound has antioxidant, antimicrobial, and anti-inflammatory properties. It favors the development of various phases of healing, especially the transition from the inflammatory to the proliferative phase, which causes wound contraction and subsequent remodeling, high collagen deposition, neovascularization, rapid re-epithelialization, and tissue formation [40]. The effect of various secondary metabolites on wound repair is described in Table **2**.

Table 2: Compounds with wound regeneration effects.

Compound	Plant species	Biological model	Mechanism of action	Reference
Acemannan	*Aloe vera* Synonym *A. barbadensis*	Male Sprague Dawley rats (8-week-old, 200-250 g) wound healing assay	↑ cell proliferation ↑KGF-1, VEGF, and type I collagen ↓ wound area ↑ epithelial coverage	[41]
Asiaticoside and madecassoside	*Centella asiatica*	Male Sprague-Dawley rats (250-300 g) Burn wound whit hot plate (75℃) (3.5x4.6 cm)	↑ collagen synthesis ↓ oxidative stress ↑vasodilatation, cell proliferation and growth ↑VEGF and FGF	[31]
Madecassic acid, madecassoside, asiatic acid, and asiaticoside	*Centella asiatica*	Male ICR mice 12 weeks (20–25 g) Excision wound model	↑wound repair ↑fibroblast proliferation and collagen synthesis ↑contraction and epithelization	[39]
3α-hydroxymasticadienoic acid (3MA), masticadienoic acid (MA), anacardic acid (ANA)	*Amphipterygium adstringens*	Male Wistar rats (170–200 g) Excision wound model	3MA and ANA: ↑wound closure better collagen matrix architecture ANA and MA: ↓inflammatory infiltrate ↑mature epithelium and dermal papillae	[42]
3'4-O-dimethylcedrusin and proanthocyanidins	*Croton* spp	Female Wistar rats (250-300 g) Excision wound model	↑contraction of the wound ↑new collagen regeneration of the epithelial layer stimulation of fibroblast spread	[43]
Curcumin	*Curcuma longa*		↑granulation tissue ↑collagen deposition, remodeling and wound contraction.	[44]
Rosmarinic acid	*Rosmarinus officinalis*	Sprague Dawley rats (180–220 g) Excision wound model	↑wound contraction ↑cell adhesion, epithelial migration, and high hydroxyproline content	[45]
Epigallocatechin gallate	*Camellia sinensis*	Wistar rat (180–220 g and 3–5 weeks of age) Excision wound model	↑wound regeneration process ↑vascularization, modulation growth factors and inflammatory cytokines	[46]
Hesperidin		Adult Sprague Dawley rats (male, 180- 220 g) diabetics Excision wound model	↓VEGF-c, Ang-1/Tie-2, TGF-β and Smad-2/3 ↑angiogenesis and vasculogenesis	[47]

Taxifolin		Male Wistar rats (250-300 g) Burn wound	regeneration and reparation of hair follicles and sebaceous glands	[48]
Naringin		Adult male Wistar rats (250-270 g) Excision wound model	Naringin 6% downregulating the expression of inflammatory factors (NF-κB, TNF-α and interleukins) and apoptotic factors (pol-γ and BAX). Upregulates the expression of VEGF and TGF-β1, which are associated with the enhancement of collagen I synthesis and angiogenesis.	[49]
Quercetin		Human skin fibroblasts (HSF), mouse skin fibroblasts (MSF) C57BL/6 mice	↑proliferation and migration of fibroblasts Restores the content of collagen fibers, ↓inflammatory factors, (TNF-α, IL-1β and IL-6) ↑ VEGF, FGF and SMA.	[50]
NR: Not reported; ↑: increase; ↓: decrease				

Biotechnology in wound regeneration

The activity of natural products on the skin is limited by poor solubility in water, high hydrophobicity, low solubility, photosensitivity, etc. Various formulations are being developed to favor the bioavailability of substances by improving solubility, permeability on the skin, and avoided degradation (chemical and/or enzymatic) (Fig. **2**).

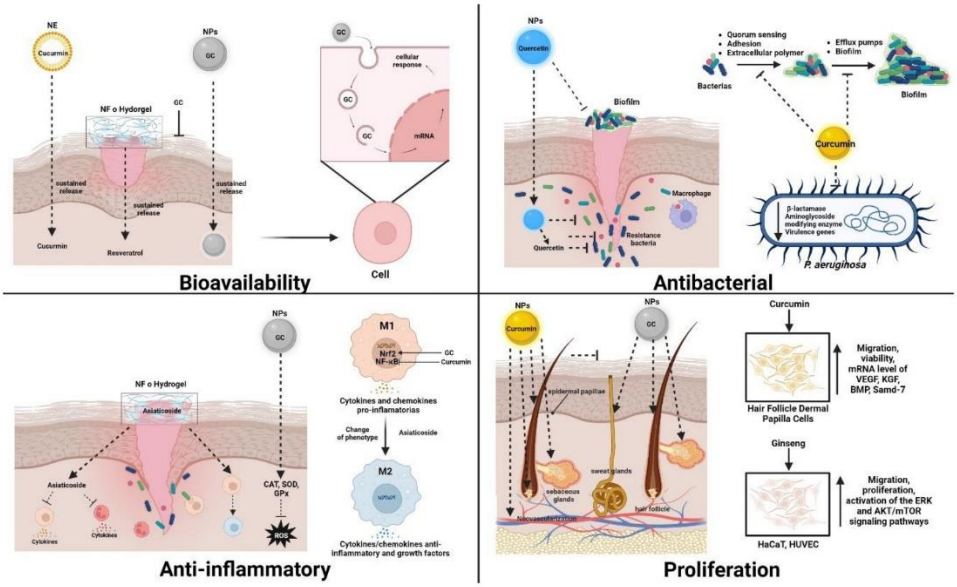

Figure 2: Effect of biotechnological formulations on the penetration and bioavailability of different secondary metabolites and their effect on skin regeneration. CAT: Catalase, GC: Gallocathequin; GPx: Glutathione peroxidase, M1: Macrophage type M1, M2: Macrophage type M2, NE: Nanoemulsion, NPs: Nanoparticles, ROS: Reactive oxygen species, SOD: Superoxide dismutase.

Hydrogels

One technological strategy in regenerative medicine is the use of formulations/scaffolds for dressing and adjuvant drugs, mostly hydrogels, in the treatment of wound regeneration [51]. The hydrogel is a material of three-dimensional networks whose main characteristic is that it retains large amounts of water without dissolving, thus maintaining a humid environment that helps reduce the formation of scars. Additionally, high porosity allows gas exchange, and

hydrogels can be loaded with bioactive molecules, in addition low adherence reduces pain for patients [52]. Therefore, the investigation of hydrogels loaded with extracts or secondary metabolites is essential for wound regeneration. Quercetin is a flavonoid that decreases fibrosis and scar formation, when loaded into liposomes and integrated in hydrogels, enhanced its bioavailability and maintaining its qualities [53]. Moreover, hydrogels enable the sustained release of metabolites. For example, polyvinyl alcohol hydrogel with inebrin of *Lagochilus inebrians* it has a sustained release of the drug for up to 60 hours [54]. The combination of resveratrol and curcumin in a nanoemulgel enhanced controlled release, was applied in burns and showed histopathological features similar to those of normal skin [55].

Secondary metabolites also function as scaffolds for the formulation of biomaterials such as hydrogels.

Resveratrol in a gallic acid aqueous solution, promotes self-assembly of gallic acid to form a fibrous hydrogel that is also therapeutic carrier and shows slow release, antibacterial effects, and regulation of inflammatory factors in bacteria-infected wounds [56]. Tannic acid, acrylamide, and soy protein constituting the hydrogel used to treat wounds exhibited good adhesion, antibacterial activity, and tissue regeneration [57].

Nanotechnology

Nanotechnology is a field in science involving the manipulation of matter in the nanoscale range (10-1000 nm), whit different approaches such as medical area [58]. Their use as a carrier enhances bioavailability, increases biological activity and allows the use of a lower dose of the active substance [59]. Nanotechnology itself applied in wounds enhanced healing and regeneration. In the treatment of regeneration of the skin the use of nanoparticles predominates, mainly applied together with hydrogels to a lesser extent and other nanomaterials designed to function as dressings.

Nanoparticles

Nanoparticles (NPs) in chronic wounds promote regeneration of skin, as shown by epidermal appendage formation -hair follicles, sweat and sebaceous glands-, formation of dermal papillae, adipocyte migration, and inhibition of scar formation [60, 61]. Moreover, NPs as administration vehicles keep the drug isolated from possible bioreactions and allow its controlled release after reaching the lesions [62], and NPs can enter the tissue by hydrophobic interactions and cells by endocytosis,

acting as vehicle and drug delivery [63]. Skin acts as a natural barrier; in this case, it prevents most drugs from penetrating, mainly hydrophobic molecules with a large molecular weight [64]. Moreover, when the molecules pass through the stratum corneum, they are more retained in the dermis and hypodermis [65, 66]. Therefore, developing methods to avoid the stratum corneum and facilitate drug entry is essential in topical administration [67].

The modifications in NPs are essential since they will allow NPs to penetrate tissues such as the stratum corneum or even determine the specificity of the cellular target. In AuNPs their size, shape, and modifications of surface chemistry (charges, ligands, antibodies, polymers), determine whether penetration may occur through skin (hair follicles, intercellularly, or transcellularly), as well as release in response to pH, biomolecules, or light [68].

Medicinal plants and metabolite secondaries, as mentioned earlier, also have activities related to enhanced wound healing, promote the regeneration of skin and epidermal appendages. This activity is enhanced by their integration of NPs. *Cimifuga dahurica* in AgNPs alone and in hydrogel promotes healing skin wounds and formation of epidermal appendages [69]. *Calendula officinalis* is widely known for its healing activity; when it is integrated with AgNPs in chitosan hydrogels and applied in patients with very large ulcers (10 x 8 cm approx.) in the lower extremities that do not respond to treatment, decreased inflammation and pain occur, wounds heal completely and promote tissue regeneration [70].

The possible improvement in the activity of the extracts when integrated into NPs and/or hydrogels could be because of the increased bioavailability of the secondary metabolites. Some of these compounds have low bioavailability, skin absorption and sustained release problems. For example, flavonoids have a high molecular weight more when be glycosylated, aromatic ring that confers hydrophobicity and steric hindrances, have little probability of transport across cell membranes, and the aglycones enters by passive diffusion but are pumped out by ABC transporters [71]. When flavonoids are integrated into NPs and/or hydrogels, their bioavailability improves.

Gallocatechin (GC) integrated into AgNPs increased wound healing, restauration of dermis and epidermal appendages, enhanced the expression of antioxidant enzymes, and growth factors [11], increased Nrf2 and regulated expression of NFκB both of which are associated with changes in the phenotype of M1 to M2 macrophages [11]. Higher expression of M2 plays a role in the resolution of inflammation, antifibrotic activity and regeneration of tissues [10]. As mentioned,

curcumin has various properties that favor regeneration wound -antibacterial, antioxidant and anti-inflammatory (NF-κB) activities- but has poor solubility and low bioavailability [72]. However, their bioavailability is enhanced with is integrate in NPS of Fe-SiO_2 or NPS of silk fibroin/alginate, inhibits scar formation and promote follicle regeneration in bacterial-infected wound; and increased cell migration and production of growth factors in hair follicles in the DP [73, 74]. In this case, the different material of NPs does not affect the activity since both improved tissue regeneration.

Hence, the use and application of NPs increase the liberation of drugs and prolong the release of metabolites. Alginate nanoparticles as capsaicin vehicle (embedded in nanofibers) prolonged the release of metabolites from 120 to 500 hours in the treatment of cancer [75]. Triterpene saponins such as Asiaticoside are poorly soluble and lipophilic but are loaded in polymeric NPs and incorporated in hydrogel, improve bioavailability, enable sustained release three times more that metabolites alone and enhance therapeutic effects in diabetic wounds [76]. Moreover, asiaticoside loading into polylactic-co-glycolic acid nanofibers promotes M2 polarization, and downregulates inflammatory cytokines, which could promote tissue regeneration [77]. Secondary metabolites yields are influenced by biotic and abiotic factors, and industrial manufacturing is complicated due to its chemical complexity. Therefore, it is especially important make the most of the resources.

The widespread use of antibiotics has increased antimicrobial resistance; for examples are apparition of β-lactamase enzymes and creation of biofilms. Nanomaterials exhibit antibacterial properties, which accelerate wound regeneration [78]. AgNPs have notorious antibacterial activities *per se* against gram-negative and gram-positive.

Secondary metabolites act on bacteria then: 1) compromise the cell wall/membrane; 2) inhibit the production of biomolecules; and c) cause death by ROS [79]. Moreover, wound dressings loaded with AgNPs have antimicrobial activity that downregulates β-lactamase and other resistance genes [80]; as previously mentioned, by integrating bioactive compounds such as GC, they act synergistically and favor skin regeneration [11]. Quercetin-borate NPs in poly vinyl alcohol exhibited excellent bacteriostasis and functional restoration of skin [60]. Biofilms inhibit the healing of chronic wounds; treatment to remove them is complicated by the presence of an extracellular polymeric barrier (EPB) that is permeable to drugs [81]. Nanomaterials, owing to their size, can penetrate and deliver antibacterial

agents in tissues and biofilms [82]. Sonodynamic therapy with emodin NPs inhibited the growth of multi-bacterial biofilms, and curcumin NPs in biofilms of multidrug-resistant *Pseudomonas aeruginosa*, both burn wound bacterial isolates, had antibiofilm activity by decreasing expression of virulence factors [83, 84]. Therefore, the formulation with nanoparticles and natural products could be a good alternative for the treatment of wounds with bacterial resistant and biofilm, promoting of tissue regeneration.

Metabolites are not only being used as bioactive compounds but also for the construction of NPs. Glycosylated flavonoids such as rutin are used as scaffolds of NPs (rutin NPs) incorporated into cryogels to increased IL-10, have antioxidant properties, and demonstrate their antiscarring effect [85]. Another example is the fabrication of NPs with Ginseng extract which increased cell migration and proliferation (ERK, AKT/mTOR), angiogenesis, dermis similar to normal and with hair growth [86].

Nanofibrous

Another application of nanotechnology for regenerative medicine is the design of biomaterials that provide essential structural "scaffolding" to create new structures that mimic natural tissues that are biocompatible [87]. Nanofibrous scaffolds (NFS) or matrix is a biomaterial that forms a 3D framework composed of synthetic or natural polymer to carry and deliver drugs facilitating tissue regeneration in wounds [60]. Investigation of this material with extract or metabolites it´s still limited because most of the research that has been done only reaches the *in vitro* phase. *Aloe vera* loaded in NFS zein/polycaprolactone/collagen had antibacterial activity against *S. aureus* and *E. coli* [88]. Essential oils have excellent biological properties, but low solubility and stability under external factors limit their use [59]. Integration in NFS enhanced its stability. Polyvinyl alcohol/gelain NFS with *Thymus daenesis* essential oil and *Glycyrrhiza glabra* extract promote the migration of fibroblasts [89]. NFS with quercetin in graphene oxide NPs and incorporation in polycaprolactone solution promoted the liberation of quercetin by approximately 70% after 15 days and had antibacterial effect [90].

Nanoemulsion

Nanoemulsion is a mix of two immiscible liquids in the presence of surfactants; one of the liquids disperses in another liquid and forms small spherical droplets [72]. In the case of skin, mono- and sesquiterpenes penetrate fastest and deeper, this is time-dependent and these compounds enhance chemical absorption of other triterpenes more complex that do not penetrate the skin easily [91, 92]. However, when

integrated into a nanoemulsion triterpenes improve bioavailability. For example, a nanoemulsion with triterpenes extract of *Poria cocos* loaded in hydrogels for topical application stimulates skin regeneration in diabetic wounds [93]. Nanoemulsion of curcumin induces skin regeneration [72].

CONCLUDING REMARKS

When the integrity of the skin is lost and a wound is generated, a repair process begins that can restore the functionality of this organ through two mechanisms: healing with the formation of a fibrotic scar or skin regeneration where the skin annexes are recovered, such as hair follicles and glands. The occurrence of either mechanism depends on a complex regulation process that is still not fully understood, this process involves molecular mechanisms that activate and regulate re-epithelialization, formation of epidermal appendages, and neovascularization.

Plant extracts and their active components tip the balance toward regeneration; however, bioavailability in many cases is limited. The development of hydrogels and various nanotechnological strategies -nanoparticles, nanofibers and nanoemulsions- promote the penetration, bioavailability, and improvement of the therapeutic effect of plants.

In many cases, the low doses of the active compounds reduce the possible risk of presenting side effects. Therefore, the use of technology integrating natural products is an important point within research to find effective treatments for chronic wounds that can lead to loss of tissue function, amputation of limbs and even death. However, it is essential to continue researching the natural products to understand how they promote the regeneration of skin wounds.

CONSENT FOR PUBLICATON

None Declare

CONFLICT OF INTEREST

None Declare

ACKNOWLEDGEMENT

DGAPA-PAIIT- IN212623 and the CONACyT (CVU 775307) doctoral scholarship.